PHYSICAL MODEL SIMULATIONS OF SALT

LEACHING BY BRINE PUMPING METHOD

Rhattanachat Rhattanapong

A Thesis Submitted in Partial Fulfillment of the Requirements for the

Degree of Master of Engineering in Geotechnology

Suranaree University of Technology

Academic Year 2010

แบบจำลองเชิงกายภาพของการละลายเกลือหินโดยวิธีการสูบน้ำบาดาลเค็ม

นายรัตนชาติ รัตนพงศ์

PHYSICAL MODEL SIMULATIONS OF SALT LEACHING

BY BRINE PUMPING METHOD

Suranaree University of Technology has approved this thesis submitted in partial fulfillment of the requirements for the Master's degree.

Thesis Examining Committee

_____

(Asst. Prof. Thara Lekuthai)

Chairperson

_____

(Assoc. Prof. Dr. Kittitep Fuenkajorn)

Member (Thesis Advisor)

_____

(Dr. Prachaya Tepnarong)

Member

_____   _____

(Prof. Dr. Sukit Limpijumnong)   (Assoc. Prof. Dr. Vorapot Khompis)

Vice Rector for Academic Affairs   Dean of Institute of Engineering

รัตนชาติ รัตนพงศ์ : แบบจำลองเชิงกายภาพของการละลายเกลือหินโดยวิธีการสูบน้ำ
บาดาลเค็ม (PHYSICAL MODEL SIMULATIONS OF SALT LEACHING BY BRINE
PUMPING METHOD) อาจารย์ที่ปรึกษา : รองศาสตราจารย์ ดร.กิตติเทพ เฟื่องขจร,
185 หน้า.

วัตถุประสงค์ของงานวิจัยนี้เพื่อจำลองผลกระทบของการสูบน้ำบาดาลเค็ม โดยใช้รูปแบบ
การย่อส่วนทางกายภาพในห้องปฏิบัติการและมีการประเมินผลกระทบของตำแหน่งที่ตั้งของบ่อสูบ
ความหนาของชั้นหินปิดทับ อัตราการสูบน้ำและทิศทางการไหลของน้ำใต้ดินในขนาดต่อขนาด
และตำแหน่งของโพรงที่ถูกละลาย และต่อการตอบสนองของการทรุดตัว ในการจำลองของชั้นหิน
ปิดทับใช้ทรายที่ถูกคัดขนาดแล้ว 0.6-0.8 มิลลิเมตร ชั้นเกลือถูกจำลองด้วยเกลือละเอียดขนาด 0.6
มิลลิเมตร ความเข้มข้นของน้ำเกลือที่ถูกสูบออกมาและการทรุดตัวจะถูกสังเกตอย่างต่อเนื่องใน
ระหว่างการทดสอบ การทดสอบทั้งหมดจะอยู่ภายในอุณหภูมิห้อง ผลการทดสอบระบุเห็นว่าท่อ
สูบที่อยู่ลึก (ใกล้ผิวเกลือ) ทำให้เกิดการทรุดตัวของผิวเกลือและผิวดินมีมากกว่า ท่อสูบที่อยู่ใน
ระดับตื้นขึ้นมา การทรุดตัวมีมากขึ้นเมื่อท่อสูบอยู่ใกล้ผิวเกลือและลดลงเมื่อท่อสูบอยู่สูงจาก
ผิวเกลือ ภายใต้อัตราปั้มที่เท่ากัน ขอบเขตความกว้างของการทรุดตัวที่ผิวดินที่อยู่ใกล้ผิวเกลือนั้น
มีน้อยกว่าที่อยู่ไกลจากผิวเกลือ ยิ่งระดับน้ำอยู่ลึกการทรุดตัวของผิวดินและผิวเกลือยิ่งมากตามไป
ด้วย แต่ระดับความลึกของน้ำบาดาลนี้ไม่มีผลกระทบต่อขอบเขตความกว้างของการทรุดตัว
ส่วนของอัตราการสูบน้ำบาดาล มีผลต่อการทรุดตัวและขอบเขตความกว้างของการทรุดตัวด้วย
และอาจจะกล่าวได้ว่า ตำแหน่งของแหล่งที่มาของน้ำจืด และตำแหน่งของบ่อสูบนั้นเป็นปัจจัยหลัก
ที่ควบคุมขนาดและตำแหน่งของการทรุดตัวหรือหลุมยุบ

สาขาวิชา <u>เทคโนโลยีธรณี</u> ลายมือชื่อนักศึกษา_____

ปีการศึกษา 2553   ลายมือชื่ออาจารย์ที่ปรึกษา_____

RHATTANACHAT RHATTANAPONG : PHYSICAL MODEL SIMULATIONS

OF SALT LEACHING BY BRINE PUMPING METHOD. THESIS ADVISOR :

ASSOC. PROF. KITTITEP FUENKAJORN, Ph.D., P.E. 185 PP.

SUBSIDENCE/SOLUTION/WATER FLOW/BRINE PUMPING /SALT LEACHING

The objectives of this research are to simulate the impacts of brine pumping process using a scaled-down or physical test model in laboratory, and to assess the effects of location of the well, overburden thickness, pumping rate, and groundwater flow direction on the magnitude and location of the leached caverns and their corresponding subsidence. Sorted sand (0.6-0.8 mm) is used to simulate the overburden. Pure crushed salt (0.6 mm) simulates the underlying salt bed. Salinity of the pumped brine is continuously monitored during the flow test. All tests are performed under room temperature. The results suggest that deeper pumping tubes (closer to the salt surface) induce greater magnitude of surface and formation subsidence than does the shallower tube. The subsidence magnitude induced closer to the salt surface is greater than that for away from salt surface. Under the same pumping rate The extent of the surface subsidence over the shallow salt bed is smaller than that over the deeper salt bed. The deeper groundwater level tends to show greater magnitude of surface and formation subsidence. The groundwater level however has no impact on the extent of the subsidence area. The higher rate of brine pumping, the greater magnitude and the lesser extent of the subsidence is obtained. The location of subsidence is mainly controlled by the positions of the fresh water sources and of the pumping well.

School of <u>Geotechnology</u>   Student's Signature_____

Academic Year 2010   Advisor's Signature_____

TABLE OF CONTENTS

TABLE OF CONTENTS (Continued)

TABLE OF CONTENTS (Continued)

TABLE OF CONTENTS (Continued)

LIST OF TABLES

LIST OF FIGURES

LIST OF FIGURES (Continued)

LIST OF FIGURES (Continued)

LIST OF FIGURES (Continued)

LIST OF FIGURES (Continued)

LIST OF FIGURES (Continued)

LIST OF FIGURES (Continued)

LIST OF FIGURES (Continued)

LIST OF FIGURES (Continued)

LIST OF FIGURES (Continued)

LIST OF FIGURES (Continued)

LIST OF FIGURES (Continued)

LIST OF FIGURES (Continued)

LIST OF FIGURES (Continued)

LIST OF FIGURES (Continued)

LIST OF FIGURES (Continued)

LIST OF SYMBOLS AND ABBREVIATIONS

A	=	Cross-sectional area of flow (area)
b	=	Constant
B	=	Maximum radius of cavern area
B/2	=	Radius of influence
c	=	Arbitrary constant
d	=	The diameter of the specimen
d	=	Cavern depths
D	=	Depth of cavern
E	=	Extraction ratio of the mine
E_m	=	Deformation modulus
G	=	Maximum slope
G(x)	=	Slope
H	=	The head difference
H	=	Cavern height
i	=	Hydraulic gradient (unitless)
k	=	Coefficient of permeability (length/time)
L	=	The length of the specimen
N	=	Model parameters
Q	=	Flow rate (volume/time)
r_i	=	Distance from data point 'i' to the center of the group of data

LIST OF SYMBOLS AND ABBREVIATION Continued)

R_s	=	Roof deformation
$S(r_i)$	=	Subsidence magnitude at point 'i', where i varied from 1 to the total number of measurements, n)
$S(x)$	=	Vertical displacement
S_{max}	=	Maximum subsidence
t	=	Time since excavation
$u(x)$	=	Horizontal displacement
w	=	Cavern diameters
w_{cri}	=	Critical cavern diameters
x	=	Horizontal distance
x_i	=	Coordinates of subsidence measured at point 'i'
y_i	=	Coordinates of subsidence measured at point 'i'
Y_o	=	Model parameters
Y_{ss}	=	Model parameters
z	=	Vertical displacements of the ground surface
Z_u	=	Ultimate surface displacement at any location
γ	=	Angle of draw
β	=	Model parameters
$\varepsilon(x)$	=	Horizontal strain
ρ	=	Maximum curvature
$\rho(x)$	=	Curvature
ϕ	=	Friction angle

ACKNOWLEDGEMENTS

Rhattanachat Rhattanapong

CHAPTER I

INTRODUCTION

1.1 Rationale and Background

Salt and associated minerals in the Khorat and Sakon Nakhon basins, northeast of Thailand have become important resources for mineral exploitation and for use as host rock for product storage. For over four decades, local people have extracted the salt by using an old fashioned technique, called here as brine pumping method. A shallow borehole is drilled into the rock unit directly above the salt. Brine (saline groundwater) is pumped through the borehole and left to evaporate on the ground surface. Relatively pure halite with slight amounts of associated soluble minerals is obtained. This simple and low-cost method can however cause an environmental impact in the form of unpredictable ground subsidence, sinkholes and surface contamination. Even though the brine pumping industry has been limited to strictly controlled areas, isolated from agricultural areas and farmlands, severe surface subsidence and sinkholes have commonly found outside the controlled areas, particularly on the upstream side of the groundwater flow. The subsidence is caused by deformation or collapse of the cavern roof at the interface between the salt and overburden. Due to the complexity of groundwater circulation, infiltration of fresh surface water, salt solubility, brine pumping rates, and number and intensity of the pumping wells, the location and magnitude of the subsidence are very unpredictable. Even though the subsidence problems have long been recognized, theoretical and experimental studies on the issues

have been rare. In particular, no attempt has been made to obtain a true understanding of the formation and surface subsidence caused by the brine pumping process.

1.2   Research Objectives

The objectives of this research are to simulate the impacts of brine pumping process using a scaled-down or physical test model in laboratory, and to assess the effects of overburden thickness, well depth, pumping rate, and groundwater flow direction on the magnitude and location of the leached caverns and their corresponding subsidence. The efforts primarily involve as follows.

1. Designing and fabricating a scaled-down vertical test frame to simulate a two-dimensional cross-section of the pumping well and surrounding formations.

2. Preparing test samples to simulate overburden rocks and underlying salt.

3. Conducting series of flow testing under a variety of overburden configurations and pumping parameters.

4. Developing relationships between the cavern and subsidence characteristics and the flow parameters.

1.3   Scope and Limitations

1. The study area is limited to Khorat and Sakon Nakhon basins

2. Scaled-down physical models are used to simulate the salt leaching in two dimensions

3. Fine sand with nominal diameter of 0.6-1.2 mm. is used to simulate the overburden formations.

4. The overburden thickness above the salt rock = 10-50 cm,

    the groundwater = 10-20 cm, the depth of pumping = 5-35 mm

5. Periodic and continuous withdrawal rates will be performed

6. Two flow directions will be simulated.

7. SALT_SUBSID is used to simulate the subsidence profiles and compared with the model test results.

8. No field testing will be preformed

1.4   Research Methodology

Figure 1.1 depicts the research plan.

1.4.1   Literature Review

Literature review will be carried out to improve an understanding of surface subsidence knowledge. The sources of information are from journals, technical reports, and conference papers. A summary of the literature review is given in the thesis.

1.4.2   Construction of The Physical Model

The test platform for physical model test will be constructed in Geomechanical Laboratory in Suranaree University of Technology. The testing space (area) is about 1.6×1 m. Shown in Figure 8 and 9 show the test platform. .

1.4.3   Model Testing

The subsidence is caused by deformation or collapse of the rock salt at the interface between the salt and overburden. Photo of the surface movement in the model will be recorded the test parameters (variables) include as follows;

    1. Sources of fresh water

        - Vertical infiltration

- Horizontal flow

2. Withdrawal rate (20-100 cc/min)

   - Periodic withdrawal

   - Continuous withdrawal

3. Depth of pumping (5-35 mm)

4. Overburden thickness (10-50 cm)

5. Groundwater level (5-20 cm)

1.4.4 Numerical Simulation

A computer software SALT_SUBSID will be used to simulate the subsidence measured from the model testing. Results obtained from computer program will be compared with the physical model from the testing.

1.4.5 Comparisons

Results obtained from testing will be compared with the solutions from the with the computer program results. Similarity and discrepancies will be discussed

1.4.6 Thesis Writing and Presentation

All research activities, methods, and results will be documented and compiled in the thesis. The contents or findings will be published in the conference, proceedings or journals.

1.4.7 Expected Results

The results from this research will be applicable to the analysis and design of salt leaching by brine pumping method. The physical model can be used as teaching and research tools to reveal the two-dimensional salt leaching process from this research will be useful in predicting the location, depth and size of the solution caverns that are developed by the brine pumping activity.
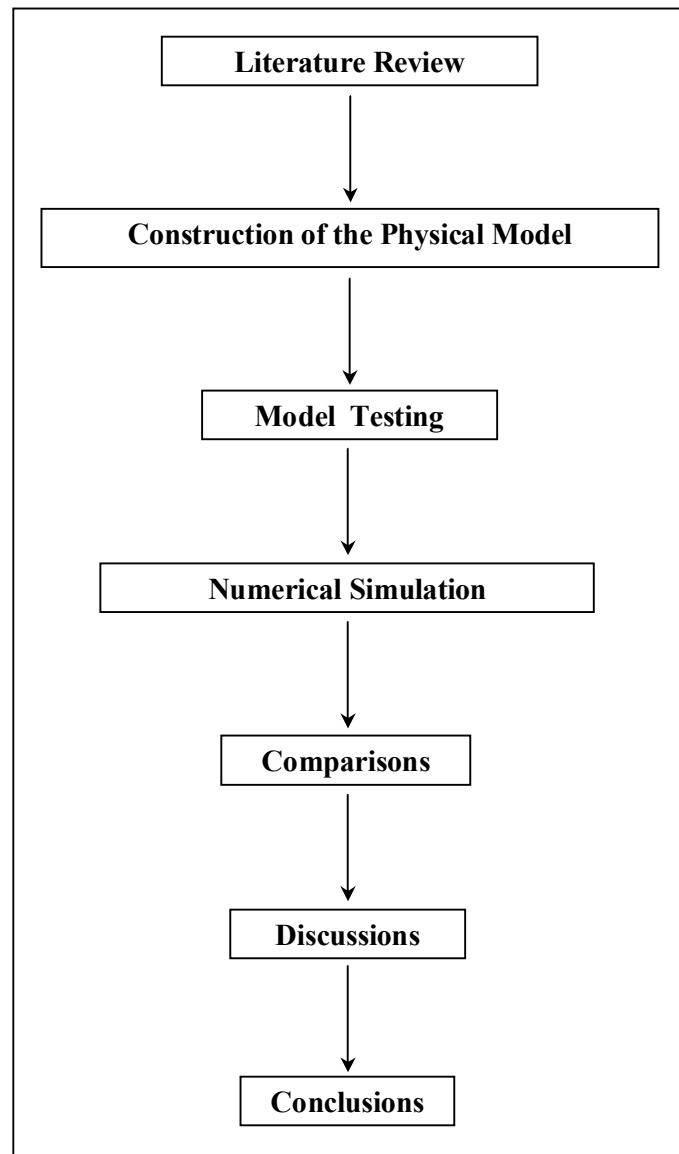
Figure 1.1 Research methodology.

1.5   Thesis Contents

Chapter I states the objectives, rationale, and methodology of the research. Chapter II summarizes results of the literature review on surface subsidence knowledge. Chapter III Construction of the Physical Model. Chapter IV describes Model testing Chapter V describes the profiles of surface subsidence are simulated using a profile function. Chapter VI describes the profiles of surface subsidence are simulated using a Salt_SUBSID program. Chapter VII describes the profiles of surface subsidence are simulated using a finite difference flow program (FEFLOW). Describes develop mathematic relationships, Model testing and Numerical Simulation Conclusions and recommendations for future research needs are given in Chapter VIII.

CHAPTER II

LITERATURE REVIEW

2.1 Introduction

Topics relevant to this research are reviewed to improve an understanding of surface subsidence knowledge. These include rock salt in the northeast of Thailand, calculation of surface subsidence profiles (profile function), and SALT_Subsid program, physical model simulation. Results from the review are summarized as follows.

2.2 Rock Salt in Northeast Region of Thailand

Rock salt formation in Thailand is located in the Khorat plateau as shown in Figure 2.1. The Khorat plateau covers 150,000 square kilometers, from 14° to 19° northern latitude and 101° to 106° eastern longitude. The northern and eastern edges of the plateau lie close to Laos and the southern one close to Cambodia (Utha-aroon, 1993).

Rock salt is separated into 2 basins: Sakon Nakhon Basin and Khorat Basin. The Sakon Nakhon Basin in the north has an area about 17,000 square kilometers. It covers the area of Nong Khai, Udon Thani, Sakon Nakhon, Nakhon Phanom, and Mukdahan provinces and extends to some part of Laos. The Khorat Basin is in the south, which has about 33,000 square kilometers. The basin covers the area of Nakhon Ratchasima, Chaiyaphum, Khon Kaen, Maha Sarakham, Roi Et, Kalasin, Yasothon, Ubon Ratchathani provinces and the north of Burirum, Surin, and Sisaket provinces (Suwanich, 1986).
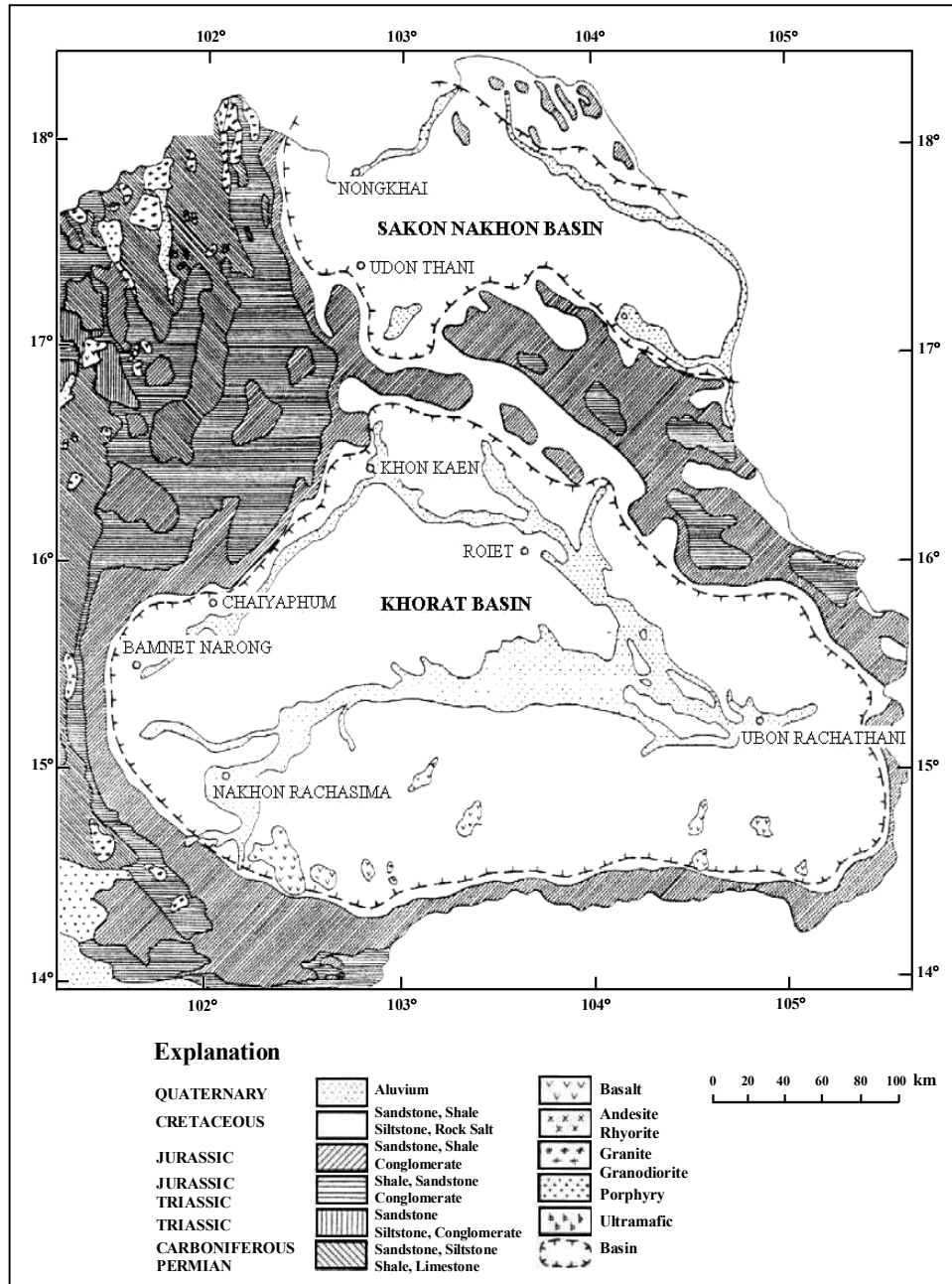
Figure 2.1 Sakon Nakhon and Khorat Basins containing rock salt in the northeast of Thailand (modified from Rattanajarurak, 1990 and Utha-aroon, 1993 adapted from Geological Map of Thailand, scale 1:2,500,000).

The Department of Mineral Resources had drilled 194 drilled holes between 1976 and 1977 for the exploration of potash (Japakasetr, 1985; Japakasetr and Workman, 1981; Sattayarak, 1983, 1985; Japakasetr, 1992; Japakasetr and Suwanich, 1982). Some holes were drilled through rock salt layers to the Khok Kruat Formation (Yumuang et al., 1986; Supajanya et al., 1992; Utha-aroon, 1993; Warren, 1999). The sequences of rock layers from the bottom of this formation up to the top of the Maha Sarakham Formation are as follows.

1) Red bed sandstone or dense greenish gray siltstone sometime intercalated with reddish-brown shale.

2) Basal anhydrite with white to gray color, dense, lies beneath the lower rock salt and lies on the underlying Khok Kruat Formation.

3) Lower rock salt, the thickest and cleanest rock salt layer, except in the lower part which contains organic substance. The thickness exceeds 400 meters in some areas and formed salt domes with the thickness up to 1,000 meters, with the average thickness of 134 meters.

4) Potash, 3 types were found; carnallite ($KCl.MgCl_2.6H_2O$) with orange, red and pink color, sylvinite (KCl) rarely found, white and pale orange color, an alteration of carnallite around salt domes, and techydrite ($CaCl_2.2MgCl_2.12H_2O$) often found and mixed with carnallite, orange to yellow color caused by magnesium, the dissolved mineral occurred in place.

5) Rock salt, thin layers with average thickness of 3 meters, red, orange, brown, gray and clear white colors.

6) Lower clastic, clay and shale, relatively pale reddish-brown color and mixed with salt ore and carnallite ore.

7) Middle salt, argillaceous salt, pale brown to smoky color, thicker than the upper salt layer with average thickness of 70 meters, carnallite and sylvite may be found at the bottom part.

8) Middle clastic, clay and shale, relatively pale reddish brown color and intercalated with white gypsum.

9) Upper salt, dirty, mixed with carbon sediment, pale brown to smoky color or orange color when mixed with clay and 3 to 65 meters thick.

10) Upper anhydrite, thin layer and white to gray color.

11) Clay and claystone, reddish brown color, occurrence of siltstone and sandstone in some places, and

12) Upper sediment, brownish gray clay and soil in the upper part, and sandy soil and clay mixed with brown, pink and orange sandy soil in the lower part.

Cross-sections from seismic survey across the Khorat-Ubon and Udon-Sakon Nakhon Basins (Sattayarak and Polachan, 1990) reveal that rock salt can be categorized into 3 types according to their appearances namely, rock salt beds, rock salt fold and salt domes. The Maha Sarakham and Phu Tok Formations fold in harmony with the Khorat megasequence. A part of the cross section through the Khorat Basin is illustrated in Figure 2.2.

2.3   Site Conditions

Figure 2.3 also shows the areas where the brine pumping have been practices. Depths of the shallowest salt in those areas vary from 40 m to 200 m. It belongs to the Middle or Lower member, depending on locations. Most of the brine pumping practices is however in the areas where the topography is flat, groundwater table
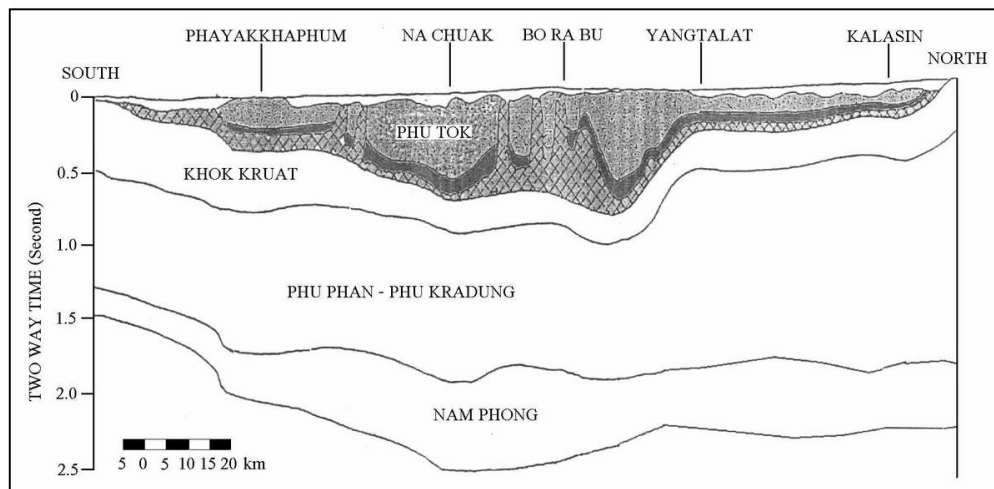
Figure 2.2 Cross-section showing rock salt in the Khorat Basin (Sattayarak N., 1985).
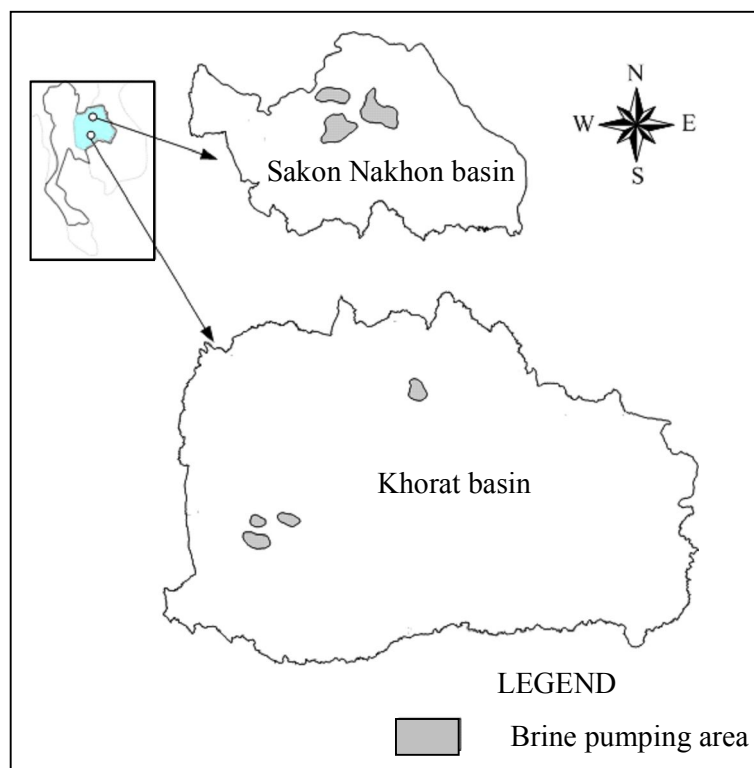
Figure 2.3 Brine pumping area in Khorat and Sakon Nakhon salt basins.

in near the surface, and the salt depth is less than 50 m in the Sakon Nakhon basin, and about 100 m in the Khorat basin (Jenkunawat, 2005; Wannakao et al., 2005). Based on field investigation, Jenkunawat (2007) states that the surface subsidence normally occurs in the areas where depth of the shallowest salt is less than 50 m. The overburden consists mainly of mudstone siltstone and sandstone of the Middle Clastic, and claystone and mudstone of the Lower Clastic, with fractures typically dipping less than 30 degrees, and rarely at 70 degrees (Crosby, 2007). The members are characterized by abundant halite and anhydrite-filled fractures and bands with typical thickness of 2 cm to 5 cm.

Direct shear tests performed in this research yield the cohesion and friction angle of 0.30 MPa and 27° for the smooth saw-cut surfaces prepared from the Middle Clastic siltstone. More mechanical properties for these clastic members are summarized by Wannakao et al. (2004) and Crosby (2007).

2.4 Brine Pumping

Wannakao and Walsri (2007) state that one third of the northeast is generally underlain by sedimentary rocks of Maha Sarakham Formation, sequences of rock salt and clastic rocks. The deposits are divided into the Khorat and Sakon Nakhon basins. Salt productions from brine groundwater are common in both basins. A brine groundwater well is 4 in diameter with 2 in air pumping line at about 60-100 meters depth. The brine is pumped to salt storage bin, then conveyed to salt paddy field for solar evaporation. There are many surface subsidence reported in salt production area in Ban Non Sabaeng, Sakon Nakhon province

Fuenkajorn (2002) give a general guideline developed for the design of salt solution-mined cavern in Sako Nakorn and Khorat basins. Laboratory testing calibrates the mechanical and rheological properties of the salt formation. Via a series of numerical analysis, conservative configurations of the solution mine caverns are determined. It is recommend that the caverns be arranged in an array of single well system and should have the maximum diameter and height of 80 m and 60 m, respectively The minimum spacing is estimated to be 240 m. the cavern field would yield an extraction ratio of 1.96 x 10^6 m^3 of rock salt per one square kilometer. The salt roof and floor should be greater than 200 m to prevent excessive movement of the cavern ground.

Jenkunawat (2007) studies the occurrence of salt cavities induced by brine pumping. The main purpose is to delineate disaster area and monitor land subsidence. Drill holes were totally 12 with depth ranged 100-200 m. A number of holes were cased them with PVC pipes. Drilling results showed claystone at top, salt dome located under the salt production area at depth of 40-50 m. Rock salt was located at depth 40-200 m. Anhydrite and gypsum were observed in holes around the salt dome. Sinkholes are circular in shape, with diameter of 50-100 m. Land usually starts subsiding at pumping well and moves in a series of subsidence which can be traced in a line. They occur in only on a salt dome, where there are fractures, brine zone and dissolution of salt. Areas out of the salt dome are not under risk of salt subsidence.

2.5   Salt Solubility

Potter et al. (1981) show that the solubility of sodium chloride in water has been the subject of several investigations. The earlier measurements were subject to an error

of 0.1 weight percent of salt below 373 K and 0.3weight percent salt above 373 K. Undertook a redetermination of the solubility using a specially designed bomb lined with platinum and attained a precision of 0.01 or 0.1 weight percent of salt over the entire temperature range. A comparison of the solubility obtained by various investigators is shown in Figure 2.4
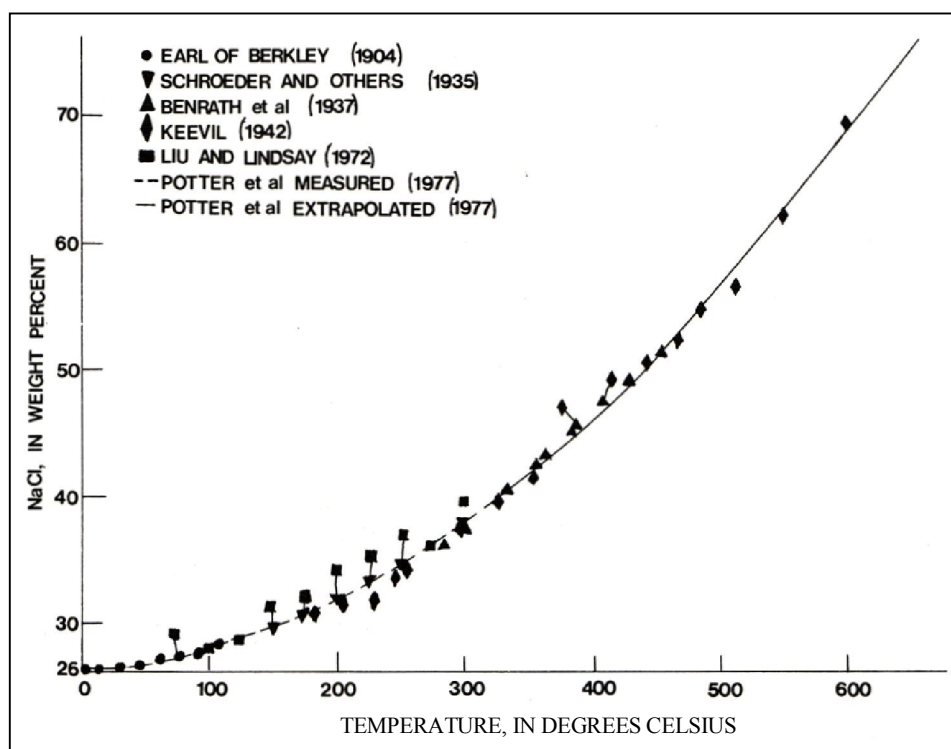
Figure 2.4 A comparison of the solubilities of sodium chloride in water.

(from Potter et al 1981)

Gil et al. (2006) perform computer simulations of salt solubility to provide an animated, visual interpretation of the different solubilities of related salts based on simple entropy changes associated with dissolution: configurational disorder and thermal disorder. This animation can also help improve students' conceptual

understanding of chemical equilibrium before any quantitative interpretation of equilibrium constants is attempted.

2.6   Calculation of Surface Subsidence

2.6.1   Theory and Criterion

Singh (1992) states that subsidence is an inevitable consequence of underground mining – it may be small and localized or extend over large areas, it may be immediate or delayed for many years. During recent years, with the expansion of urbanization and increased concern for the environment, it is no longer possible to ignore its aftermath.

The major objectives of subsidence engineering are (1) Prediction of ground movement, (2) Determining the effects of such movements on structures and renewable resource and (3) Minimizing damage due to subsidence.

Whenever a cavity is created underground, due to the mining of minerals or for any other reason, the stress field in the surrounding strata is disturbed. These stress changes produce deformations and displacements of the strata, the extent of which depends on the magnitude of the stresses and the cavity dimensions. With time, supporting structures deteriorate and the cavity enlarges, resulting in instability. This is induces the superjacent strata to move into the void. Gradually, these movements work up to the surface, manifesting them selves as a depression. This is commonly referred to as subsidence. Thus mine subsidence may be defined as ground movements that occur due to the collapse of overlying strata into mine voids. Surface subsidence generally entails both vertical and lateral movements.

Surface subsidence manifests itself in three major ways: (1) cracks, fissures, or step fractures, (2) pits or sinkholes and (3) troughs or saga. Surface fractures may be in the form of open cracks, stepped slips, or cave - in pits and reflect tension or shear stresses in the ground surface. Subsidence consists of five major components, which influence damage to surface structures and renewable resources are vertical displacement, horizontal displacement, slope, vertical strain, and vertical curvature.

Calculation by profile function;

Subsidence:

$$S(x) = \frac{1}{2} S_{max} \left[1 - \tanh\left(\frac{cx}{B}\right) \right] \qquad (2.1)$$

Slope:

$$G(x) = S'(x) = -\frac{1}{2} S_{max} \frac{c}{B} \operatorname{sech}^2\left(\frac{cx}{B}\right) \qquad (2.2)$$

Curvature:

$$\rho(x) = S''(x) = S_{max} \frac{c^2}{B^2} \left[\operatorname{sech}^2\left(\frac{cx}{B}\right) \tanh\left(\frac{cx}{B}\right) \right] \qquad (2.3)$$

Horizontal displacement:

$$u(x) = -\frac{1}{2} S_{max} \frac{bc}{B} \operatorname{sech}^2\left(\frac{cx}{B}\right) \qquad (2.4)$$

Horizontal strain:

$$\varepsilon(x) = S_{max} \frac{bc^2}{B^2}\left[\text{sech}^2\left(\frac{cx}{B}\right)\tanh\left(\frac{cx}{B}\right)\right] \tag{2.5}$$

where S_{max} is the maximum subsidence, D is depth of cavern, γ is angle of draw, x is horizontal distance, c is arbitrary constant, b is constant, and B is maximum radius of cavern area.

2.6.2 Calculation with SALT_SUBSID Program

SALT_SUBSID code developed by RE/SPEC Inc. (Nieland, 1991) has been used to predict the three-dimensional surface subsidence for predicting configurations of solution cavern on top of salt bed. SALT_SUBSID is designed to calculate the subsidence profile induced by dry mining (underground openings) and solution mining (brine caverns). The key parameters used in SALT_SUBSID including Y_{ss}, Y_o, β and N have been calibrated using the subsidence results computed by the finite element analysis. This makes the predicted subsidence profile over the cavern field more site-specific. Definition of these parameters is described in details by Nieland (1991).

$$Z(x,y,t) = Z_u(x,y).G(t) \tag{2.6}$$

$$G(t) = Y_{ss}.t + Y_o[1\text{-}\exp(-\beta E^N t)], \text{ and} \tag{2.7}$$

$$G(t) = 1; \text{ if } Y_{ss}.t + Y_o[1\text{-}\exp(-\beta E^N t)] > 1 \tag{2.8}$$

where Y_{ss}, Y_o, β, N are model parameters, t is time since excavation, E is extraction ratio of the mine, and Z_u is ultimate surface displacement at any location.

The condition that $G(t) = 1$ is applied when a cavity is completely closed. The parameter Y_{ss} represents the steady-state closure rate and Y_o represents the ultimate transient closure. The parameters β and N are empirical constants used to model the transient closure rate. In the case of dry mining, the parameter Y_{ss} is set to zero.

Aracheeploha et al. (2009).An analytical method has been developed to predict the location, depth and size of caverns created at the interface between salt and overlying formations. A governing hyperbolic equation is used in a statistical analysis of the ground survey data to determine the cavern location, maximum subsidence, maximum surface slope and surface curvature under the sub-critical and critical conditions. A computer program is developed to perform the regression and produce a set of subsidence components and a representative profile of the surface subsidence under sub-critical and critical conditions. Finite difference analyses using FLAC code correlate the subsidence components with the cavern size and depth under a variety of strengths and deformation moduli of the overburden. Set of empirical equations correlates these subsidence components with the cavern configurations and overburden properties. For the super-critical condition a discrete element method (using UDEC code) is used to demonstrate the uncertainties of the ground movement and sinkhole development resulting from the complexity of the post-failure deformation and joint movements in the overburden. The correlations of the subsidence components with the overburden mechanical properties and cavern geometry are applicable to the range of site conditions specifically imposed here (e.g., half oval-shaped cavern created at the overburden-salt interface, horizontal rock units, flat ground surface, and saturated

condition). These relations may not be applicable to subsidence induced under different rock characteristics or different configurations of the caverns. The proposed method is not applicable under super-critical conditions where post-failure behavior of the overburden rock mass is not only unpredictable but also complicated by the system of joints, as demonstrated by the results of the discrete element analyses. The proposed and the corresponding subsidence components induced by the brine pumping practices are shown in Figure 2.5
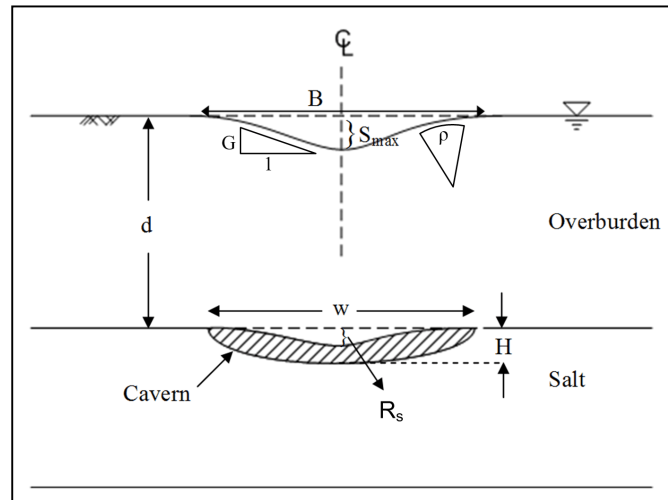
Figure 2.5 Variables used study (by Aracheeploha, 2009).

2.7   Physical Model

Physical modeling of structures formed by salt withdrawal; implications for deformation caused by salt dissolution by creating 15 physical models, they investigated deformation above subsiding tabular salt, salt walls, and salt stocks. Dry quartz sand simulated a brittle sedimentary roof above viscous silicone representing salt. The modeled diapiric walls had linear planforms and rectangular, semicircular,

triangular, or leaning cross sectional shapes; the stock was cylindrical. In models where the source layer (or allochthonous salt sheet) was initially tabular, a gentle, flat-bottomed syncline bounded by monoclinal flexures formed above a linear zone where the silicone was locally removed. Above all subsiding diapirs, the deformed roof was bounded by an inner zone of steep, convex-upward reverse faults and an outer zone of normal faults. Above subsiding diapiric walls, extensional and contractional zones were balanced. Above the subsiding salt stock, conical, concentric fault zones comprised inner reverse faults and outer normal faults by Ge et al, (1998).

Asadi et al. (2005) state that increasing world demand for energy and mineral resources has resulted in much mechanization and rapid excavation techniques by modern mining operations. Exploitation of minerals using caving methods such as the longwall mining method will result in surface subsidence. This phenomenon can cause environmental problems and damage to surface and subsurface structures. In order to protect the environment and structures from these damages, precise subsidence prediction is essential. When a horizontal seam is mined, the subsidence trough has symmetric shape, whereas in inclined seams it is non-symmetric and complicates the prediction of the surface subsidence profile. In some countries, large volumes of coal reserves of high quality are classified as inclined and steep strata. For economic reasons, these deposits have to be extracted and, consequently, the problems of surface subsidence of these types of deposits are still highly relevant. During the last decades, several new models of subsidence prediction for level, inclined, and steep seams have been developed worldwide (Figure 2.6). Still, there are some complexities in the prediction of subsidence profiles in inclined and steep seam mining.
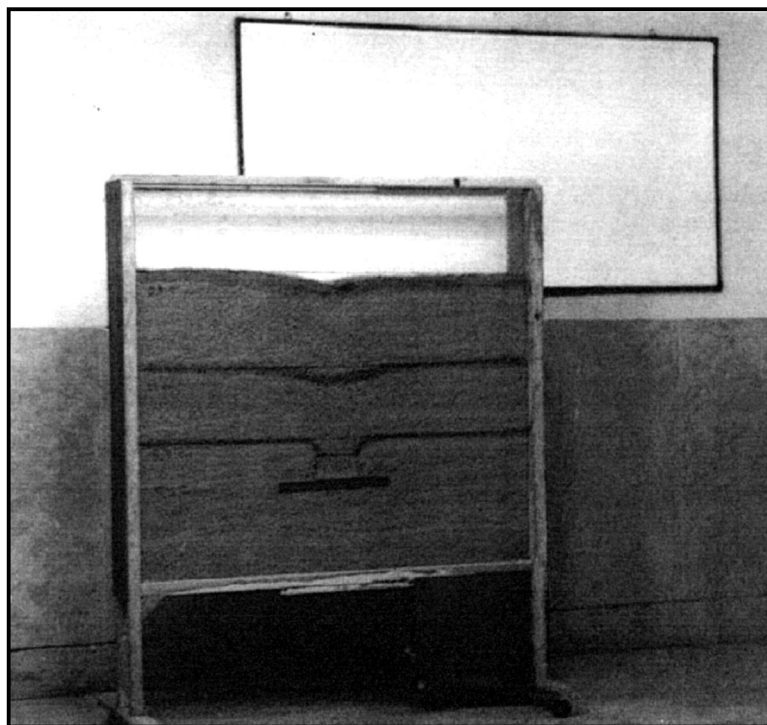
Figure 2.6 A physical model for prediction of subsidence (from Asadi et al, 2005)

Lourenco et al. (2006) show that implications for rainfall-induced landslides. It mentions Field observations and theoretical analysis have been used in the literature to assess slope instability caused by permeability variations. This investigation aims to study the influence of permeability variations on slope behaviour by experimental means. It focuses particularly on the pore water pressure generation in the vicinity of soils with different permeabilities, and the corresponding failure mode. A series of generated failures in a model with 2 soil layers was performed by means of a flume device. The soil layers were made of a medium-sized sand and a fine sand, placed in horizontal layers. A combination of photography and pore water pressure measurements was used to examine the relationship between the pore water pressure generation and failure modes. Experiments were conducted for different arrangements of soil layers by

changing the soil layer position (Figure 2.7). the bottom of the lower layer (b) for tests performed by upward infiltration. Testing procedure comprises on alternating the layers' position and the infiltration direction.
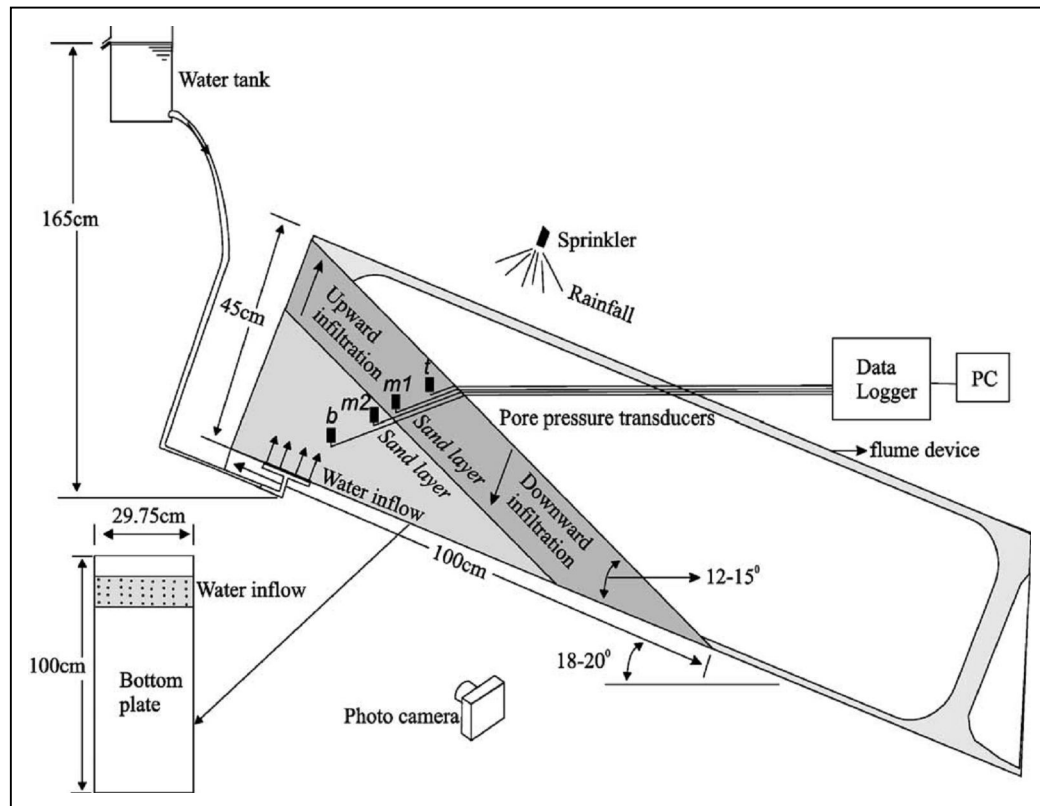
Figure 2.7 Experimental arrangement. The arrangement illustrated corresponds to the right triangle configuration. Two transducers were always placed near the layers surface contact (m1 and m2). The third was placed at the uppermost part of the upper layer (t) for tests performed by downward infiltration (from Lourenco et al, 2006).

CHAPTER III

TEST FRAME

3.1 Introduction

This chapter describes the design and development of the test frame used in this research. It is intended to simulate the impacts of brine pumping process using a scaled-down or physical test model in laboratory, and to assess the effects of overburden thickness, well depth, pumping rate, and groundwater flow direction on the magnitude and location of the leached caverns and their corresponding subsidence. All tests are performed in the laboratory under ambient temperature.

3.2 Design of Test Frame

A test frame is constructed in Geomechanics Laboratory at Suranaree University of Technology. It is developed to represent a vertical cross section of surface subsidence caused by brine pumping. To allow visual inspection during the test two 1.6 m ×1.2 m wide with 1.5 cm thick clear acrylic plates are secured in vertical position. This provides the testing area of about 1 square-meter. They are set 1.2 cm apart using steel frames. The left, right and bottom edges are sealed with rubber plates with water-tight silicone. Figure 3.1 shows test frame used in the model simulations.

This test frame consists of two parts, testing kit and stand. The first part of this frame model is consisted of two acrylic plates to prevent sand and water from leaking from the front and back of the model. The acrylic plates are transparent and allow to monitor the salt solubility and the surface subsidence. The water tube is attached to the

rear acrylic plate which is used for water pumping. There are three rubber strips secured on both sides and the bottom. These three rubber strips are used for sealing the water and other materials from leaking out of the frame. A steel bar and two pieces of brass mesh are used to block the sand from flowing from side to side and to allow water to flow through. Eight steel beams are used for bearing the sides of the acrylic plates. The C-shape steel is used to support the bottom of the test frame, having the same length with the acrylic plates. Four 0.6 mm thick flat bars are placed at the corners. The four flat bars secure the footing at the sides of the test frame. Figures 3.2 through 3.7 show specifications and dimensions of the test frame.

3.3   Testing Materials and Layout

Pure crushed salt is used to simulate the rock salt bed, and sorted sand to simulate the overburden. The pure crushed salt is from Pimai salt factory. The size of the salt grains is 0.02 mm. It can be tightly packed after being compressed which given a low permeability salt layer. This salt does not mix with iodine. The iodine may have an effect on the results of the testing by making an error on the salinity measurements.

The 0.8 mm sorted sand is used to simulate the overburden. The color of the sand is white as it's originally color from the milling rock. In this study the white and green color sand is used. The white sand was dyed to get green colors and the dye does not dissolve in the water.

3.4   Permeability Testing of Sand

The permeability of sand lager is determined by performing a constant head test. The test set up is show in Figure 3.8.

From Equation (3.1) The flow rate Q equals to 5.2 cc/min., H is the head difference equal to 70 cm, d is the diameter of the specimen equal to 5 cm, L is the length of the specimen equal to 30 cm. and k is the coefficient of permeability, which to calculate through the equation (3.1). The hydraulic gradient i and the Area A were calculated through the equation (3.2) and (3.3) respectively.

$$Q = kAi \qquad (3.1)$$

$$i = H/L \qquad (3.2)$$

$$A = \pi d^2/4 \qquad (3.3)$$

Where: Q = flow rate (volume/time)

i = hydraulic gradient (unitless)

A = cross-sectional area of flow (area)

k = coefficient of permeability (length/time)

The coefficient of permeability k, from the calculated value was 0.11 cm / min.
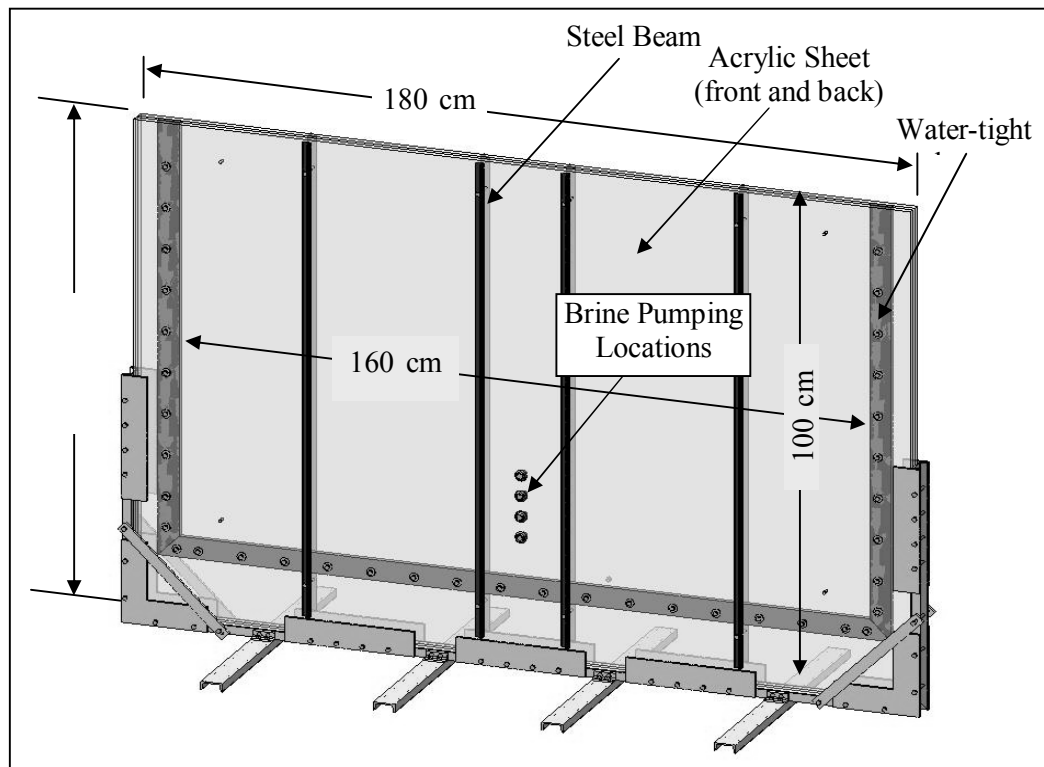
Figure 3.1 Test frame used in the model simulations.
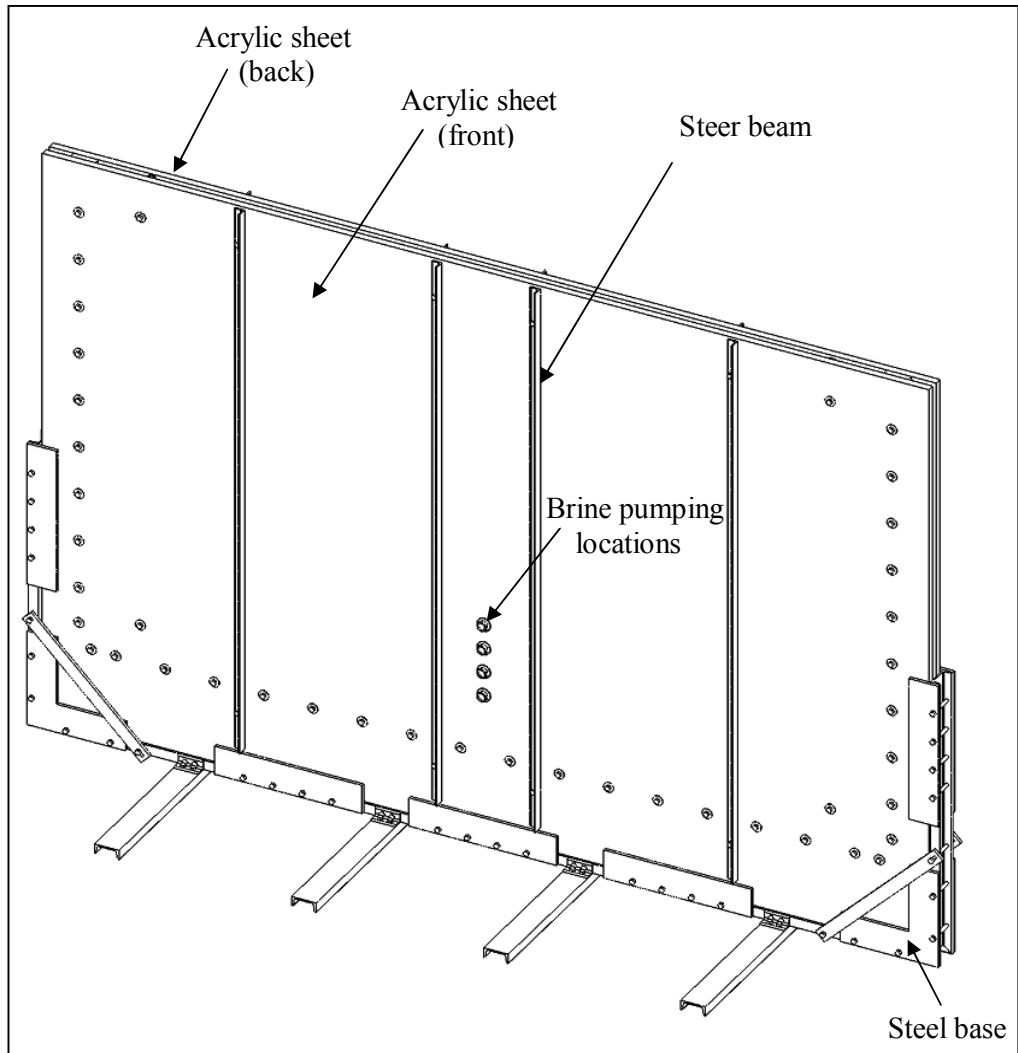
Figure 3.3 Perspective view of test frame used to simulate salt leaching.
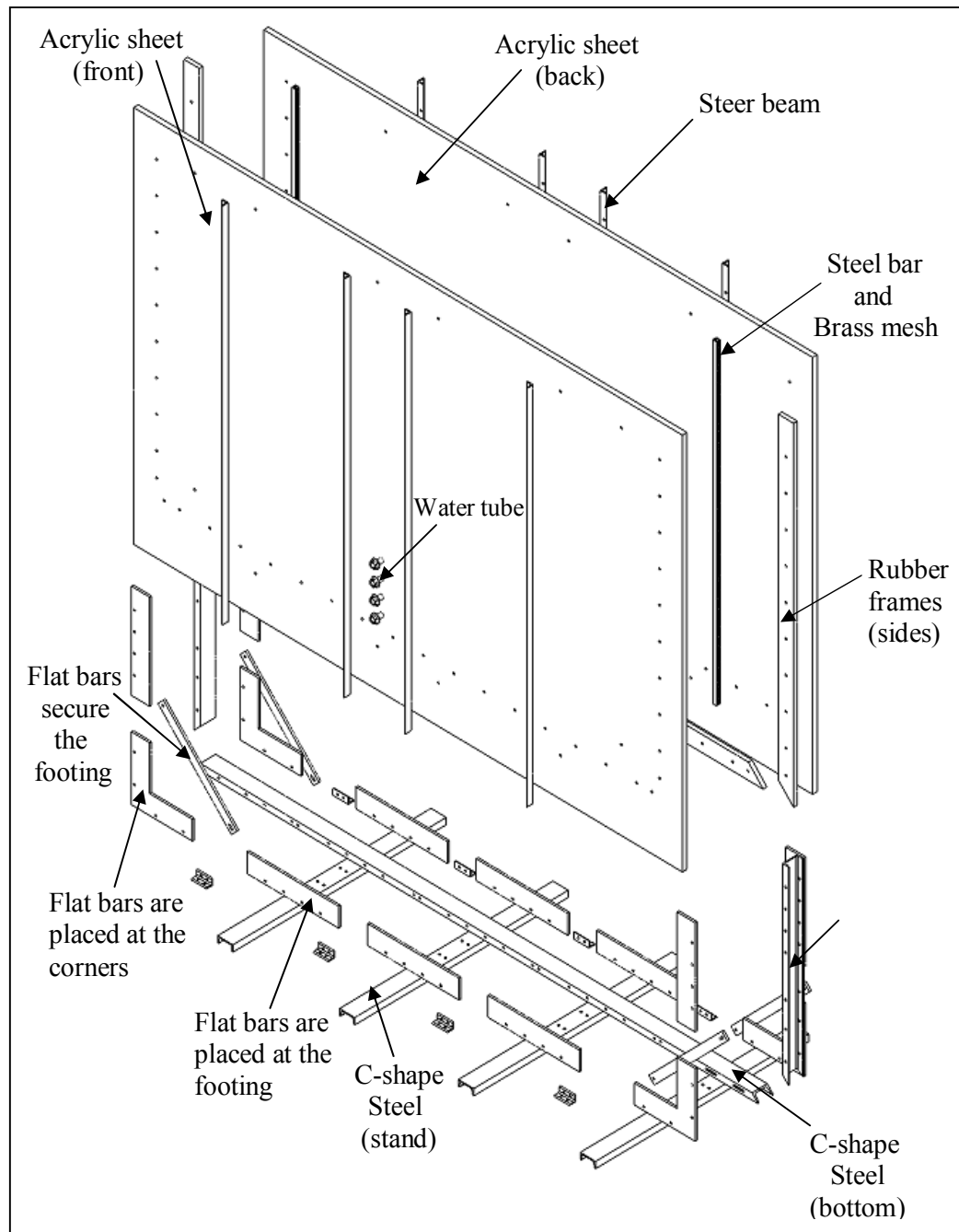
Figure 3.3 Test frame components.
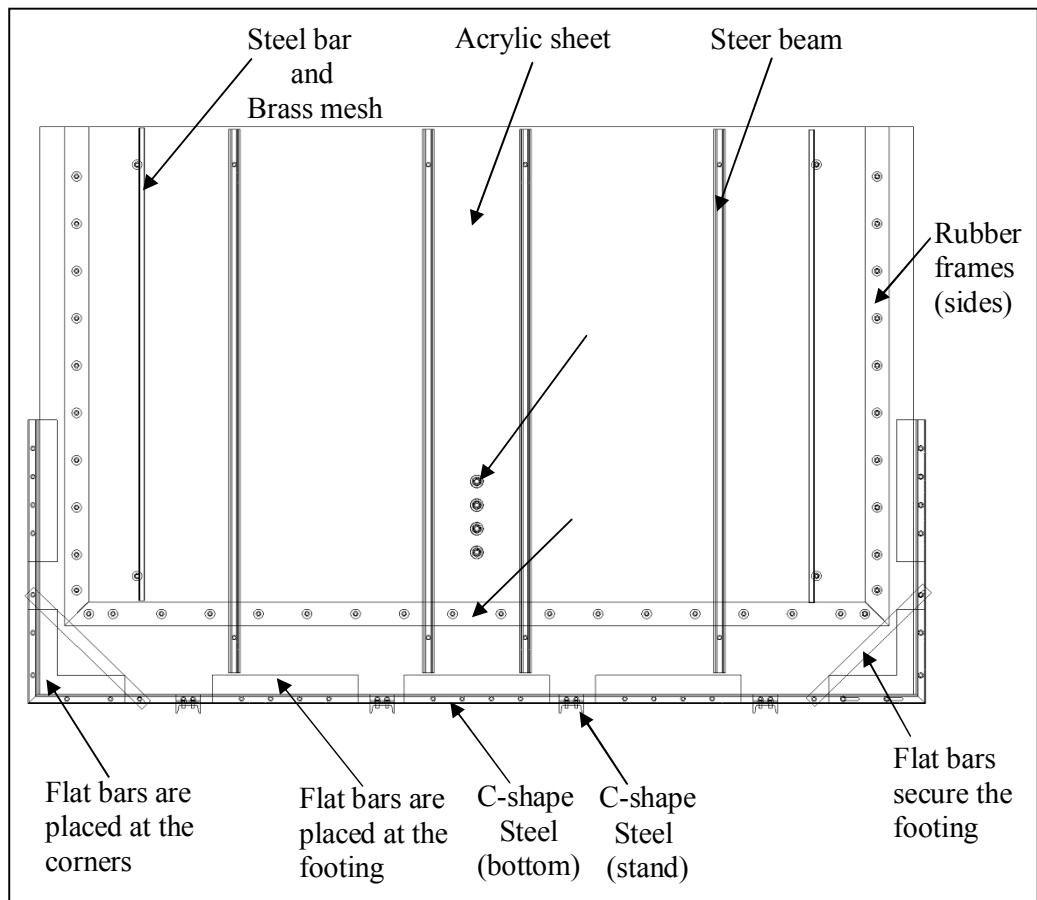
Figure 3.4 Front view of the test frame.
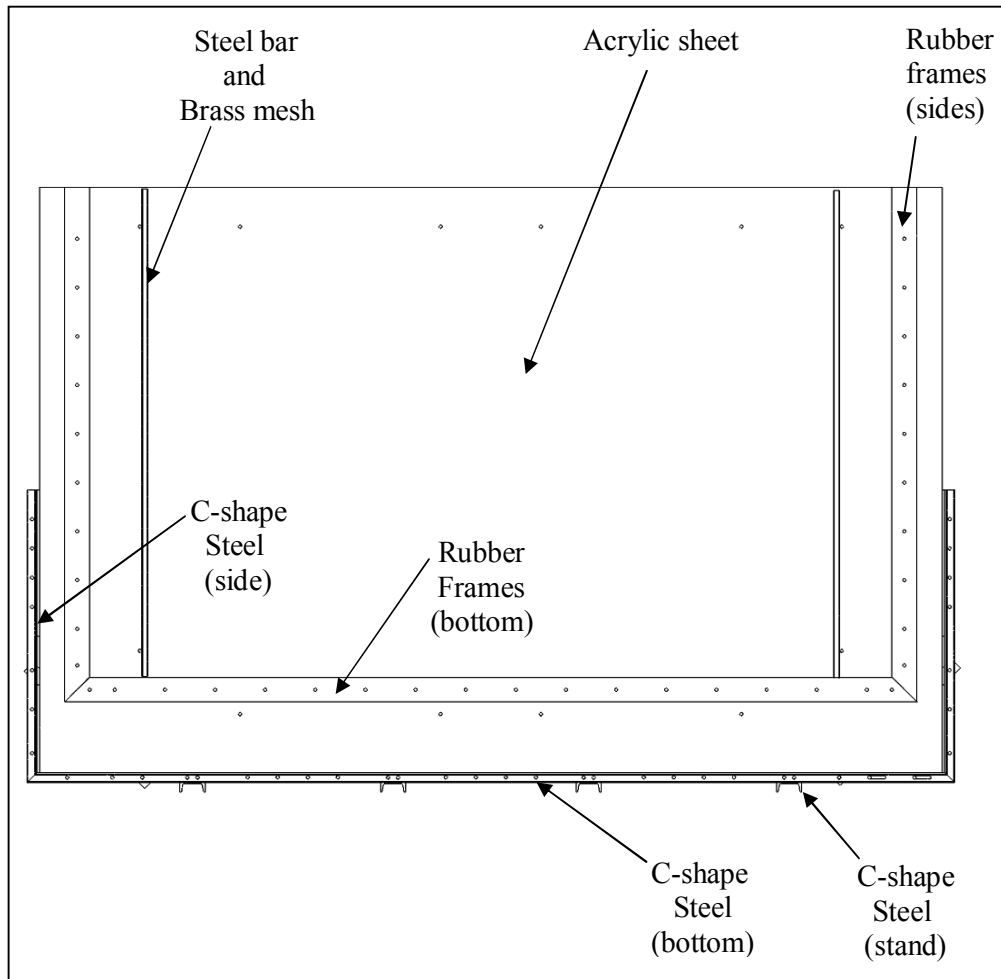
Figure 3.5 Front view of vertical cross section of the test frame.

Flat bars are placed at the corners

Acrylic sheet (back)

Acrylic sheet (front)

Water tube

Flat bars are placed at the footing

Flat bars are placed at the footing

C-shape Steel (stand)

Steel bar and Brass mesh

C-shape Steel (side)
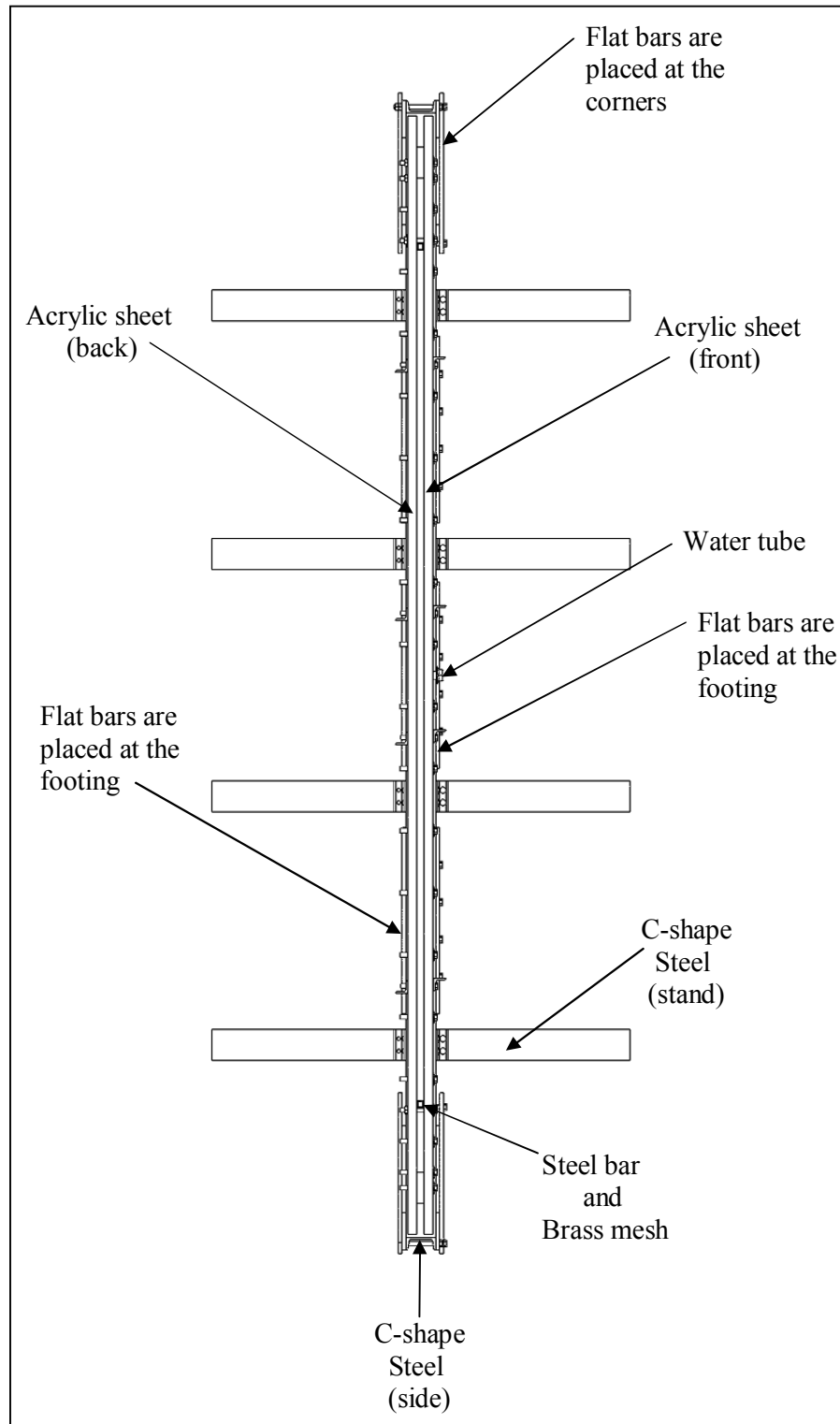
Figure 3.6 Top cross section of the test frame.
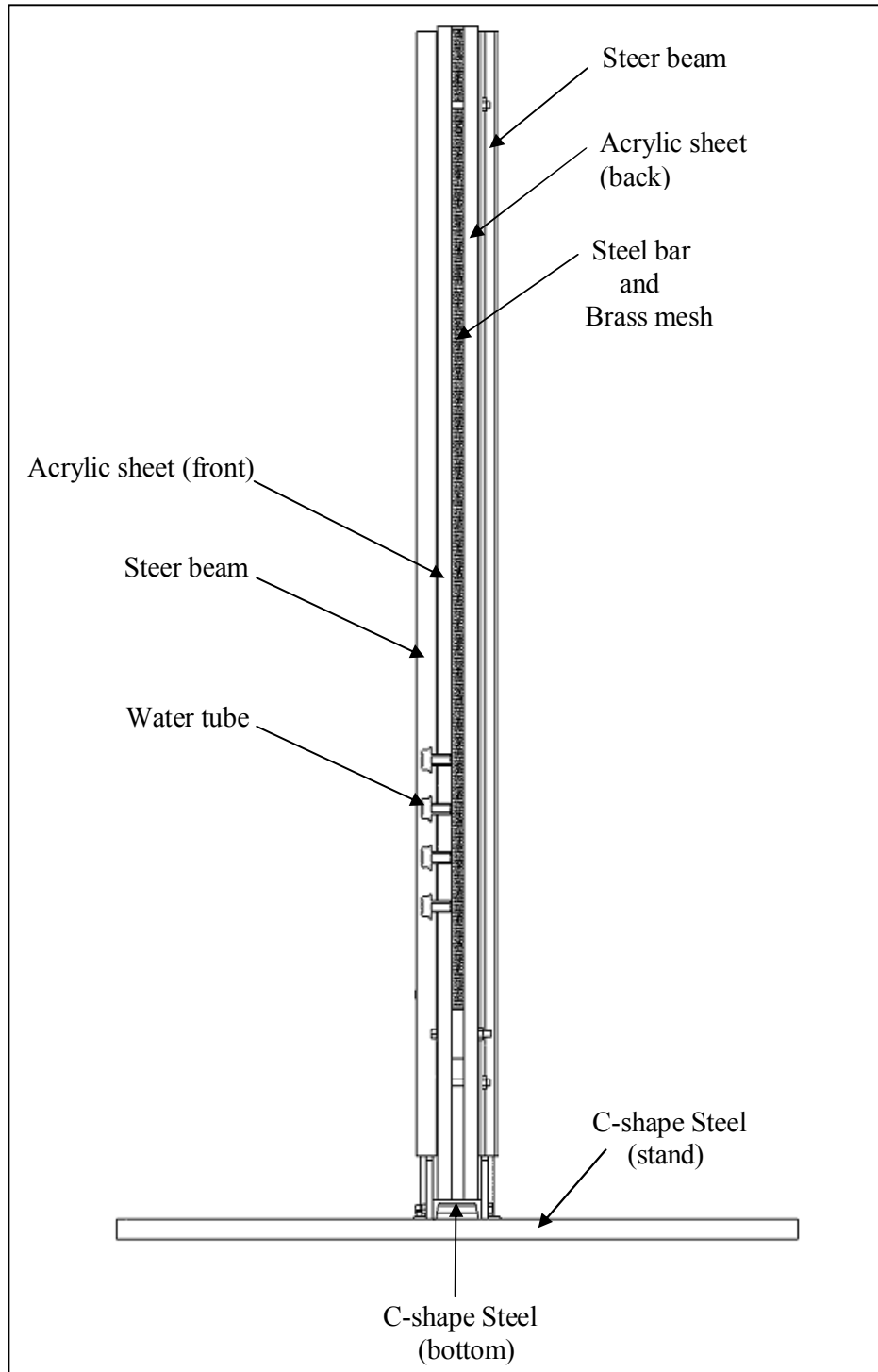
Figure 3.7 Side cross section of the test frame.
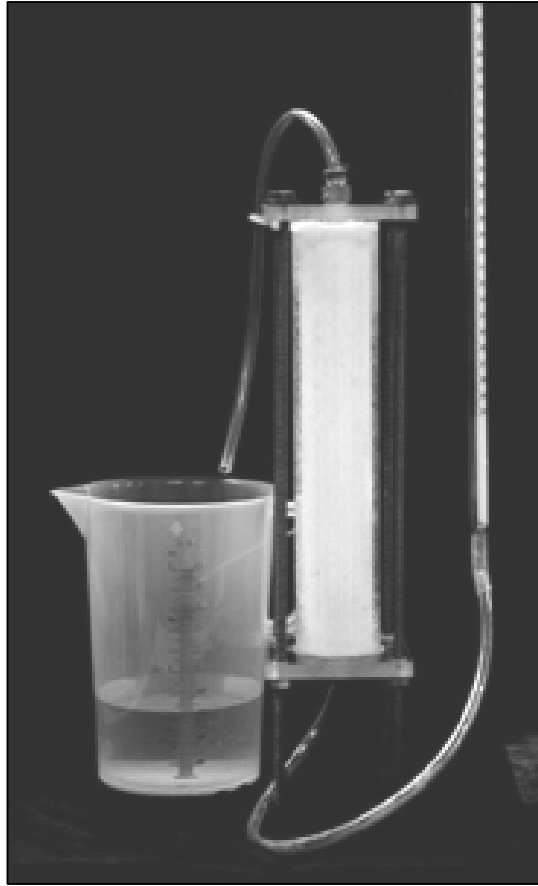
Figure 3.8 Flow of fine sand used in this study

CHAPTER IV

MODEL TESTING

4.1　Introduction

This chapter describes the test method and results of the physical model testing. The series of physical model are simulated under vertical and horizontal infiltration. The subsidence is measured under various conditions, as follows

- Groundwater level (h_w)

- Flowing rate and pressure of groundwater

- Groundwater flow direction use in salt solubility

- Withdrawal rate (pumping rate)

- Location of well pumps (h_p) and

- Overburden thickness (d_s).

4.2　Testing Method

Four series of physical model testing are performed to study the behavior of the solubility and subsidence. These four series are;

1) Testing the effect of the pumping well position. The fixed parameters are the flow direction of fresh water as vertical infiltration, the thickness of rock salt (ts) = 12.5, 11.0 and 10.5 cm, the thickness of overburden (ds) = 25 cm, the height of groundwater levels (hw) = 24 cm, and the pumping rate (Q) = 100 cubic centimeters per minute (cc/min) as shown in Figure 4.1 and Table 4.1.

2) Testing the effect of the overburden thickness. The fixed parameters are the direction of flowing fresh water. (Permeable from the top), thickness of rock salt (ts) = 11 cm, distance between the end of pumping tube to the salt surface (hp) = 2 cm and the rate of groundwater pumping (Q) = 100 cubic centimeters per minute, as shown in Figure 4.1 and Table 4.1.

3) Testing the effect of the groundwater level. The fixed parameters are; thickness of rock salt (ts) = 11 cm, distance between the end of pumping tube to the salt surface (hp) = 2 cm and thickness of overburden (ds) = 25 cm, as shown in Figure 4.1. and Table 4.1.

4) Testing the effect of the withdrawal rate. The fixed parameters are; the direction of inflow of fresh water from the top, thickness of rock salt (ts) = 11 cm, distance between the end of pumping tube to the salt surface (hp) = 2 cm and thickness of overburden (ds) = 11 cm, the height of groundwater levels (hw) = 10 cm, as shown in Figure 4.1, Figure 4.2 and Table 4.1

Purified salt is used to simulate the salt layer. The salt layer is pressed to get desired compaction and level. The dyed sand approximately 1-2 cm is put into the test frame to see the boundary of the salt layer. Saturated brine is poured into the test frame until the overburden is sunk. Left for 12 hours to settle the sand and salt layer under the natural water flow condition. The pumping well is installed at the desired high. Salt water is pumped out with defined rate while the water level is keeping constant by filling. The amount of subsidence at specified location is measured when every 2 liters of salt water is pumped out until 120-130 liters of salt water is obtained. In this way the amount of subsidence is monitored.
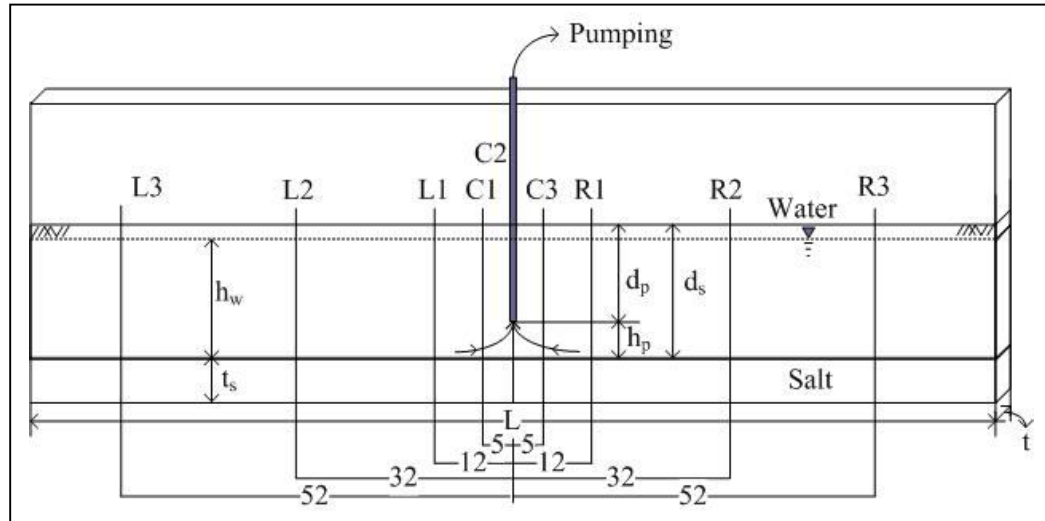
Figure 4.1   Positions and variations use in the subsidence measurement in vertical
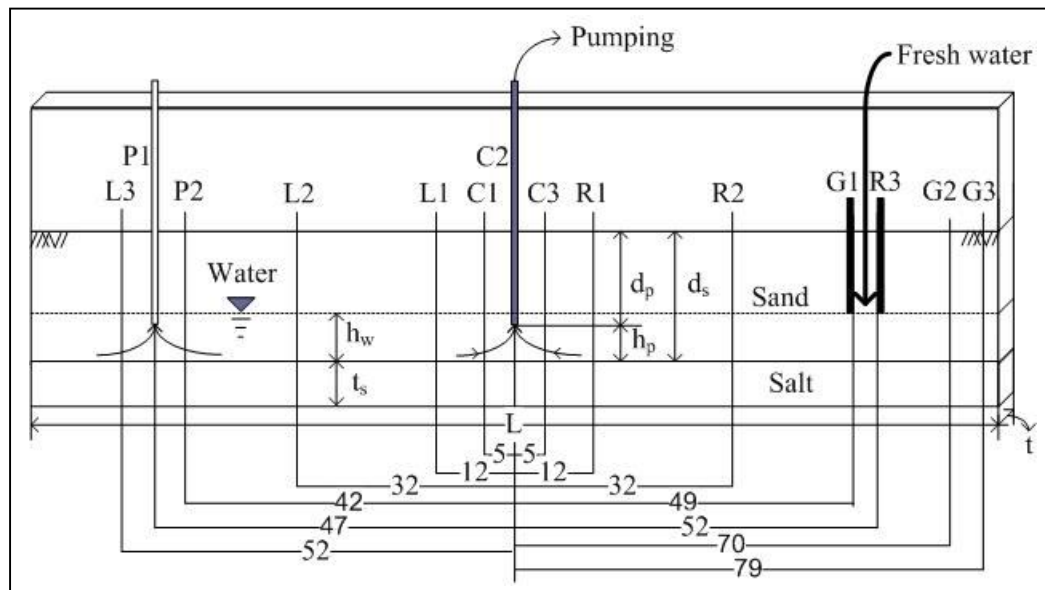
Figure 4.2   Positions and variations used in the subsidence measurement under

horizontal flow direction

Table 4.1 Variables in each test set

Testing series	Parameters variables						Flow
	Withdrawal	h_p (cm)	d_s (cm)	h_w (cm)	t_S (cm)	Pumping rate (cc/min)	
(Series 1). Depth of pumping	Periodic Pumping	0.56	11	10	12.5	100	Vertical infiltration
		2.5			10.5		
		3.5			9.5		
	Continuous Pumping	0.5	25	24	12.5		
		2			11		
		3.5			9.5		
(Series 2) Overburden Thickness	Continuous Pumping	2	11	10	11	100	
			25	24			
			50	54			
(Series 3). Groundwater Level	Continuous Pumping	2	25	6	11	100	Vertical infiltration
				12.5			
				18			
				6		100	Horizontal flow
				12.5			
				12.5	(new)		
				18	11		
				18	(new)		
				12.5	r_a (2")	100	
				12.5	r_a (6")		
(Series 4) Pumping rate.	Continuous Pumping	2	11	10	11	20	Vertical
						100	

Remarks: d_S = Overburden thickness, r_a = Size of recharge area

h_w = Water level highs,   new = new pumping well

h_p = Vertical Distance between pumping well and salt surface

4.3   Results of Simulation

Series of physical model testing have been performed under various conditions that have given different results of the surface subsidence. The subsidence measurements have been conducted in the different positions under the vertical infiltration direction (see

Figure 4.1) and the horizontal flow direction (see Figure 4.2). Figure 4.3 shows variables used to monitor the subsidence and Table 4.2 shown the results of simulation. Under the various conditions, the results are summarized as follows:

Table 4.2 Results of simulation

Test Parameters					Results			
Testing series	Withdrawal	h_S (cm)	(cm)	Flow	S_{max} (cm)	B (cm)	R_s (cm)	W (cm)
(Series 1). Depth of pumping	Periodic Pumping	0.56	d_S =11	Vertical infiltration	4.03	60	4.03	60
		2.5			3.17	70	3.17	70
		3.5			2.76	100	2.76	100
	Continuous Pumping	0.5	d_S =25		3.26	160	3.53	100
		2			2.07		2.83	
		3.5			2.34		2.49	
(Series 2) Overburden Thickness	Continuous Pumping	2	d_S = 11		2.34	100	2.34	100
			d_S = 25		0.44	160	2.59	100
			d_S = 50		0.44	160	7.5	160
(Series 3). Groundwater Level	Continuous Pumping	2	h_w = 6		0.65	160	2.53	160
			h_w = 12.5		1.94		2.56	
			h_w = 18		2.1		2.61	
			h_w = 6	Horizontal flow	2.86	70	3.41	70
			h_w = 12.5		2.86		3.61	
			(new)h_w =12.5		5.52	100	5.83	120
			h_w = 18		3.35	80	4.2	80
			(new)h_w = 18		5.57	120	6.02	120
			$r_a(2),h_w$ = 12.5		6.49	80	6.63	80
			$r_a(6),h_w$ = 12.5		3.12		4.24	
(Series 4) Pumping rate.	Continuous Pumping	2	d_S (11),Q=20	Vertical	0.35	160	1.18	160
			d_S (11),Q=100		2.34	100	2.34	100

Remarks: d_S = Overburden thickness, h_w = Water level highs, S_{max} = Maximum subsidence,

R_S = formation subsidence,   B = Extent of the surface subsidence

W = Extent of the formation subsidence

h_p = Vertical Distance between pumping well and salt surface
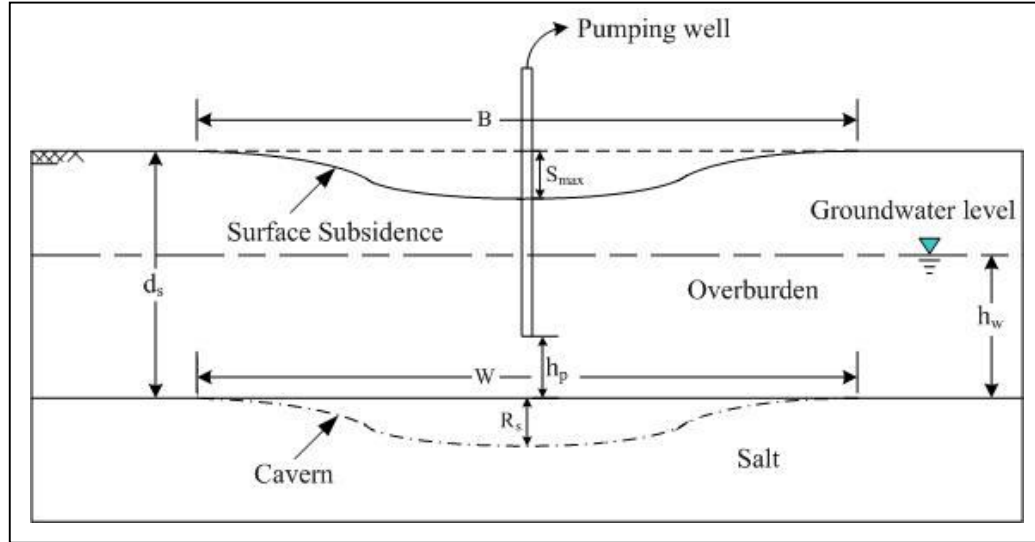
Figure 4.3 Variables used to monitor the subsidence

4.3.1 Results of The Effect of The Pumping Well Position (Depth of Pumping)

Two kinds of physical model testing (continuous pumping and periodic pumping) are carried out under vertical infiltration of fresh water conditions. The amount of subsidence and the concentration of salt are measured in continuous and periodic pumping cases. The subsidence is also measured continuously when every 2 liters of salt water is pumped out in continuous pumping.

4.3.1.1 Continuous Pumping

Three physical models (h_p = 0.5 cm and t_s = 12.5 cm, h_p = 2 cm and t_s = 11 cm, h_p = 3.5 and t_s = 9.5 cm) are simulated to understand the effect of the pumping well position under continuous pumping condition. When the pumping well is installed near to the salt layer (h_p = 0.5 cm), the subsidence occurs around the pumping area (Figure 4.4a). When the pumping well position is far from the salt layer (h_p = 2 cm), the behavior of subsidence is similar but the area of subsidence becomes

larger (Figure 4.4b). When the pumping well is moved to further distance from salt layer (hp = 3.5 cm), the subsidence around the pumping area is very small (Figure 4.4c). The subsidence and salinity are measurement as a function of time (Figures A-1 though A-3 in Appendix A). The subsidence extent does not the pumping well position.

4.3.1.2 Periodic Pumping

Three physical models (h_p = 0.5 cm and t_s = 12.5 cm, h_p = 2 cm and t_s = 11 cm, h_p = 3.5 and t_s = 9.5 cm) are simulated to understand the effect of the pumping well position under periodic pumping condition. When the pumping well is installed near to the salt layer (hp = 0.5 cm), the subsidence occurs around the pumping area in a large (Figure 4.5a). When the pumping well position is far from the salt layer (h_p = 2 cm), the behavior are area of becomes small (Figure 4.5b). When the pumping well is moved to further distance from salt layer (hp = 3.5 cm), the subsidence around the pumping area was very small (Figure 4.5c). The subsidence and salinity are measurement as a function of time (Figures A-4 though A-6 in Appendix A).

From the observation the subsidence occurred and the salinity is significantly increased when the pumping is off and the extent of subsidence is more than in the continuous pumping test. The actual figure of these can be seen in Table 4.3 and Table 4.4
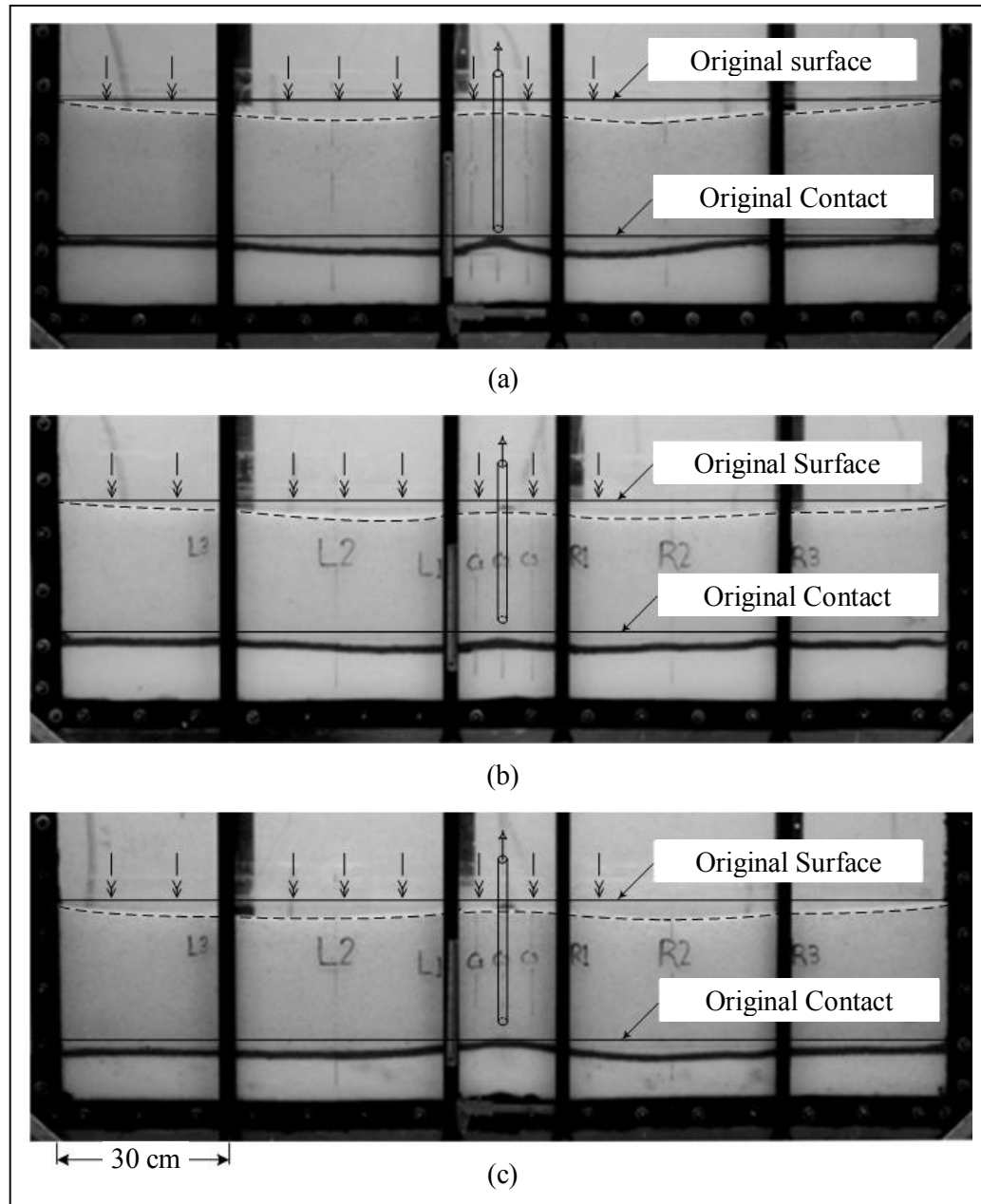
Figure 4.4 Photos of the salt solubility as affected by the depth of pumping for

continuous pumping at overburden thickness = 25 cm,

withdrawal rate = 100 cc/min., well depth = (a)

0.5 cm, (b) 2 cm and (c) 3.5 cm

(a)

(b)

← 30 cm →

(c)
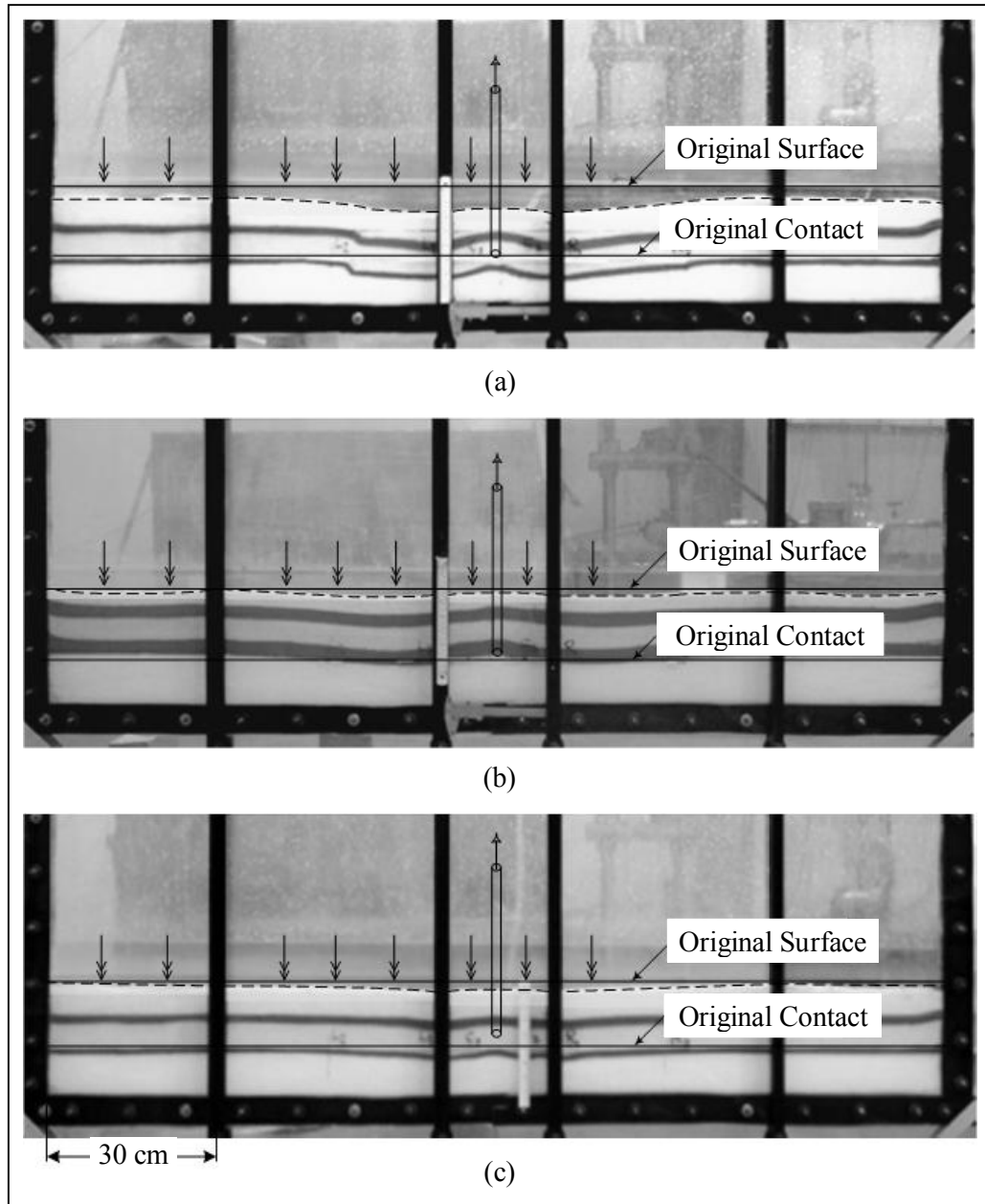
Figure 4.5 Photos of the salt solubility as affected by the depth of pumping for

continuous pumping at overburden thickness = 11 cm, withdrawal rate

= 100 cc/min., well depth = (a) 0.5 cm, (b) 2 cm and (c) 3.5 cm.
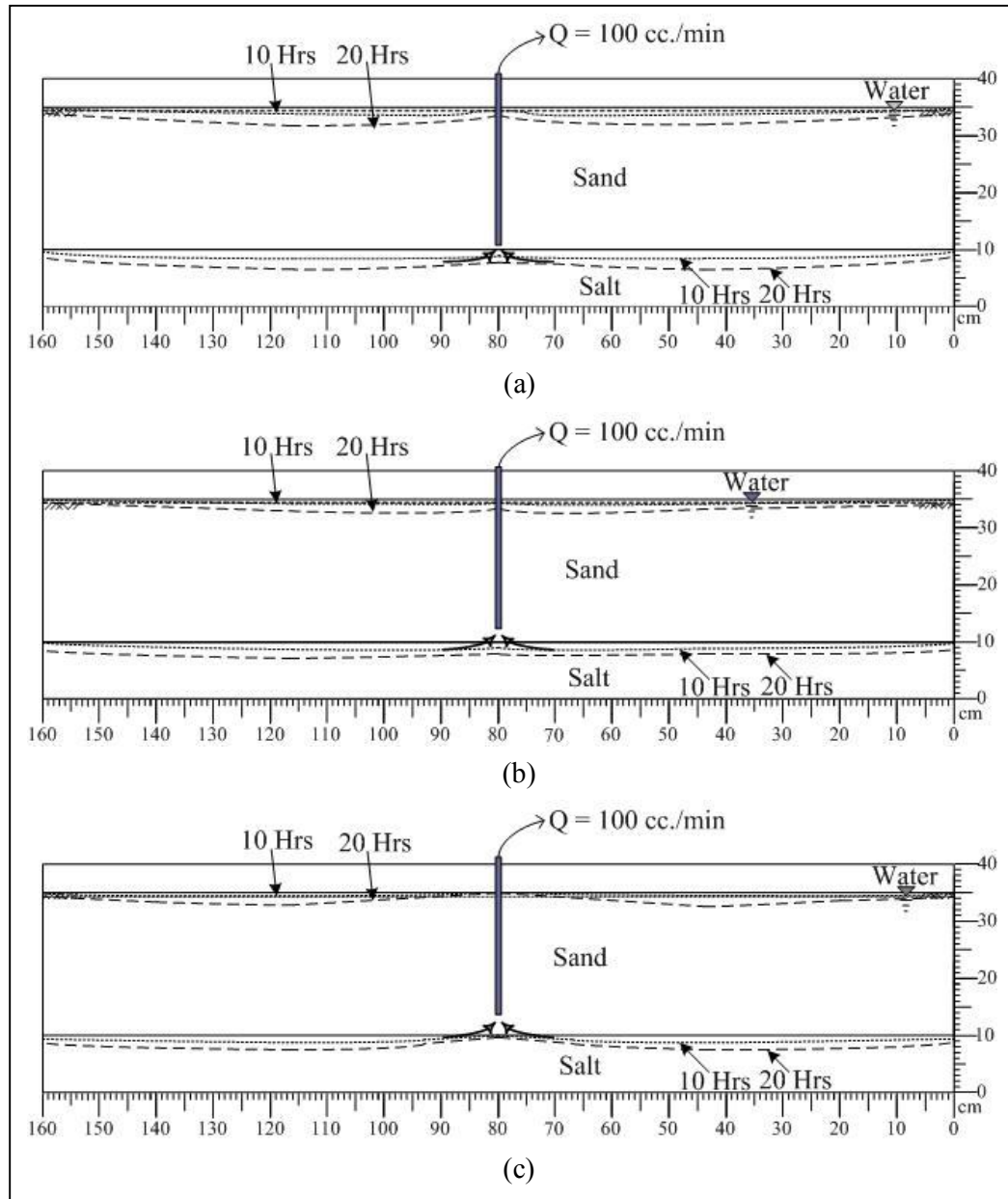
Figure 4.6 Salt solubility from as the affected by continuous pumping

at overburden thickness = 25 cm, withdrawal rate = 100

cc/min, well depth = (a) 0.5 cm, (b) 2 cm and (c) 3.5 cm.
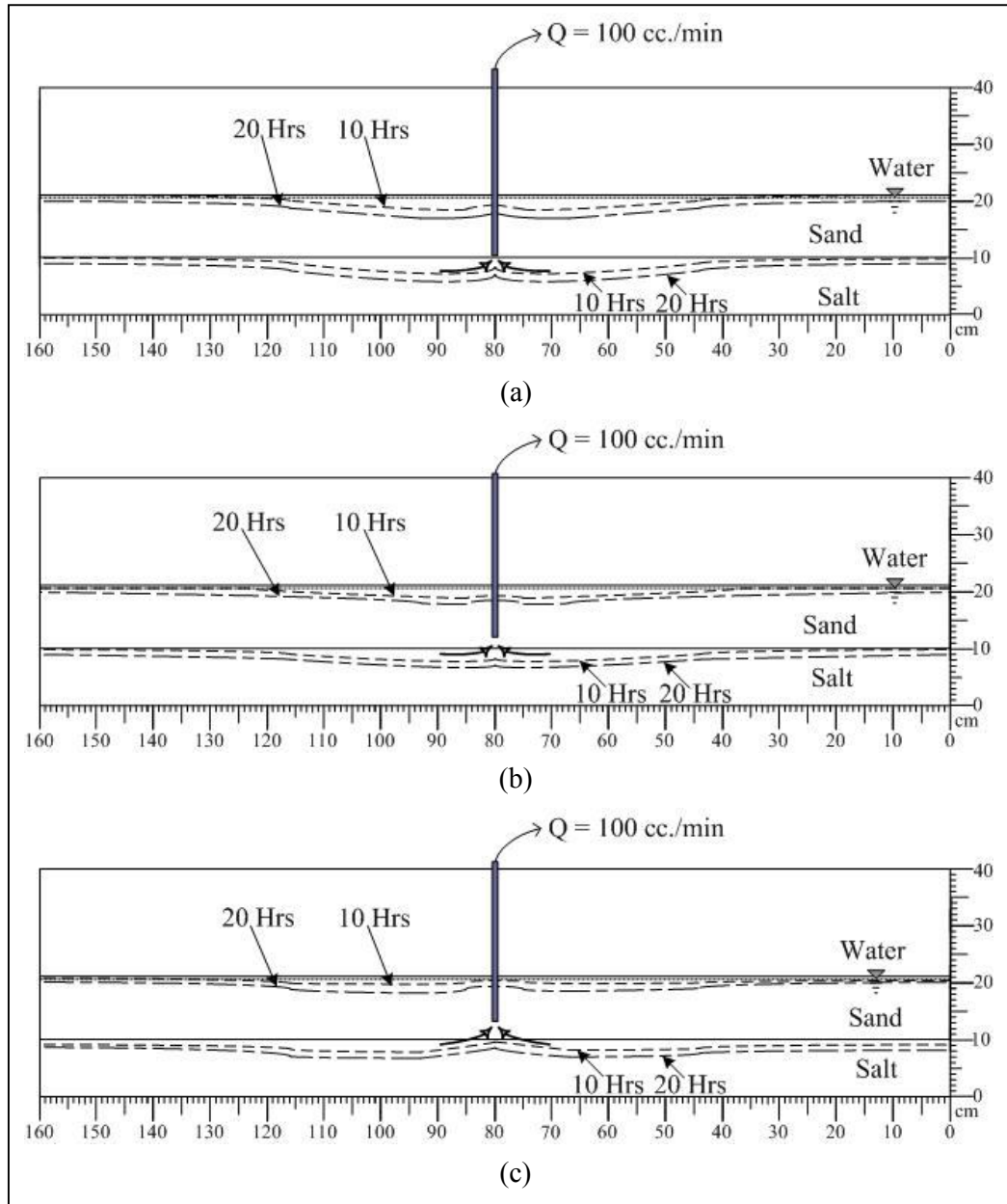
Figure 4.7 Salt solubility from as the affected by continuous pumping at overburden

thickness = 11 cm, withdrawal rate = 100 cc/min, well

depth = (a) 0.5 cm, (b) 2 cm and (c) 3.5 cm

Table 4.3 Results of the subsidence measurements under various position and time with the continuous pumping.

Height (cm.)	Time (hrs)	Subsidence (mm.)	R3	R2	R1	C3	C2	C1	L1	L2	L3
		Testing the effects of depth of pumping in vertical infiltration of fresh water									
0.5	10	surface	8.62	11.93	14.88	9.16	0	9.12	14.29	13	8.78
		formation	10.35	15.54	14.51	10.12	10.03	10.66	13.01	15.75	10.28
	20	surface	23.23	30.23	36.48	28.59	11.22	23.45	37.45	32.58	23.07
		formation	25.4	35.3	26.02	22.67	23.7	23.66	28.48	34.35	24.5
2	10	surface	5.95	8.39	10.25	8.81	4.78	8.64	8.44	7.8	4.51
		formation	8.89	11.85	11.84	12.01	9.79	11.87	13.07	13.58	8.20
	20	surface	17.14	20.64	25.56	20.47	13.67	20.61	23.86	20.85	13.71
		formation	21.27	27.33	22.48	22.3	21.3	22.65	24.34	29.32	17.84
3.5	10	surface	5.82	8.53	4.86	1.14	3.8	0.94	3.62	3.89	5.17
		formation	12.01	15.8	7.86	2.68	0	0.96	6.69	4.34	9.2
	20	surface	18.49	27.97	15.49	13.26	12.59	11.9	14.02	24.9	17.24
		formation	20.91	27.37	16.6	6.96	3.43	6.4	11.58	22.6	17.85

Table 4.4 Results of the subsidence measurements under various positions and time with the periodic pumping

Height (cm.)	Time (hrs)	Subsidence (mm.)	R3	R2	R1	C3	C2	C1	L1	L2	L3
Testing the effects of depth of pumping in vertical infiltration of fresh water											
0.5	10	surface	-	16	24.12	24.97	9.15	24.97	24.12	16	-
		formation	-	16	24.12	24.97	9.15	24.97	24.12	16	-
	20	surface	-	28.24	40.29	40.03	22.32	40.03	40.29	28.24	-
		formation	-	28.24	40.29	40.03	22.32	40.03	40.29	28.24	-
2	10	surface	-	17.23	21.37	18.33	9.48	18.33	21.37	17.23	-
		formation		17.23	21.37	18.33	9.48	18.33	21.37	17.23	-
	20	surface	-	24.95	31.73	29.84	18.72	29.84	31.73	24.95	-
		formation	-	24.95	31.73	29.84	18.72	29.84	31.73	24.95	-
3.5	10	surface	1.54	6.77	16.26	1.85	2.66	11.85	16.26	6.77	1.54
		formation	1.54	6.77	16.26	1.85	2.66	11.85	16.26	6.77	1.54
	20	surface	10.22	19.3	27.61	21.17	11.55	21.17	27.61	19.3	10.22
		formation	10.22	19.3	27.61	21.17	11.55	21.17	27.61	19.3	10.22
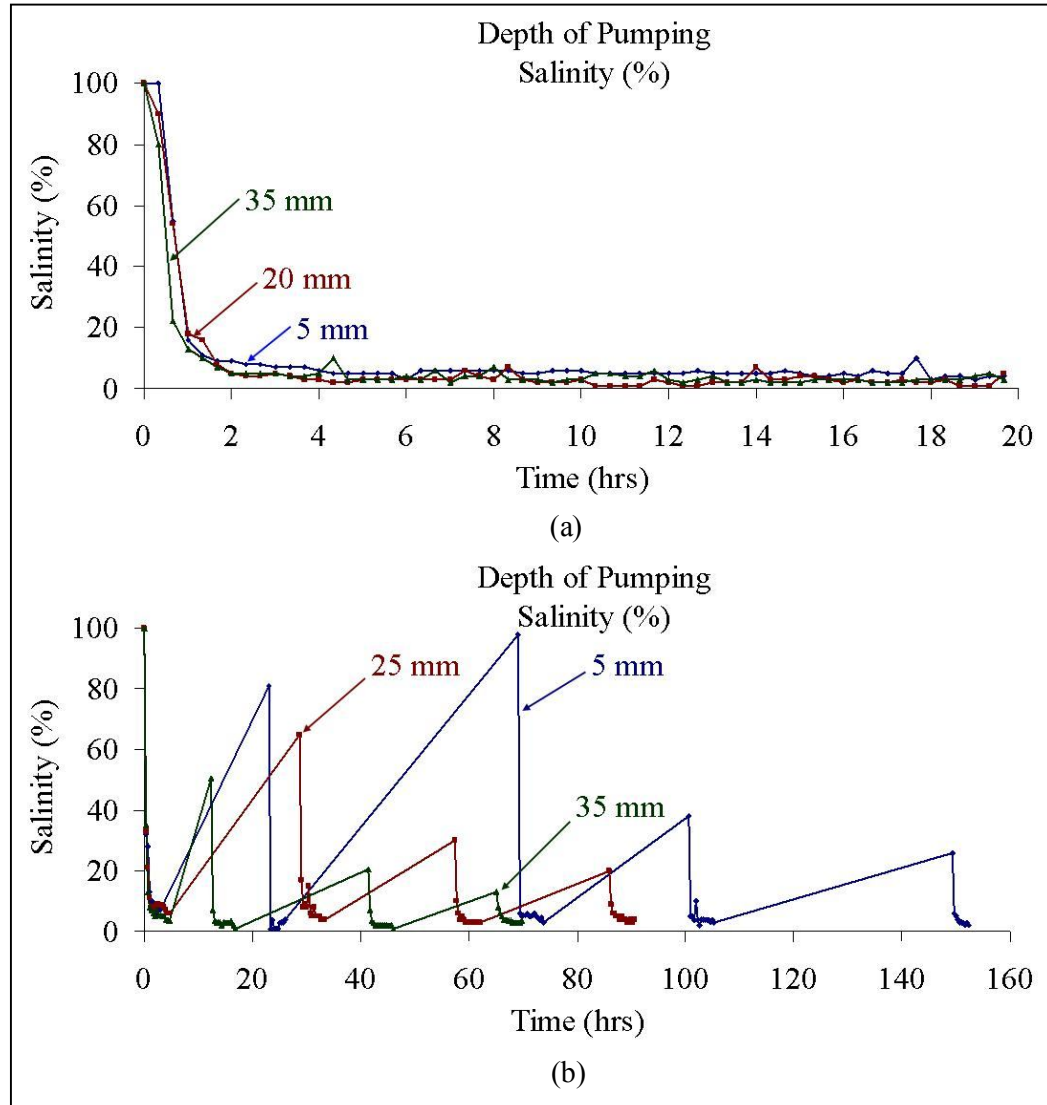
Figure 4.8 Salinity of the pumped brine measured through the test duration and the

depth of pumping of (a) the salinity of continuous pumping (b)

the salinity of periodic pumping

4.3.2 Result of The Effect of The Overburden Thickness

This physical model testing is carried out under continuous pumping and

vertical infiltration of fresh water condition. Three physical models (d_s = 11 cm, 25 cm

and 50 cm) are simulated to understand the effect of the overburden thickness. The surface and formation subsidence obtains from different overburden thickness. When the thickness is small (d_s = 11 cm), the subsidence occurs around the pumping area (Figure 4.9a). When the overburden thickness is increased (d_s = 25 cm), the behavior of subsidence is small but the area of subsidence becomes large (Figure 4.9b).When the overburden thickness is increased to some (d_s = 50 cm), the subsidence is very small (Figure 4.9c). Therefore, the results show that the thicker the overburden can give the lower the magnitudes of the surface and formation subsidence (Table 4.5). The overburden thickness also influences the salinity as the thicker overburden can give the lower percentage of the salinity (Figures 4.11). The subsidence and salinity are measurement as a function of time (Figures A-7 though A-9 in Appendix A).

4.3.3   Result of The Effect of The Groundwater Level

Two types of fresh water flow directions (vertical and horizontal infiltration) testing are conducted under continuous pumping.

4.3.3.1   Vertical Infiltration

Three physical models (h_w = 6 cm, 12.5 cm and 18 cm) are simulated to understand the effect of the groundwater level. For vertical infiltration, Table 4.2 shows the formation subsidence increases from 2.53 cm for groundwater level of 6 cm to 2.61 cm for groundwater level of 18 cm. The subsidence extent tends to be the same for these cases (Figures, 4.12 and 4.14). The subsidence and salinity are measurement as a function of time (Figures A-10 though A-12 in Appendix A).

(a)

(b)

30 cm

(c)
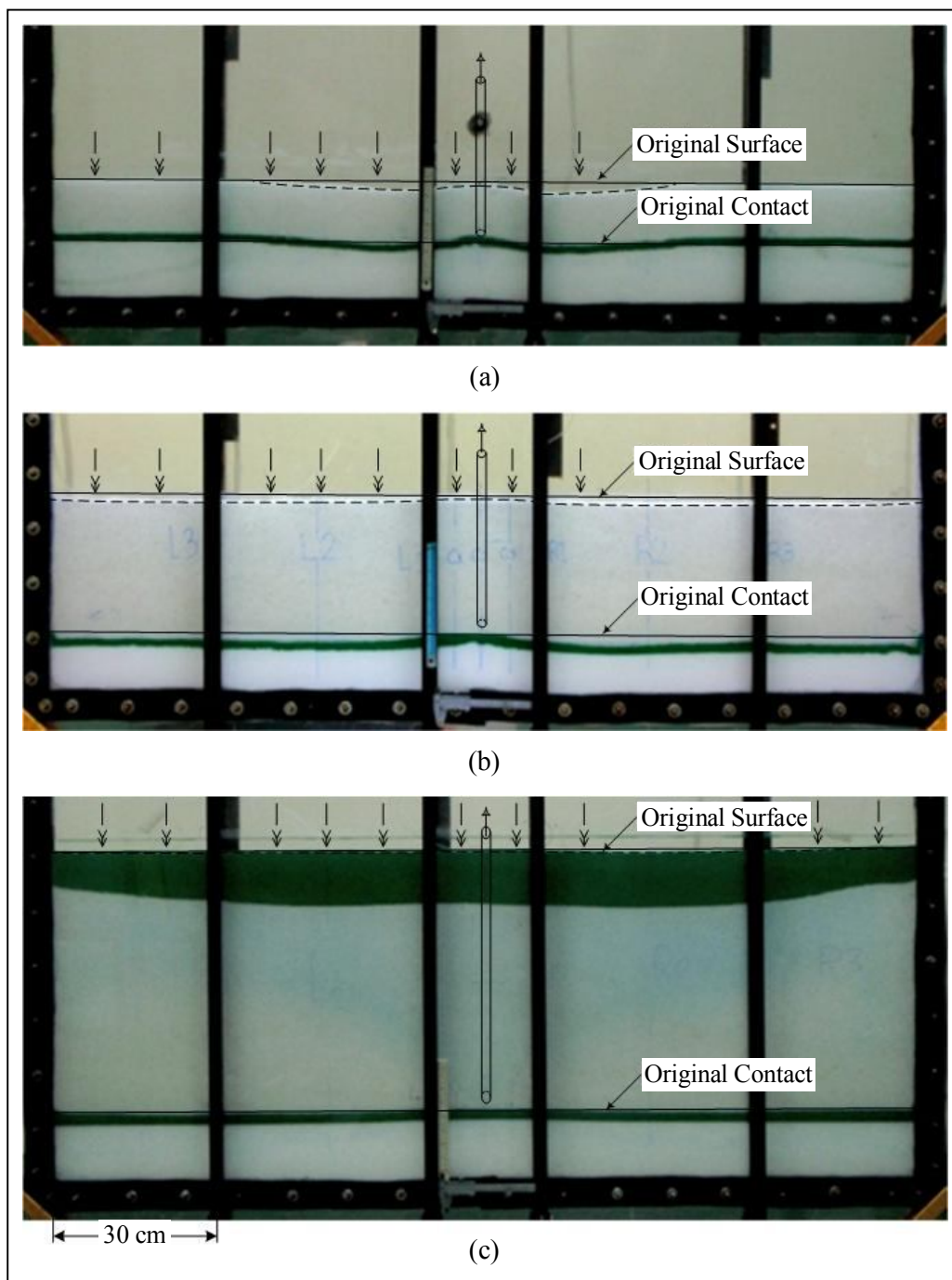
Figure 4.9 Photos of is salt solubility testing for various overburden thickness at well

depth = 2 cm, withdrawal rate = 100 cc/min and overburden

thickness = (a) 11 cm, (b) 25cm and (c) 50 cm.
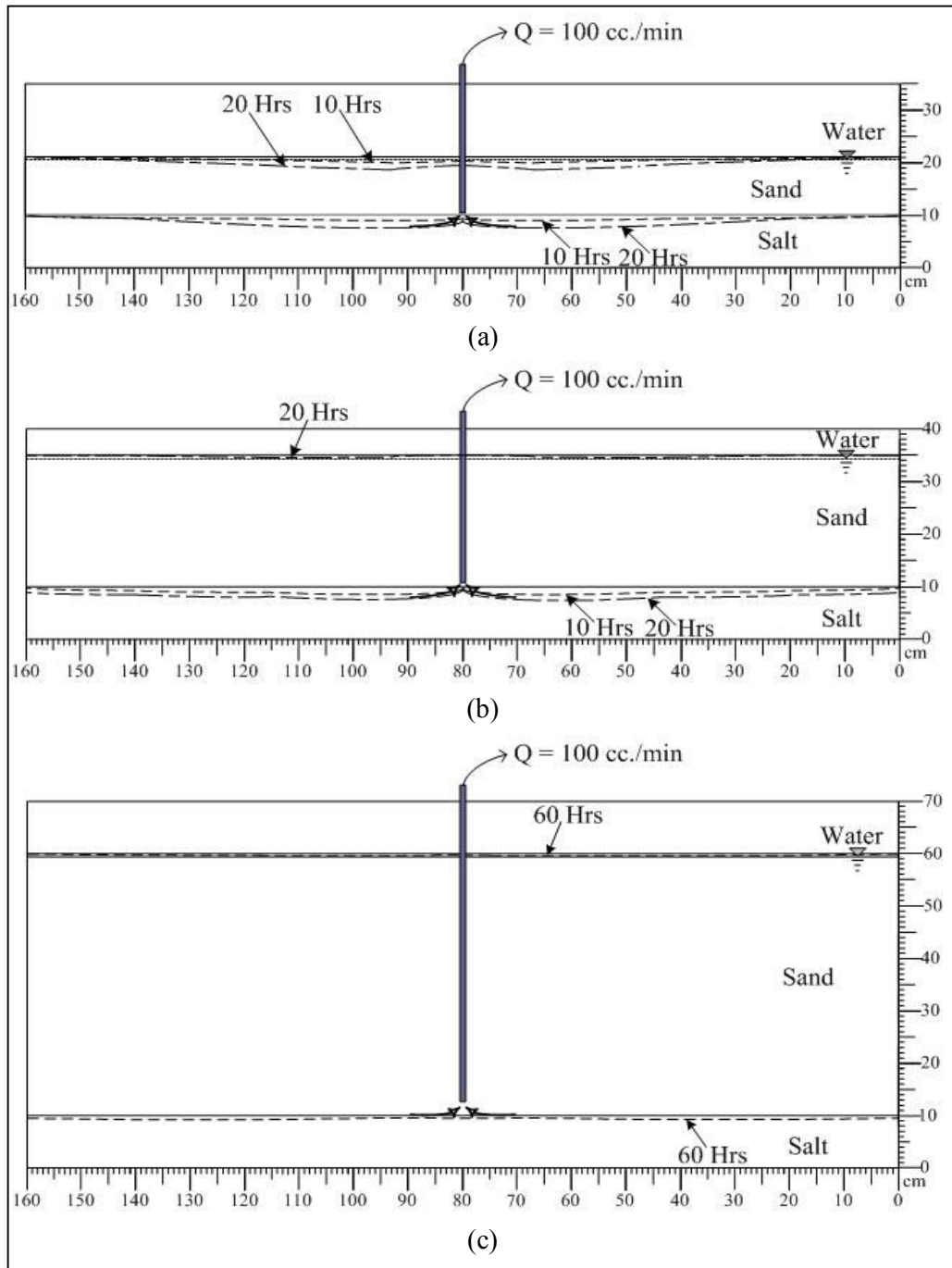
Figure 4.10 Salt solubility testing from as the affected by overburden thickness at well

depth = 2 cm, withdrawal rate = 100 cc/min and overburden

thickness = (a) 11 cm, (b) 25cm and (c) 50 cm

Table 4.5 Results of the subsidence measurements under various positions, time and the overburden thickness

Testing the effects of depth of pumping in vertical infiltration of fresh water												
Height (cm.)	Time (hrs)	Subsidence (mm.)	R3	R2	R1	C3	C2	C1	L1	L2	L3
11	10	surface	1.94	1.3	2.04	3.27	1.72	6.24	6.73	1.53	1.45
		formation	2.4	4.05	1.39	2.45	2.36	6.91	7.28	3.81	0.13
	20	surface	6.1	12.34	25.62	14.73	18.08	15.83	21.21	14.69	8.04
		formation	5.89	17.48	24.87	10.1	17.56	17.55	21.96	17.94	6.27
25	10	surface	0	0	0	0	0	0	0	0	0
		formation	4.13	5.9	11.94	1.49	9.23	8.08	9.97	5.98	2.65
	20	surface	0	4.33	2.77	0	0	0	3.39	4.54	0.28
		formation	10.92	21.97	28.04	3.98	20.67	13.63	23.79	14.29	19.76
50	10	surface	1.08	1.58	0.69	1.96	1.88	1.04	2.36	0.86	0.7
		formation	1.58	2.66	2.06	1.64	1.48	1.36	1.74	1.78	2.36
	20	surface	4.65	4.9	3.4	3.7	4.4	3.5	4.8	4	3.55
		formation	7.3	7.4	4.65	4.9	3.65	5	4.4	7.6	7.7
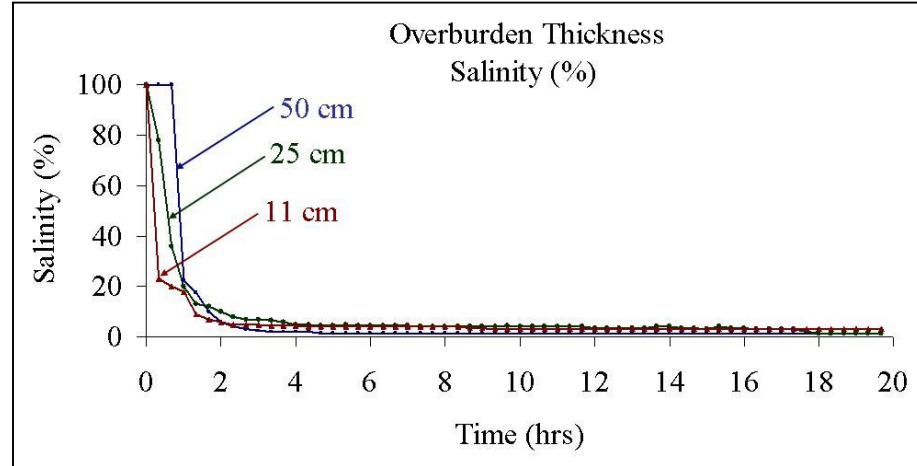
Figure 4.11 The salinity of the pumped water as a function of time

for various overburden thickness

4.3.3.2   Horizontal Infiltration

Seven physical models (h_w = 6 cm, 12.5 cm, new12.5 cm, 18 cm, new 18 cm, r_a = 2 and h_w = 12.5 cm, r_a = 6 and h_w = 12.5 cm) are simulated to understand the effect of the groundwater level and the recharge area. For horizontal infiltration, table 4.2 shows the formation subsidence (r_s) increases from 3.41 cm for groundwater level of 6 cm to 4.2 cm for groundwater level of 18 cm. This result means the horizontal flow direction has more influence on the subsidence than the vertical infiltration under the same groundwater level. The extent of the formation subsidence rises from 70 cm to 120 cm and from 80 cm to 120 cm when having a new well for groundwater level 12.5 cm and 18 cm respectively (Figures 4.13b though 4.13e). The subsidence and salinity are measurement as a function of time (Figures A-13 though A-17 in Appendix A) In addition, the formation subsidence decreases from 6.63 cm for 2 inch recharge area to 4.24 cm for 6 inch recharge area at

ground water level of 12.5 cm (Figure 4.18). The subsidence and salinity are measurement as a function of time (Figures A-18 though A-19 in Appendix A).

4.3.4 Result of The Effect of The withdrawal Rate

This physical model testing is carried out under continuous pumping and vertical infiltration of fresh water conditions. Table 4.2 shows the formation subsidence increases from 1.18 cm for the pumping rate of 20 cc/min to 2.34 cm for pumping rate of 100 cc/min (Figure 4.21). The extent of the formation subsidence decreases from 160 cm to 100 cm for the pumping rate 20 cc/min. and 100 cc/min. respectively. It means that when the pumping rate is low (Q = 20 cc/min), the extent of subsidence extent occurs around the pumping area is large (Figure 4.20a). When the pumping rate is high (Q = 100 cc/min), the extent of subsidence becomes small (Figure 4.20b). The subsidence and salinity are measurement as a function of time (Figure A-20 in Appendix A).

.
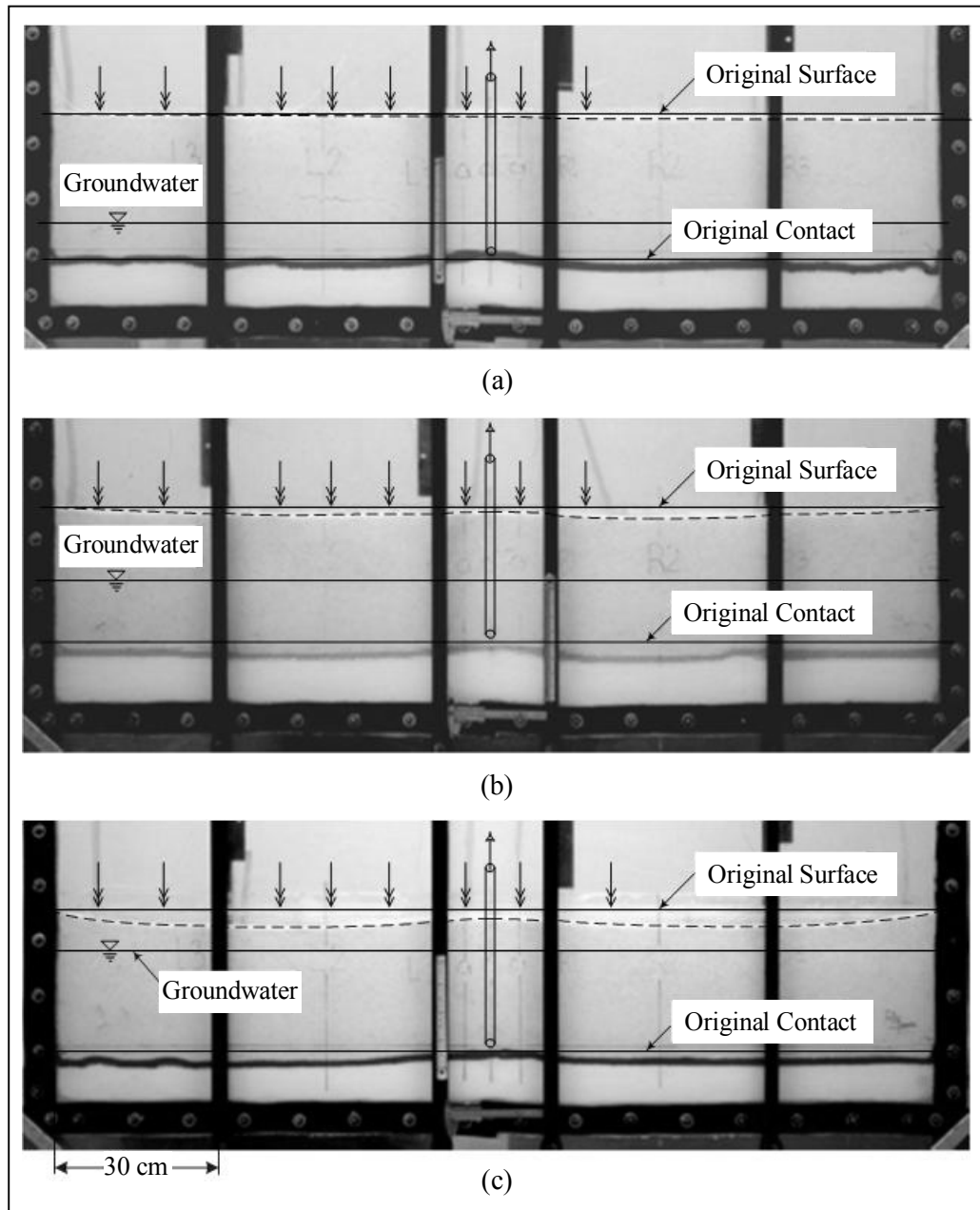
Figure 4.12 Salt solubility testing as the affected by various groundwater levels with

continuous pumping in vertical infiltration direction at overburden

thickness = 25 cm, withdrawal rate = 100 cc/min, groundwater

level = (a) 6 cm, (b)12.5cm and (c) 18 cm.
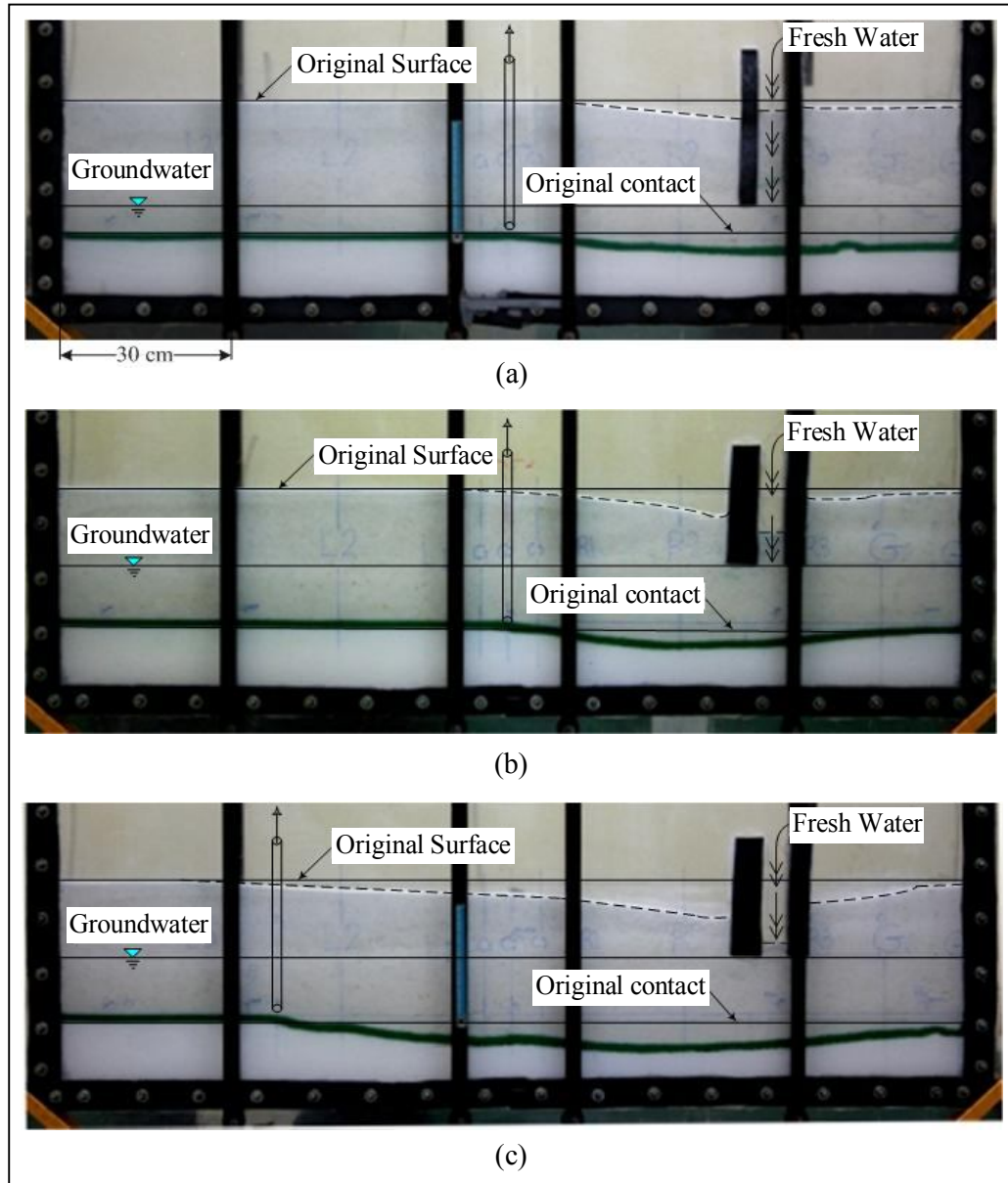
Figure 4.13 Salt solubility testing as the affected by various groundwater levels with

continuous pumping in horizontal flow direction at overburden

thickness = 25 cm, withdrawal rate = 100 cc/min, groundwater

level = (a) 6 cm, (b) 12.5 cm, (c) 12.5 cm in the new well

(d) 18 cm and (e) 18 cm with a new well
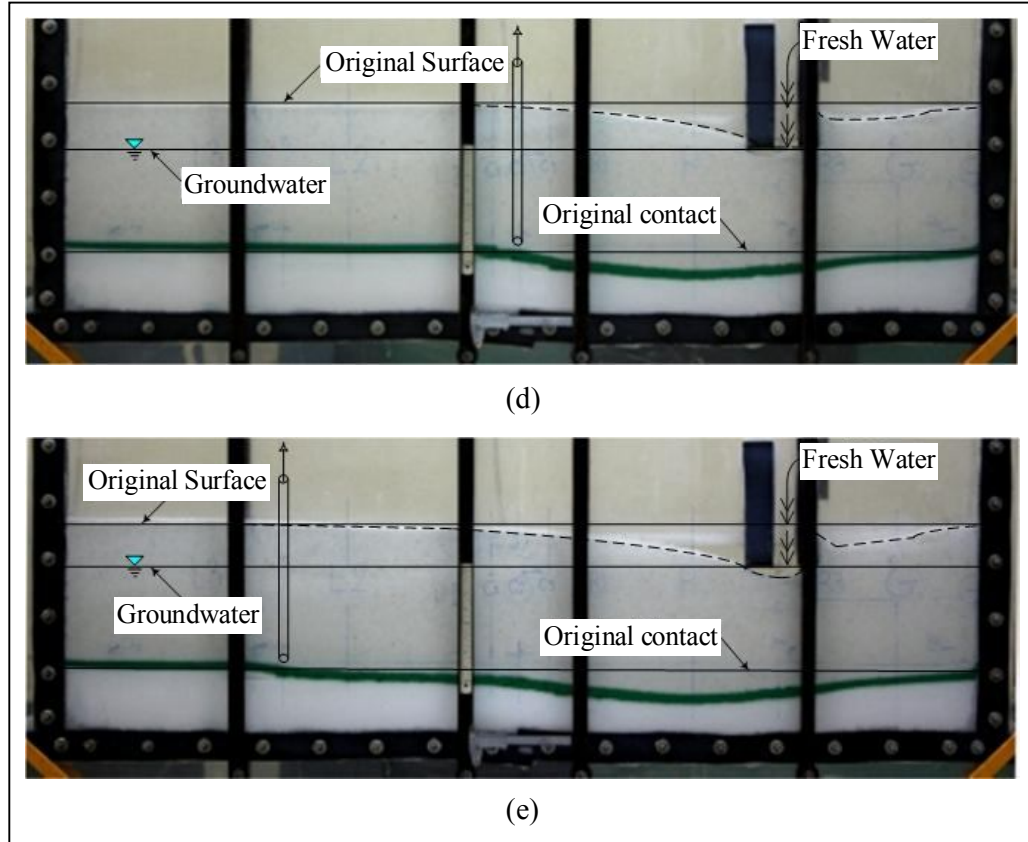
Figure 4.13 Salt solubility testing as the affected by various groundwater levels with

continuous pumping in horizontal flow direction at overburden

thickness = 25 cm, withdrawal rate = 100 cc/min, groundwater

level = (a) 6 cm, (b) 12.5 cm, (c) 12.5 cm in the new well

(d) 18 cm and (e) 18 cm with a new well (Continue).
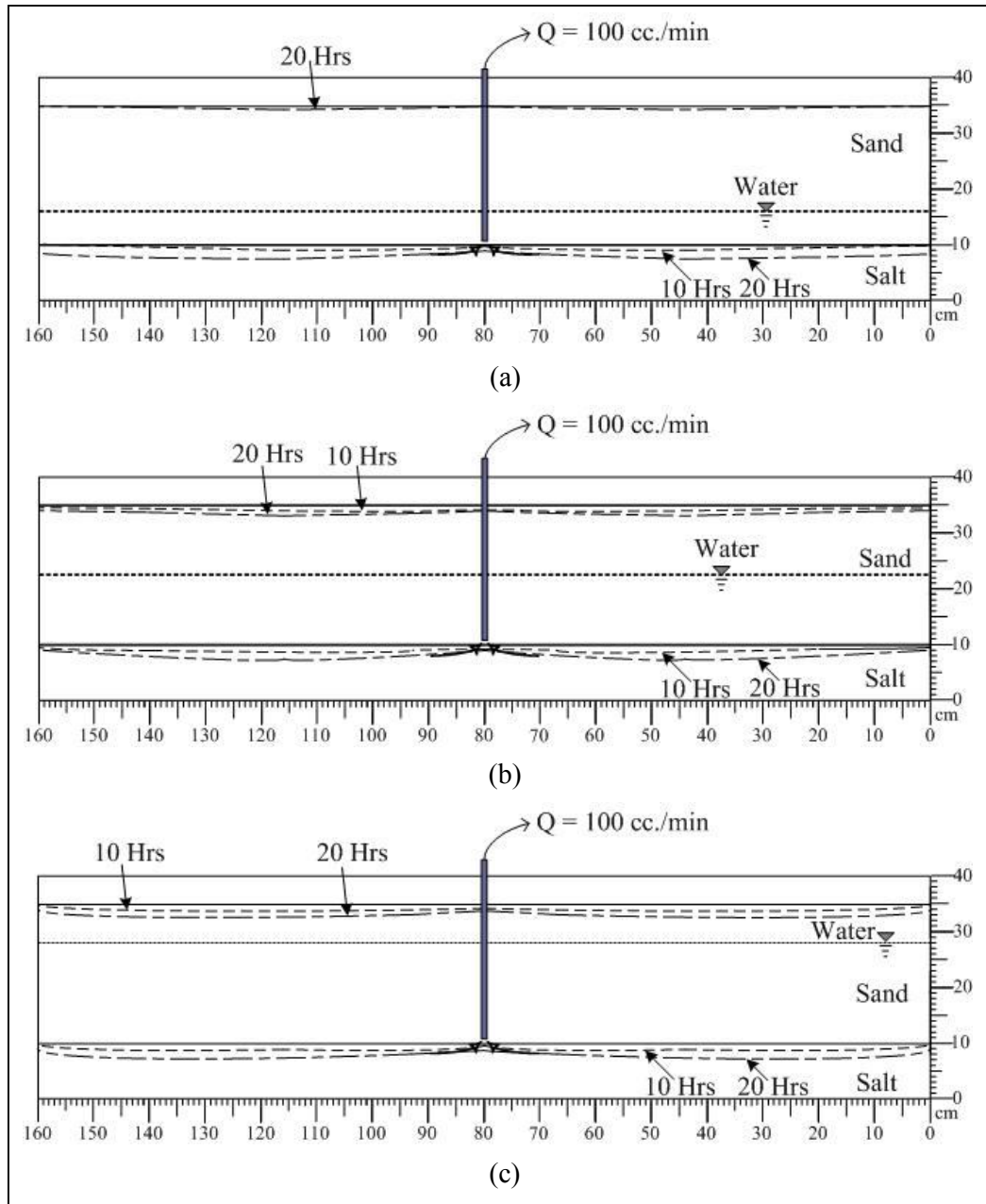
Figure 4.14 Salt solubility as the affected by groundwater levels with continuous

pumping in vertical infiltration direction at overburden thickness

= 25 cm, withdrawal rate = 100 cc/min, groundwater level

= (a) 6 cm, (b)12.5cm and (c) 18 cm
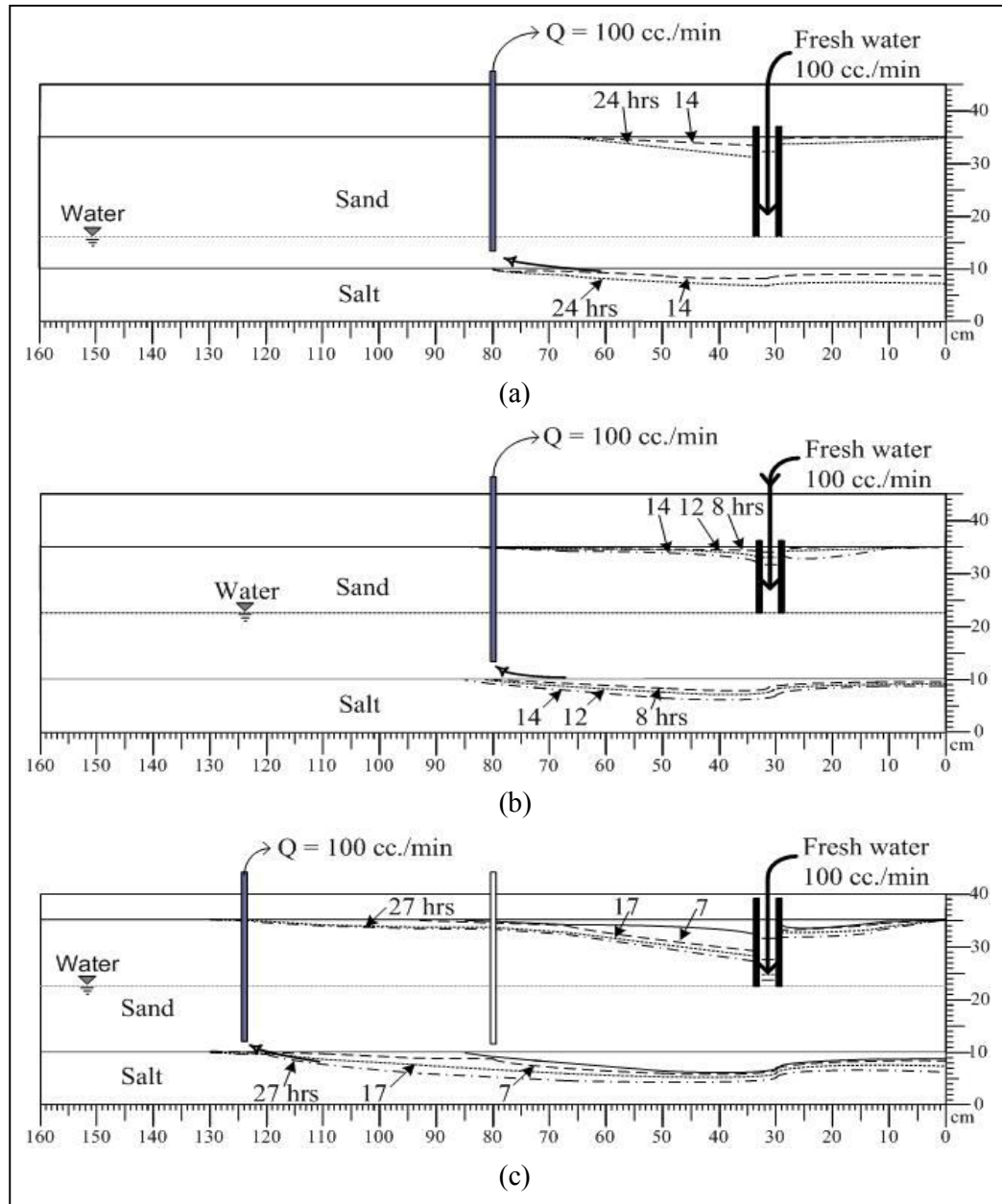
Figure 4.15 Salt solubility testing as the affected by various groundwater levels with continuous pumping in horizontal flow direction at overburden thickness = 25 cm, withdrawal rate = 100 cc/min, groundwater level = (a) 6 cm, (b) 12.5 cm, (c) 12.5 cm in the new well (d) 18 cm and (e) 18 cm with a new well
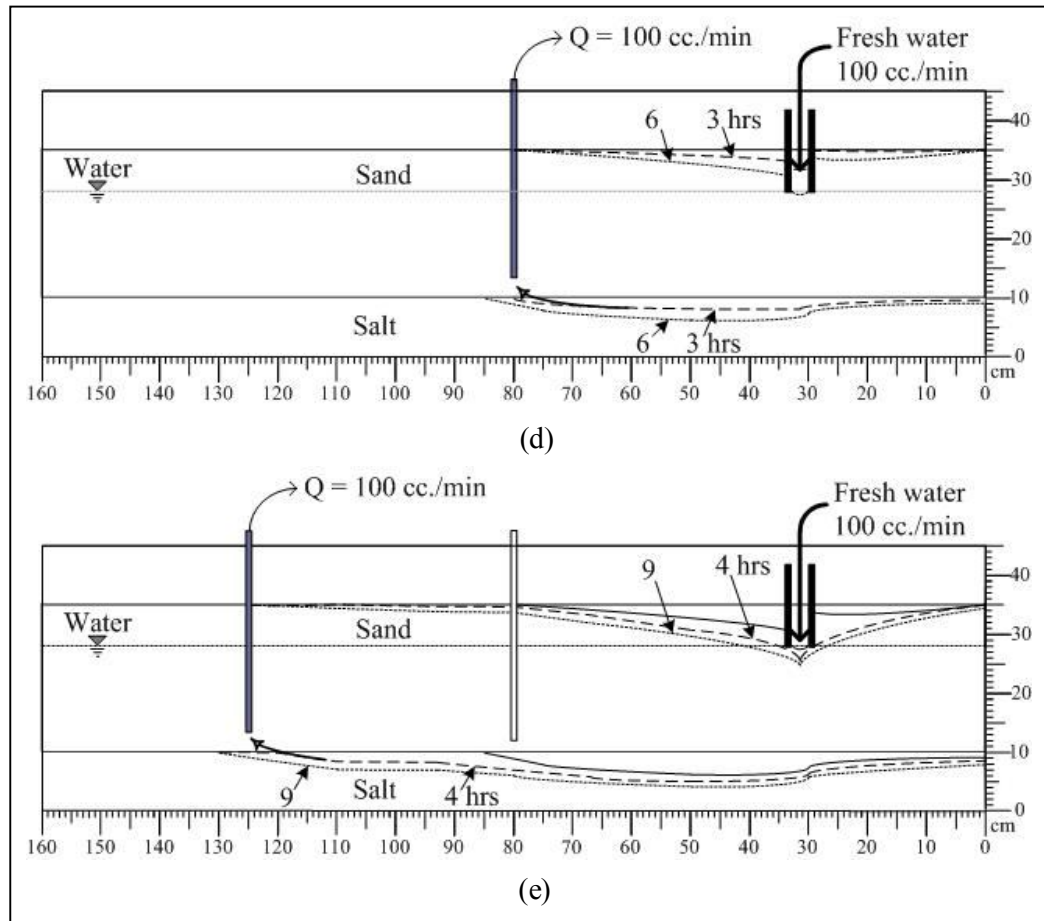
Figure 4.15 Salt solubility testing as the affected by various groundwater levels with

continuous pumping in horizontal flow direction at overburden

thickness = 25 cm, withdrawal rate = 100 cc/min, groundwater

level = (a) 6 cm, (b) 12.5 cm, (c) 12.5 cm in the new well

(d) 18 cm and (e) 18 cm with a new well (Continue).

Table 4.6 Results of the subsidence measurements under various positions, the time and the groundwater level

Height (cm.)	Time (hrs)	Subsidence (mm.)	R3	R2	R1	C3	C2	C1	L1	L2	L3
		Testing the effect of the groundwater level in vertical infiltration of fresh water									
6	10	surface	3.82	5.6	3.32	0.9	0	0.9	3.32	5.6	3.82
		formation	9.07	10.82	7.46	1.84	0	1.84	7.46	10.82	9.07
	20	surface	2.42	6.46	4.19	2.14	0	2.14	4.19	6.46	2.42
		formation	8.5	13.11	18.44	25.3	22.97	25.3	18.44	13.11	8.5
12.5	10	surface	7.48	10.44	11.8	9.77	8.92	9.77	11.8	10.44	7.48
		formation	8.01	11.99	10.68	7.52	8.55	7.52	10.68	11.99	8.01
	20	surface	13.21	19.37	15.02	12.5	10.22	12.5	15.02	19.37	13.21
		formation	20.5	25.63	17.69	11.81	10.83	11.81	17.69	25.63	20.5
18	10	surface	13.38	14.98	13.72	10.7	9.84	11.28	10.43	11.25	12.16
		formation	11.35	11.65	12.52	8.77	3.51	9.75	9.58	11.51	12.5
	20	surface	25.98	27.58	21.7	15.01	12.5	16.31	17.22	28.8	27.65
		formation	23.99	22.35	21.81	17.09	13.22	12.12	17.6	29.91	32.36

Table 4.7 Results of the subsidence measurements under various positions, the time and the groundwater level in horizontal flow

Height (cm.)	Time (hrs)	Subsidence (mm.)	G2	G1	R3	R2	R1	C3	C2	C1	L1	L2
		Testing the effect of the groundwater level in horizontal flow of fresh water										
6	20	surface	0	0	3.76	0	10.92	0	0	0	0	0
		formation	15.11	10.34	17.29	20.61	15.42	5.93	3.92	0.66	0	0
	40	surface	3.5	11.03	13.48	28.64	22.43	2.4	0.83	0	0	0
		formation	30.4	25.81	31.46	34.14	25.5	13.19	6.23	1.66	0	0
12.5	20	surface	0	0	2.61	13.37	15.41	5.38	2.53	1.32	0	0
		formation	0	13.02	23.62	94.32	45.59	19.32	9.85	8.84	6.73	1.85
	40	surface	0	3.77	9.82	69.72	28.59	8.26	3.96	2.51	0.37	0
		formation	11.23	13.56	28.5	34.46	36.11	22.47	10.7	9.41	1.89	0.29
18	20	surface	0	3.96	1.75	34.05	8.41	2.6	1.12	0	0	0
		formation	4.53	4.97	15.2	19.27	23.19	17.79	9.19	1.72	0	0
	40	surface	0	13.92	10.2	85.79	33.51	9.61	2.19	0	0	0
		formation	7.34	13.41	29.77	36.44	42.03	31.77	22.16	6.14	1.49	0
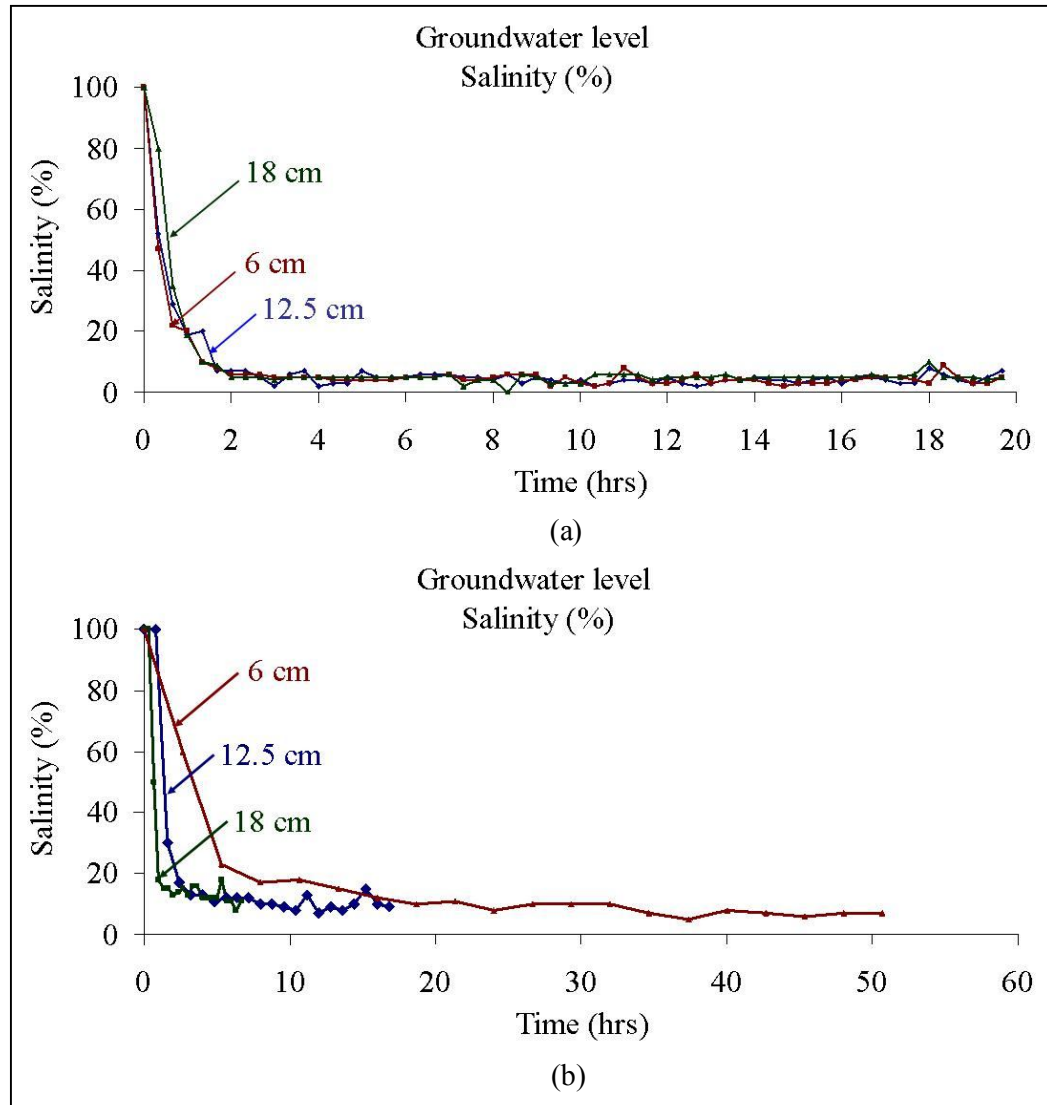
Figure 4.16 The salinity of the pumped brine measured through the test time, the

groundwater lever and the flow direction, (a) the salinity of

vertical infiltration, (b) the salinity of horizontal flow
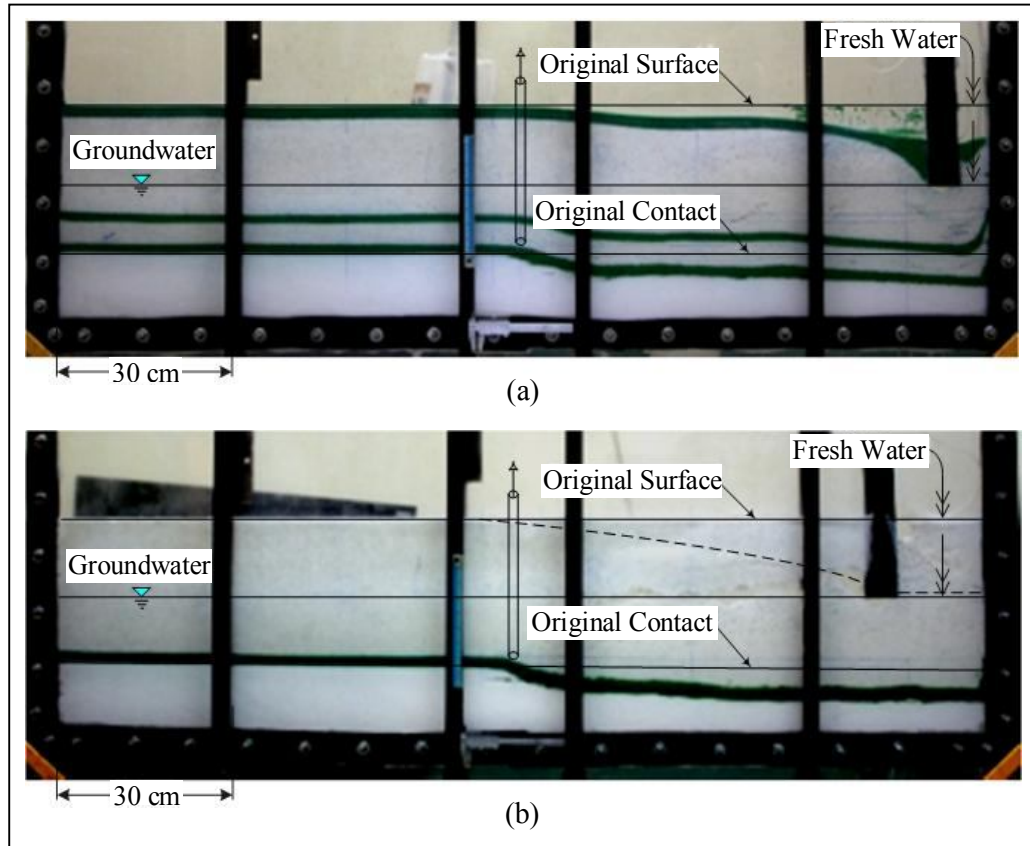
Figure 4.17 Salt solubility testing units varies the entrance width of fresh water. The

overburden thickness and the groundwater level at 25 cm and 12.5

cm does not alter respectively, but the widths of the entrance

to freshwater are (a) 6 inches and (b) 2 inches.
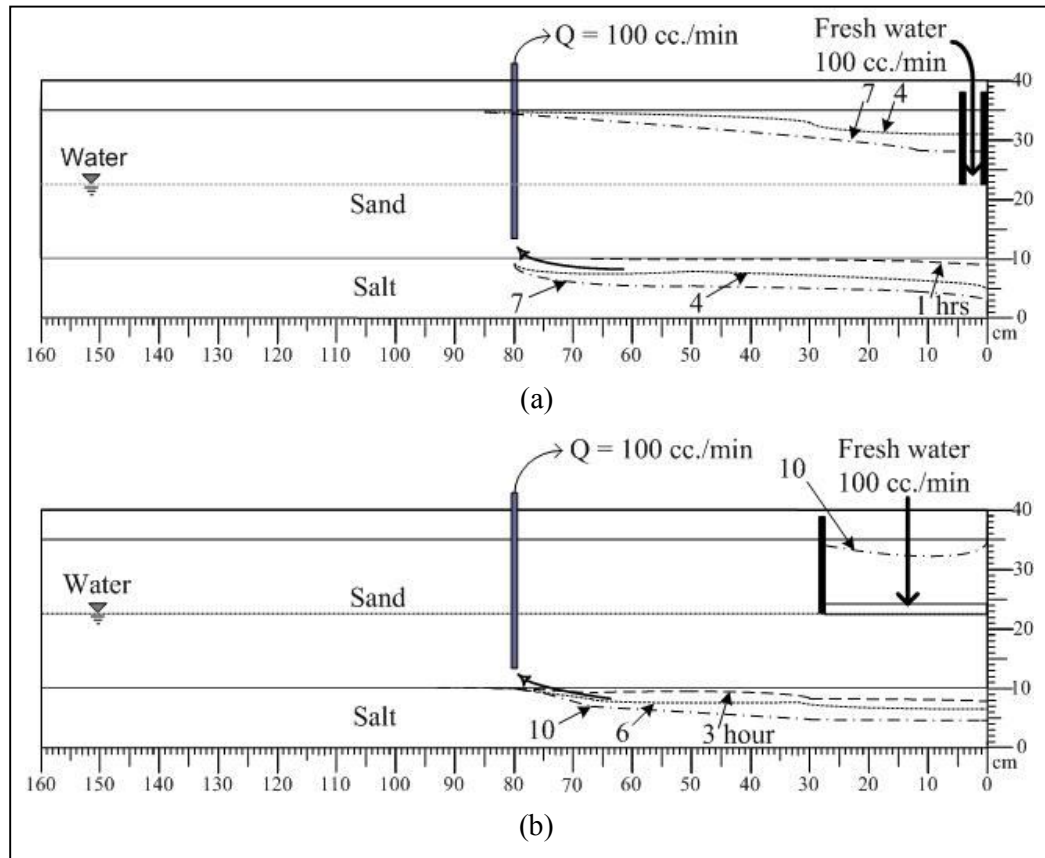
Figure 4.18 Salt solubility from variable of the water entrance width. The constant

variable is the overburden thickness and the groundwater level

was 12.5 cm and 25 cm respectively, except the freshwater

entrance width as (a) 6 inches and (b) 2 inches.

Table 4.8 Results of the subsidence measurements under various positions and time of the sources of freshwater

Recharge area	Time (hrs)	Subsidence (mm.)	G2	G1	R3	R2	R1	C3	C2	C1	L1	L2
Testing the effect of the Recharge area												
2 in	40	surface	64.11	64.93	43.04	30.26	14.26	7.75	4.76	3.45	4.3	0
	40	formation	66.35	55.8	49.15	46.29	41.24	29.77	11.2	0	0	0
6 in	20	surface	0	0.07	0.17	0.42	0.05	0	0	0	0	0
	20	formation	42.24	41.23	34.2	29.83	27.91	22.67	6.26	1.08	0.17	0
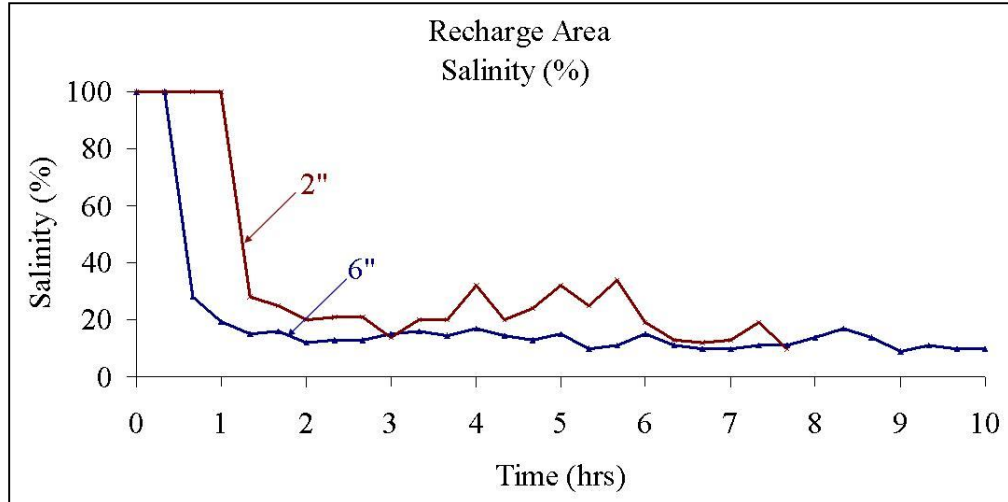
Figure 4.19 Salinity of the pumped measured under the time and variation

of the recharge Area.
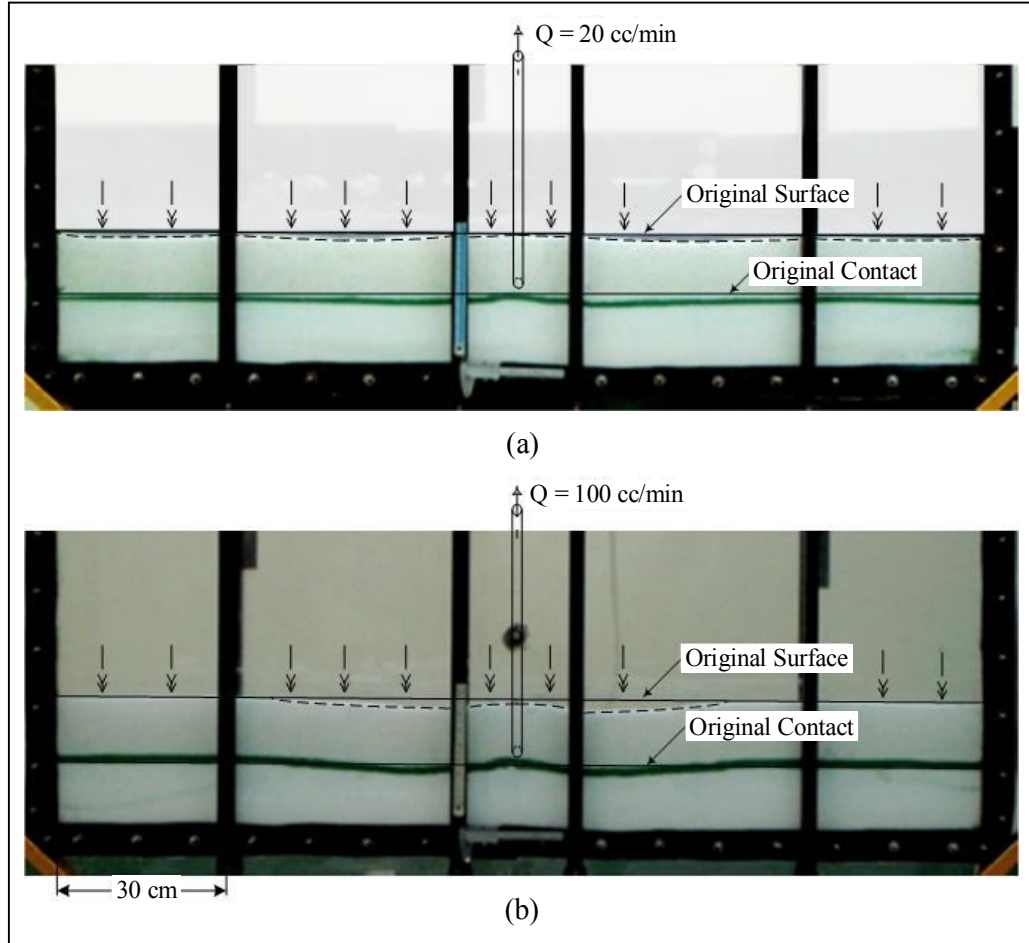
Figure 4.20 Salt solubility testing as the affected by groundwater pumping rates. The

constant variable is the overburden thickness = 11 cm and well depth

= 2 cm, but pumping rate = (a) 20 cc / min and (b) 100 cc / min
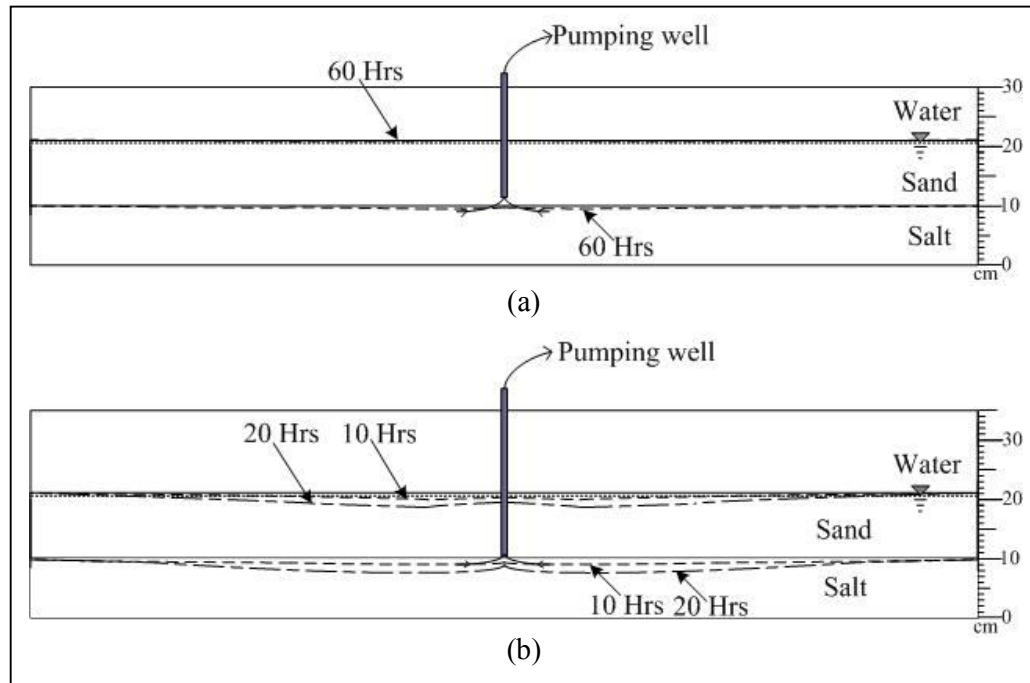
Figure 4.21 Salt solubility testing as the affected by groundwater pumping rates.

The constant variable is the overburden thickness = 11 cm

and well depth = 2 cm, but pumping rate = (a) 20

cc / min and (b) 100 cc / min.

Table 4.9 Results of the subsidence measurements under various positions and the time of variable pumping rate

Pumping rate(cc/min)	Time (hrs)	Subsidence (mm.)	R3	R2	R1	C3	C2	C1	L1	L2	L3
		Testing the effect of the pumping rate in vertical infiltration of fresh water									
20	30	surface	0	0	0	0	0	0	1.7	2.73	0.58
		formation	0.85	1.45	1.37	1.65	1.38	1.76	1.06	0.85	1.14
	60	surface	0	0.5	0	0.05	0.05	0.12	2.12	3.26	0.96
		formation	1.13	2.94	3.76	2.39	2.03	2.32	3.05	1.86	1.81
100	10	surface	1.94	1.3	2.04	3.27	1.72	6.24	6.73	1.53	1.45
		formation	2.4	4.05	1.39	2.45	2.36	6.91	7.28	3.81	0.13
	20	surface	6.1	12.34	25.62	14.73	18.08	15.83	21.21	14.69	8.04
		formation	5.89	17.48	24.87	10.1	17.56	17.55	21.96	17.94	6.27

Figure 4.22 The salinity of the pumped brine measured under the time

and variation pumping rate

CHAPTER V

PROFILE FUNCTION

5.1   Objectives

The objective of this chapter is to calculate subsidence components by using profile function. Comparison between the calculated results and the physical model simulation is made in order to verify the simulation results.

5.2   Input Parameters

There are four cases in the calculation to assess the effects of; depths of pumping, overburden thickness, groundwater level and pumping rate. It can be concluded that the profiles of the subsidence from the two methods are different in the form of the cavern profiles. As the results of the physical model which show the up cone in the middle of the well pump does not conform to cavern in the profile function calculation. This equation has been used for calculating in order to find the boundary of the slope of the subsidence toward the deepest part of the cavern. In the calculation, the form of the cavern is like basin and the deepest part would be in the middle of the well pump and there is no up cone like in the physical model. As the calculation had to use the results from the physical model such as the maximum of the subsidence and the overburden thickness and the positions used for calculating is that from the deepest point to the no subsidence point. The deepest point is given as zero to approximately two times of the boundary of the extent of the subsidence. This is to make the values s(x) in the equation 5.1 in chapter 2 (profile function) at zero and this means there is no subsidence

in that position. As such position is the boundary of the subsidence from the calculation by using Profile function. See the test parameter and results of calculation in table 5-1.

5.3   Results of Calculation

In this research, the comparison between the results of the computing and the results of the physical model simulation is mentioned in the chapter IV.

The results of finding the position and boundary of the cavern by using profile function is regardless the relevance of the feature of the cavern. There is a variance value with 10-15% of the extent of the subsidence between the calculation and the physical model. From calculation, we find an agreement when comparing with simulation direction of vertical infiltration. Result of calculation from effect of depth of pumping by continuous pumping has conformity (shown in a Figures B-1 though B-3 in Appendix B). Results of subsidence extent of periodic pumping from calculation are less than physical model (shown in a Figures B-4 though B-6 in Appendix B). Results of overburden thickness from calculation are less than physical model (show in a Figures B-7 though B-9 in Appendix B). Result effect of groundwater level from calculation less than physical model (shown in a Figures B-10 though B-12 in Appendix B). Result of effect of groundwater level with simulation flow direction of horizontal flow has unconformity because subsidence of the two sides is unequal. The subsidence occurs most in the direction of pumping well. The results of extend from calculation are less than physical model (shown in a Figures B-13 though B-17 in Appendix B). The results of effect size of Richard area with simulation flow direction of horizontal flow from calculation are less than physical model (shown in a Figures B-18 though B-19 in Appendix B). The result of effect pumping rate from calculation less is than physical model (show in a Figure B-20 in Appendix B).

Table 5-1 Test parameters and results of calculation by Profile function.

Test series	Input Parameters						Results		
	Case variables	S_{max}	D	C	γ	B	G(x)	u(x)	ε(x)
Case 1 Depth of pumping	h_p = 0.5	3.26	25	1.4	15	0.37	31.27	11.57	173.10
	h_p = 2	2.07	25				19.85	7.34	109.91
	h_p = 3.5	2.34	25				22.44	8.30	124.25
	h_p = 0.5	4.03	11				66.88	24.74	807.27
	h_p = 2.5	3.17	11				52.60	19.46	635.00
	h_p = 3.5	2.76	11				45.80	16.94	552.87
Case 2 Overburden thickness	d_S = 11	2.34	11	1.4	15	0.37	24.10	8.91	143.01
	d_S = 25	0.44	25				4.37	1.61	25.14
	d_S = 50	0.44	50				2.13	0.78	5.90
Case 3 Groundwater level	h_w = 6	0.65	25	1.4	15	0.37	6.42	2.37	36.89
	h_w = 12.5	1.94	25				19.16	7.09	110.10
	h_w = 18	2.10	25				27.76	10.27	159.48
	h_w = 6	2.86	25				27.47	10.16	152.07
	h_w = 12.5	2.86	25				27.42	10.14	151.81
	(new)h_w =12.5	5.52	25				52.94	19.59	293.10
	h_w = 18	3.35	25				31.04	11.48	180.79
	(new)h_w = 18	5.57	25				51.61	19.09	300.60
	r_a(2),h_w = 12.5	6.49	25				65.22	24.13	361.07
	r_a(6),h_w = 12.5	3.12	25				29.92	11.07	165.67
Case 4 Pumping rate	d_S (11),Q=20	0.35	11	1.4	15	0.37	3.35	1.24	18.58
	d_S (11),Q=100	2.34	11				24.10	8.91	143.01

Remark: Smax = maximum subsidence (cm),   D = Depth of cavern (cm),

B = *constant (Horizontal coefficient), γ = angle of draw (degrees),

G(x) = Slope, ε(x) =Horizontal strain, u(x) = Horizontal displacement,

C = *constant (1.8 for critical and supercritical widths/1.4 for subcritical widths)

CHAPTER VI

CALCULATION BY SALT_SUBSID PROGARM

6.1   Objectives

The objective of this chapter is to perform the surface subsidence calculation using Salt_SUBSID program to verify the results which has mentioned in the previous chapter four.

6.2   Salt_SUBSID Program Calculation

Four cases of calculation are performed as follows;

Case 1 is the effect of the pumping well position

Case 2 is the effect of the overburden thickness

Case 3 is the effect of the groundwater level

Case 4 is the effect of the pumping rate

The results from Salt_SUBSID program shows the subsidence contour in the testing set as in Figures 6-2 though 6-21. The results show the extent of the subsidence in the caver, and also the depth of the maximum subsidence and vertical cross section of subsidence extent. As consequences, the subsidence value by using Salt_SUBSID is not conformed to the results of the physical model. These may be caused by the feature of the cavern used in this computing which is the basin in the centre cavern. In this program the 3D simulation is simulated in cylinder shapes with various diameters overlapping. And this causes the feature the cavern in the vertical cross section which is used in calculation. The result of the physical model simulation has shown that there is

up cone within the cavern which is in the centre under the well pump. In this regard, the researcher could not simulate in the computing by having up cone under the well pump, Figure 6.1 (result subsidence profile for calculation of computer program and result subsidence measurement for physical model).

6.3   Result Salt_SUBSID Program

Result of calculation with program has inconsistency due to patter the feature of cavern model. Result of calculation for impact of well pump position layer with the flow direction from the vertical infiltration and continuous pumping has shown in Figures 6.2 though 6.4. Result of calculation for impact of the pumping well position layer with the flow direction from the horizontal flow and periodic pumping has shown in Figures 6.5 though 6.7. Result of calculation for impact of the overburden thickness with the flow direction from the vertical infiltration and continuous pumping has shown in Figures 6.8 though 6.10. Result of calculation for impact of groundwater levels with the flow direction from the vertical infiltration and continuous pumping has shown in Figures 6.11 though 6.13. Result of calculation for impact of groundwater levels with the flow direction from the horizontal flow and continuous pumping has shown in Figures 6.14 though 6.18. Result of calculation for impact of size of richard area with the flow direction from horizontal flow and continuous pumping has shown in Figures 6.19 though 6.20. Result of calculation for impact of pumping rate with the flow direction from the vertical infiltration and continuous pumping has shown in Figure 6.21. Therefore, the results of the computing give a higher value on the extent of the subsidence, so this program can not be used for calculating or comparing.
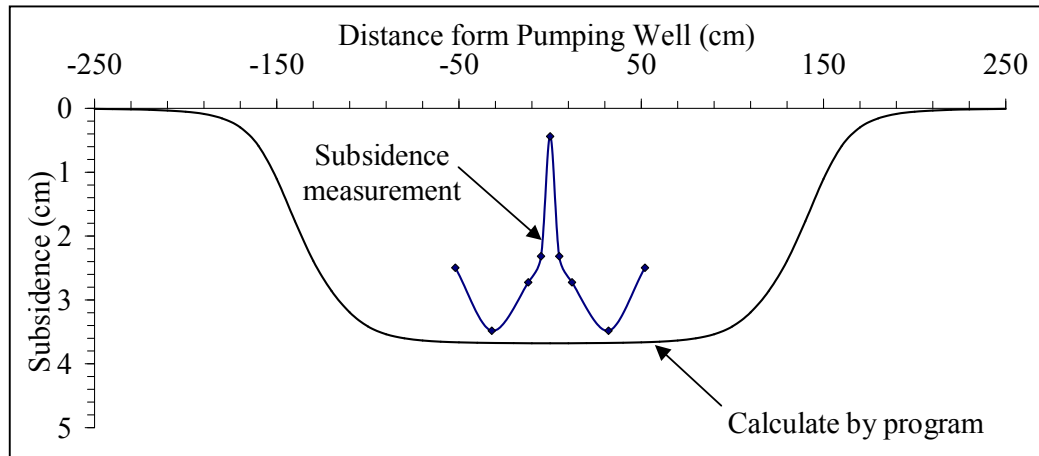
Figure 6.1 Comparison between .result subsidence in physical model

and program calculation.
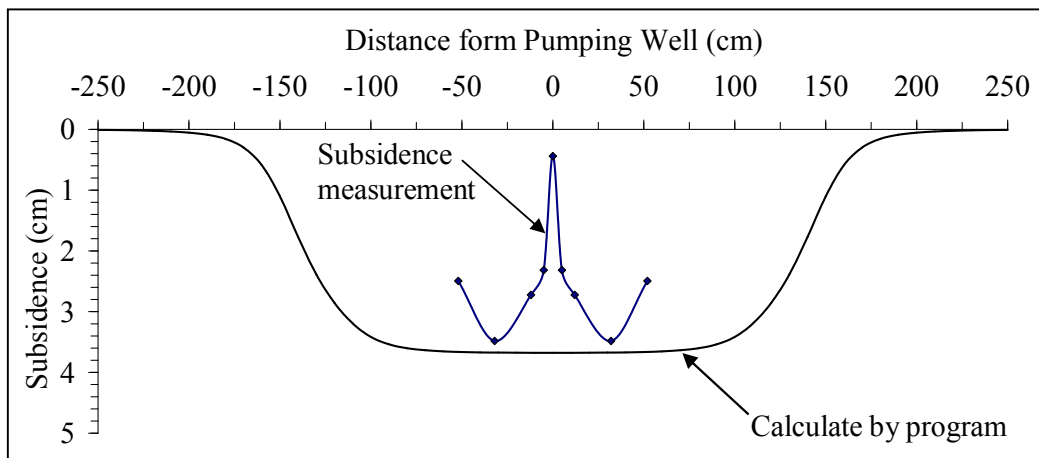
Figure 6.2 Results of Salt_SUBSID calculation (case 1) for vertical infiltration,

$h_p = 0.5$ cm, $d_s = 25$ cm, continuous pumping.
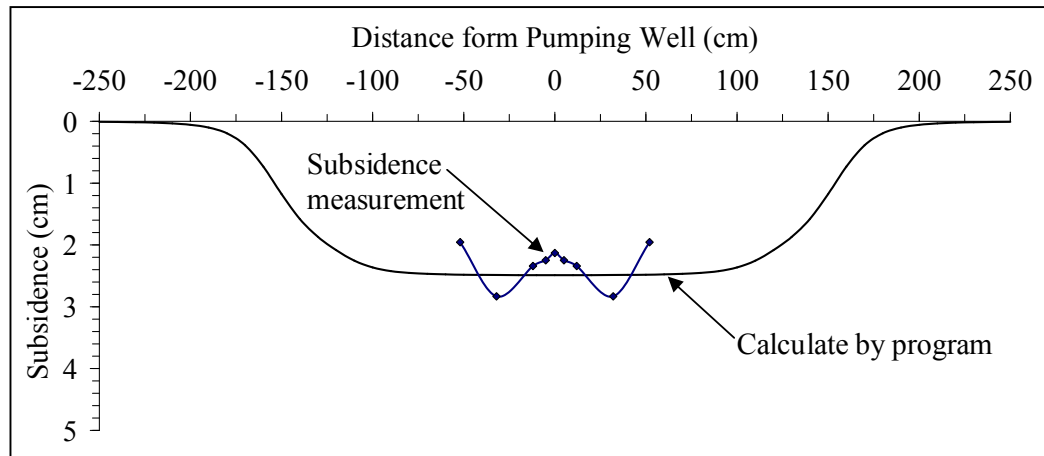
Figure 6.3 Results of Salt_SUBSID calculation (case 1) for vertical infiltration,

h_p = 2.0 cm, d_s = 25 cm, continuous pumping.
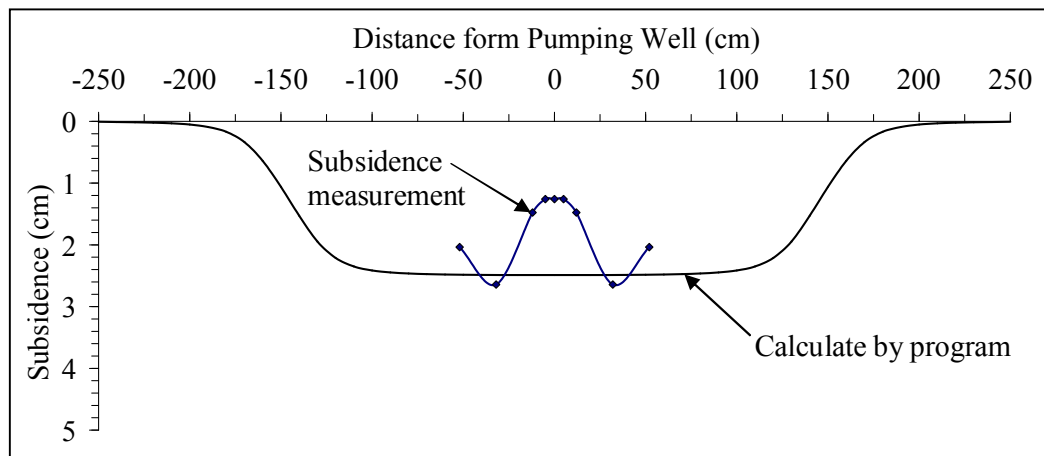
Figure 6.4 Results of Salt_SUBSID calculation (case 1) for vertical infiltration,

h_p = 3.5 cm, d_s = 25 cm, continuous pumping.
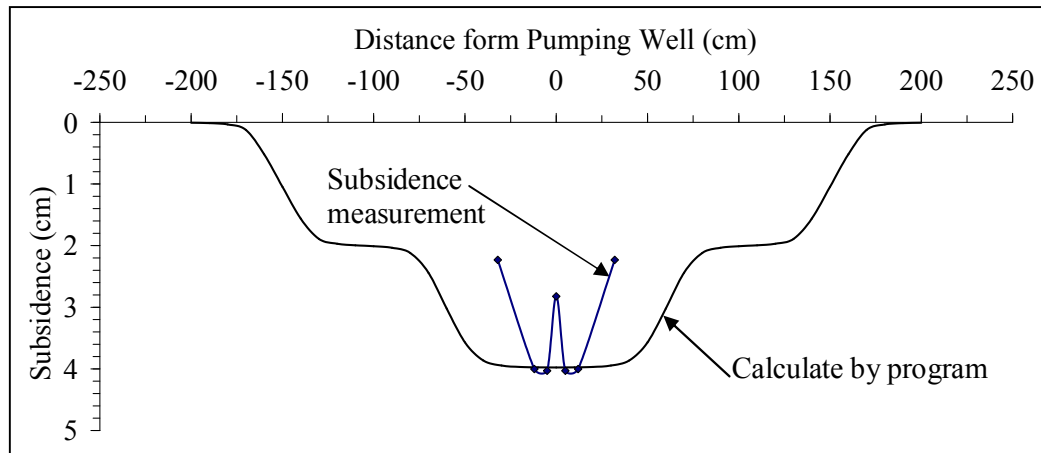
Figure 6.5 Results of Salt_SUBSID calculation (case 1) for vertical infiltration,

$h_p = 0.5$ cm, $d_s = 11$ cm, periodic pumping.
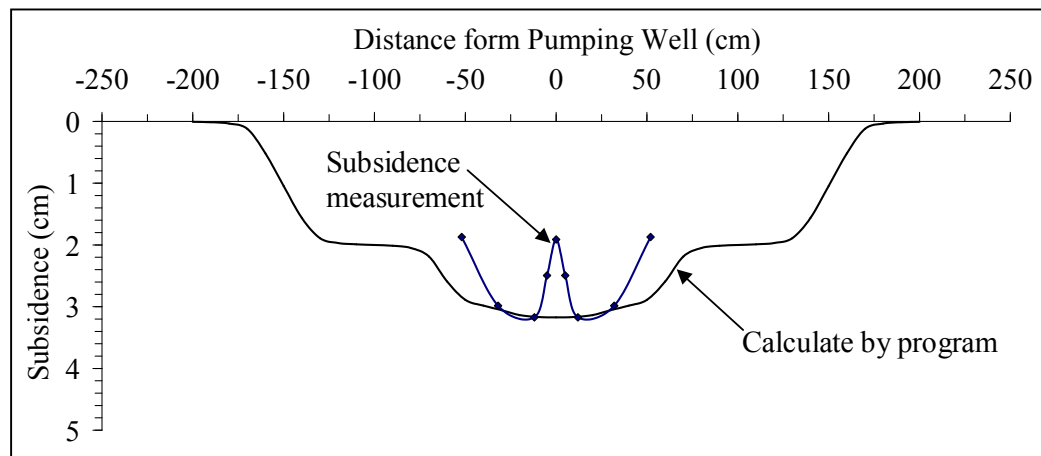
Figure 6.6 Results of Salt_SUBSID calculation (case 1) for vertical infiltration,

$h_p = 2.0$ cm, $d_s = 11$ cm, periodic pumping.
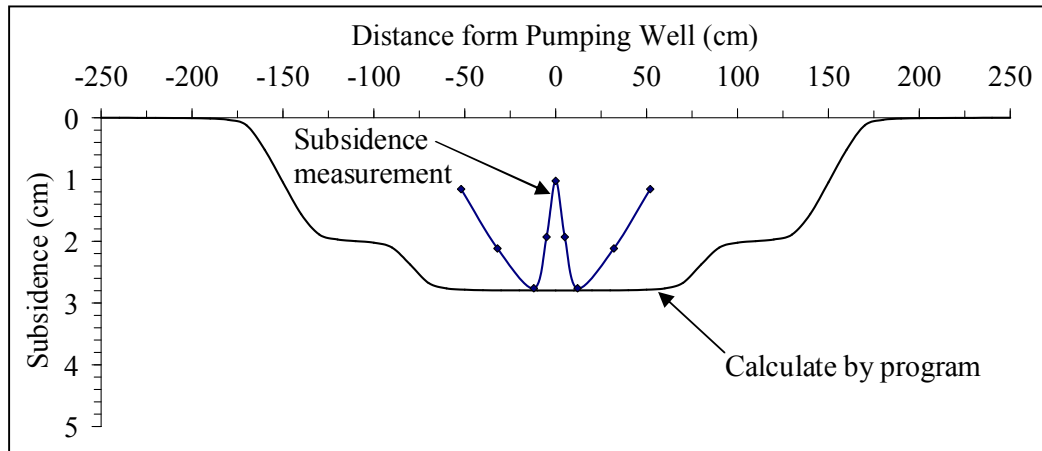
Figure 6.7 Results of Salt_SUBSID calculation (case 1) for vertical infiltration,

h_p = 3.5 cm, d_s = 11 cm, periodic pumping.
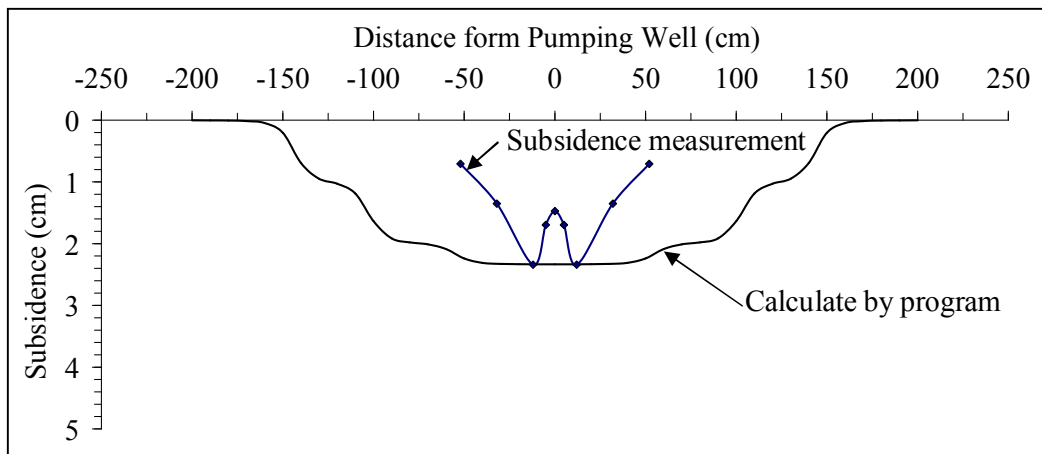
Figure 6.8 Results of Salt_SUBSID calculation (case 2) for vertical infiltration,

d_s = 11 cm, h_p = 2 cm, h_w = 10 cm, and the continuous pumping.
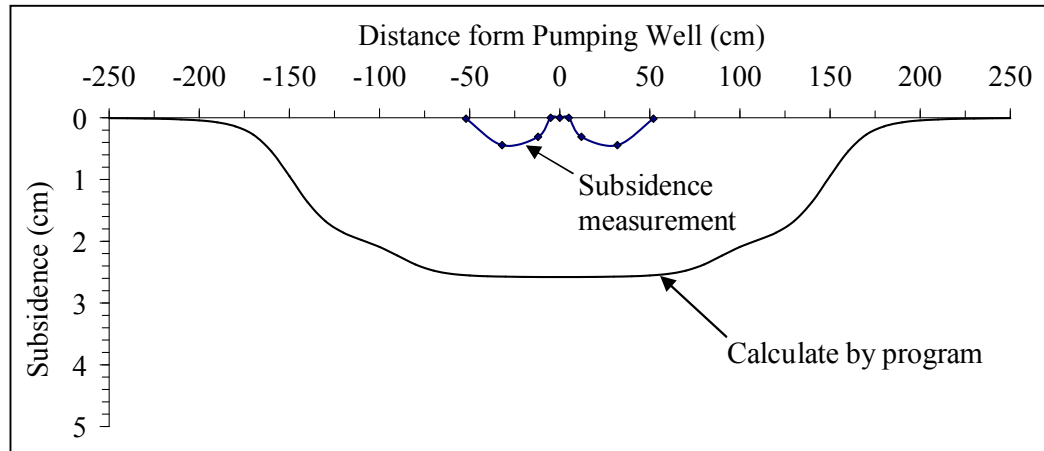
Figure 6.9 Results of Salt_SUBSID calculation (case 2) for vertical infiltration,

$d_s = 25$ cm, $h_p = 2$ cm, $h_w = 24$ cm, and the continuous pumping.
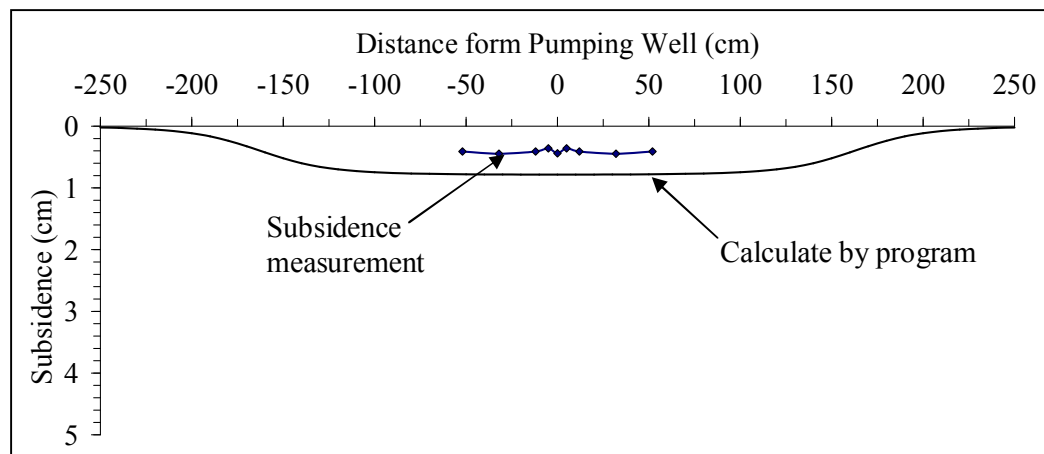
Figure 6.10 Results of Salt_SUBSID calculation (case 2) for vertical infiltration,

$d_s = 50$ cm, $h_p = 2$ cm, $h_w = 49$ cm, and the continuous pumping.
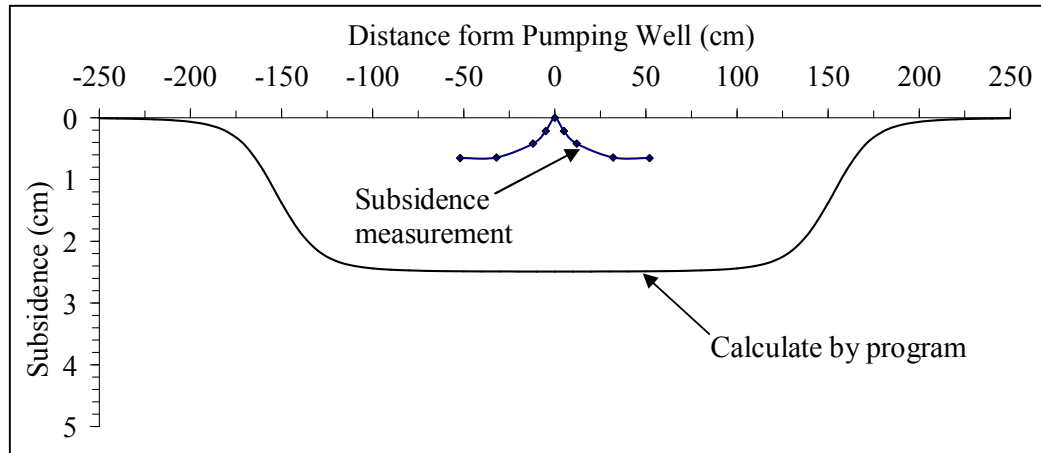
Figure 6.11 Results of Salt_SUBSID calculation (case 3) for vertical infiltration,

h_w = 6 cm, h_p = 2 cm, d_s = 25 cm and the continuous pumping.
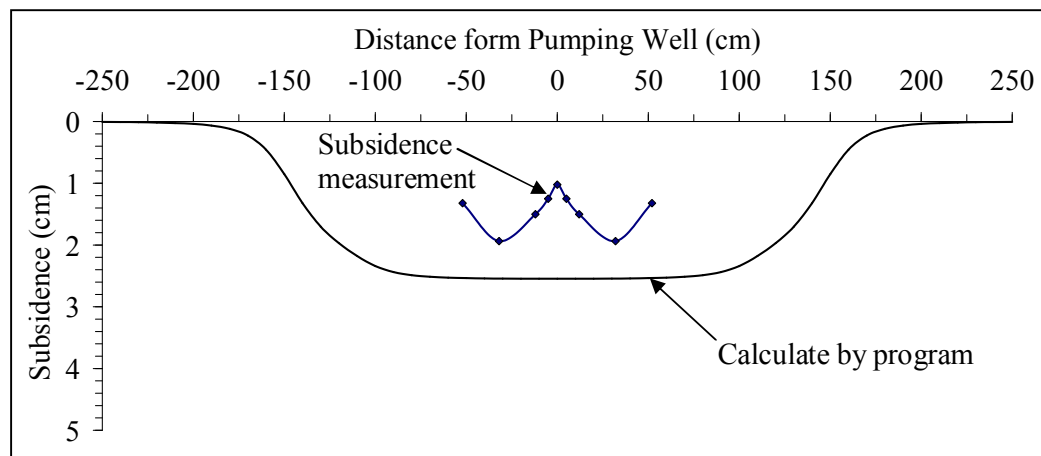
Figure 6.12 Results of Salt_SUBSID calculation (case 3) for vertical infiltration,

h_w = 12.5 cm, h_p = 2 cm, d_s = 25 cm and the continuous pumping.
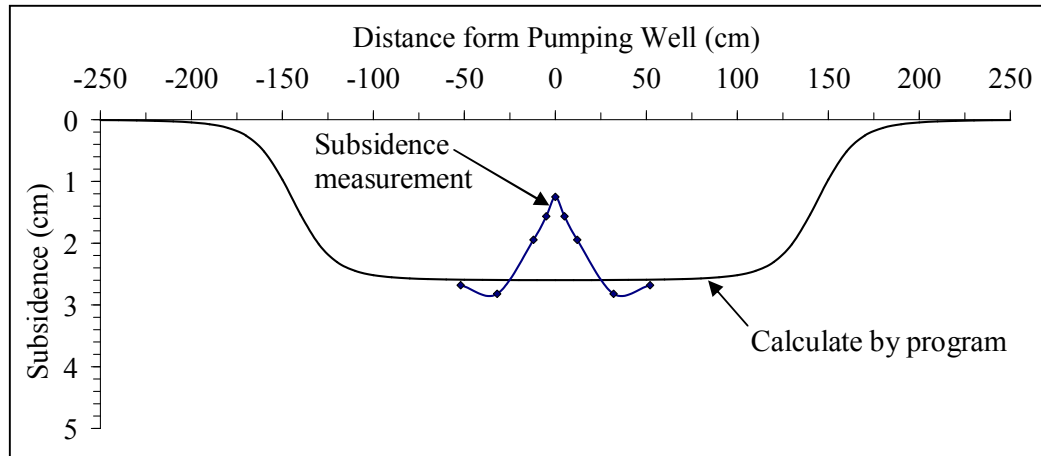
Figure 6.13 Results of Salt_SUBSID for calculation (case 3) for vertical infiltration,

$h_w = 18$ cm, $h_p = 2$ cm, $d_s = 25$ cm and the continuous pumping.
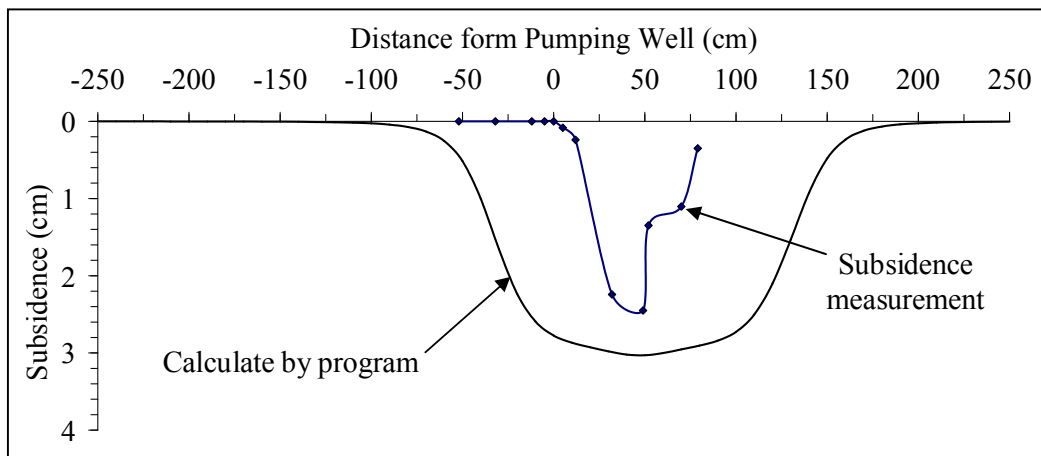
Figure 6.14 Results of Salt_SUBSID calculation (case 3) for horizontal flow,

$h_w = 6$ cm, $h_p = 2$ cm, $d_s = 25$ cm and the continuous pumping.
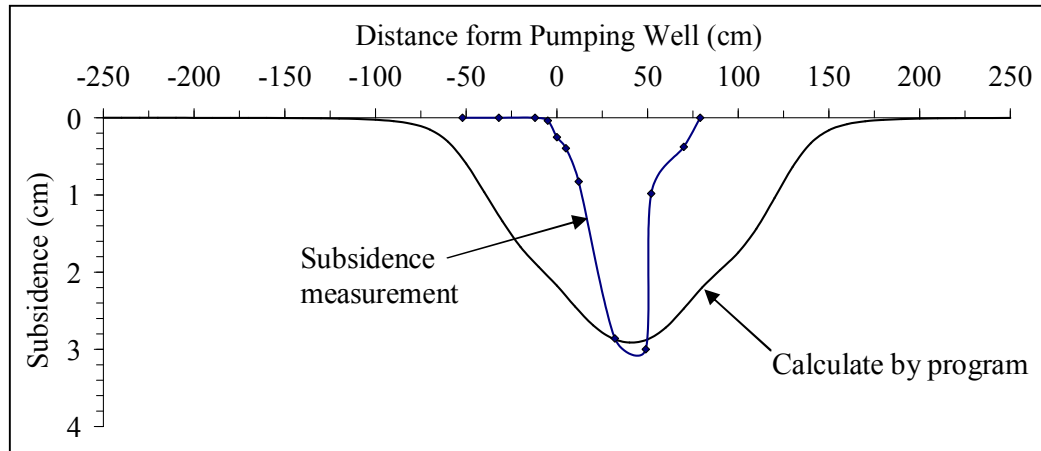
Figure 6.15 Results of Salt_SUBSID calculation (case 3) for horizontal flow,

$h_w =$ 12.5 cm, $h_p = 2$ cm, $d_s = 25$ cm and the continuous pumping.
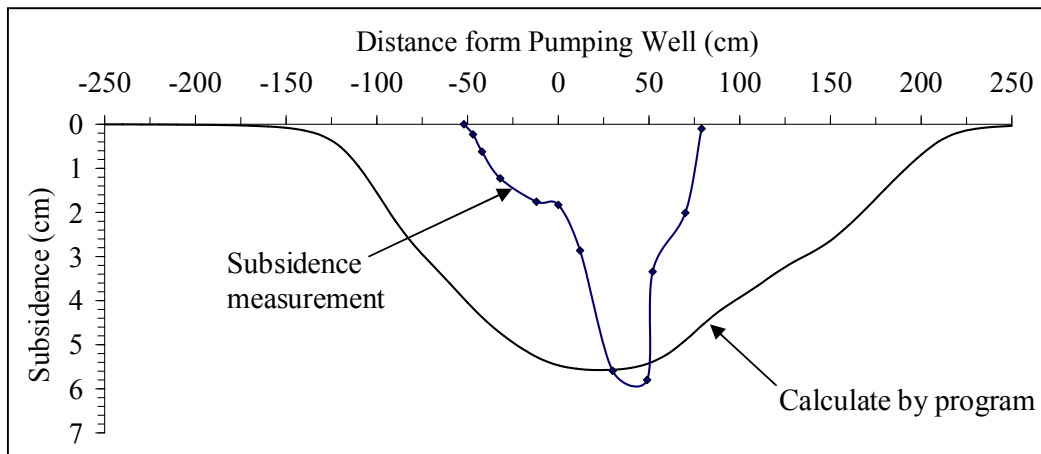
Figure 6.16 Results of Salt_SUBSID calculation (case 3) for horizontal flow, $h_w = 12.5$

cm, $h_p = 2$ cm, $d_s = 25$ cm and the continuous pumping in a new well.
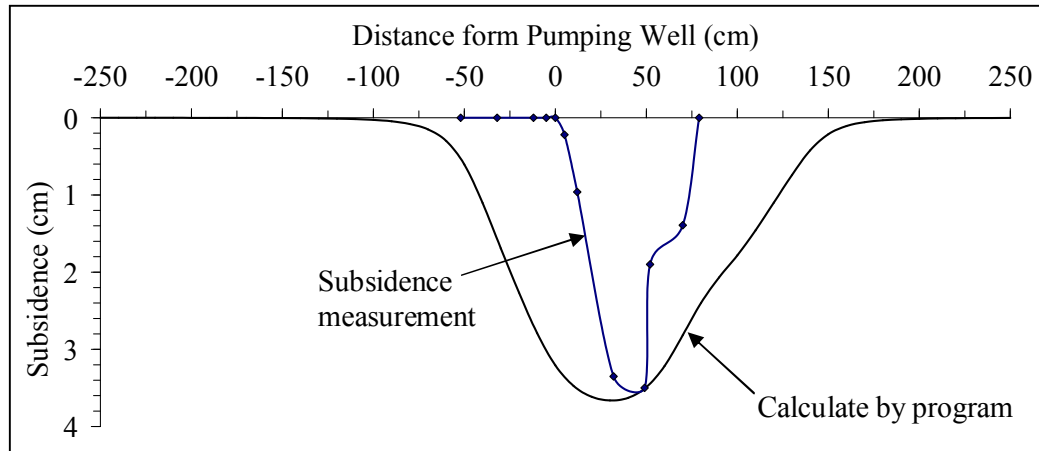
Figure 6.17 Results of Salt_SUBSID calculation (case 3) for horizontal flow,

h_w = 18 cm, h_p = 2 cm, d_s = 25 cm and the continuous pumping.
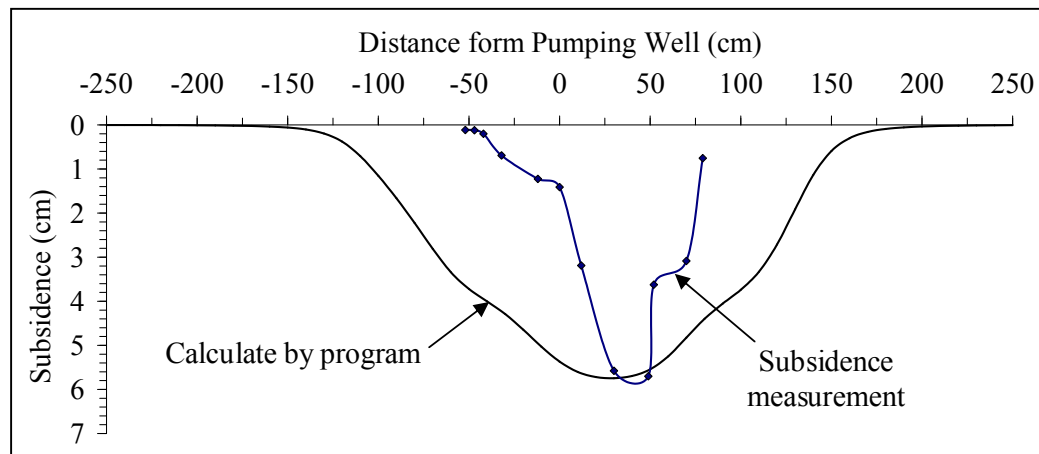
Figure 6.18 Results of Salt_SUBSID calculation (case 3) for horizontal flow,

h_w = 18 cm, h_p = 2 cm, d_s = 25 cm and the continuous

pumping in a new well.
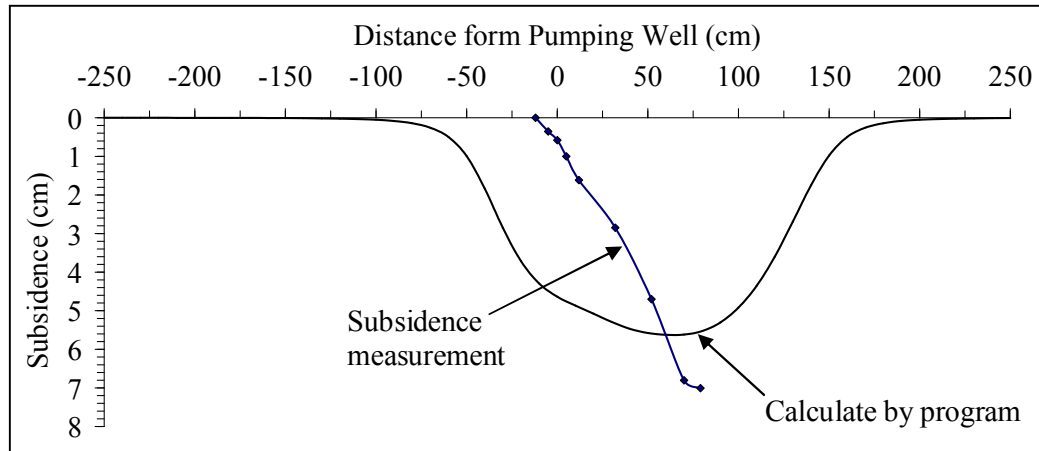
Figure 6.19 Results of Salt_ SUBSID calculation (case 3) for horizontal flow, 2 in

recharge area, h_w = 12.5 cm, h_p = 2 cm, d_s = 25 cm and

the continuous pumping.
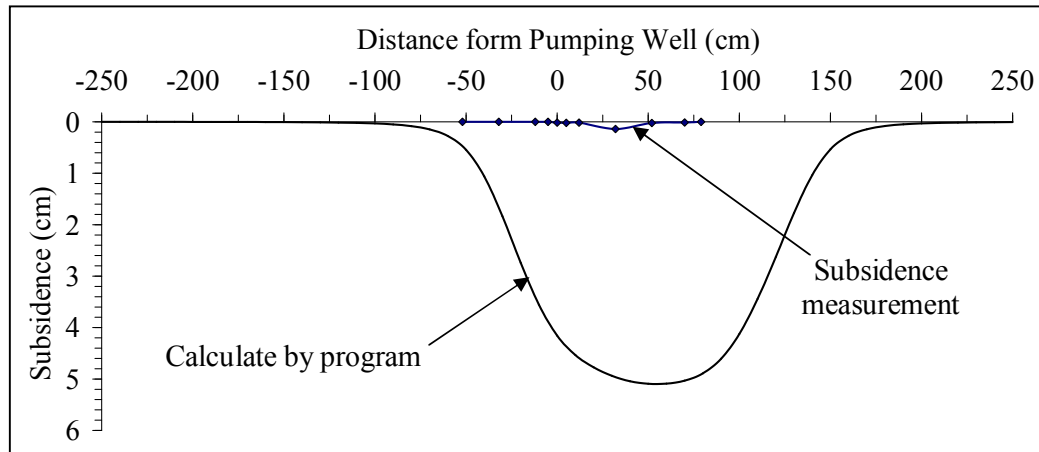
Figure 6.20 Results of Salt_ SUBSID calculation (case 3) for horizontal flow, 6 in

recharge area, h_w = 12.5 cm, h_p = 2 cm, d_s = 25 cm and

the continuous pumping.
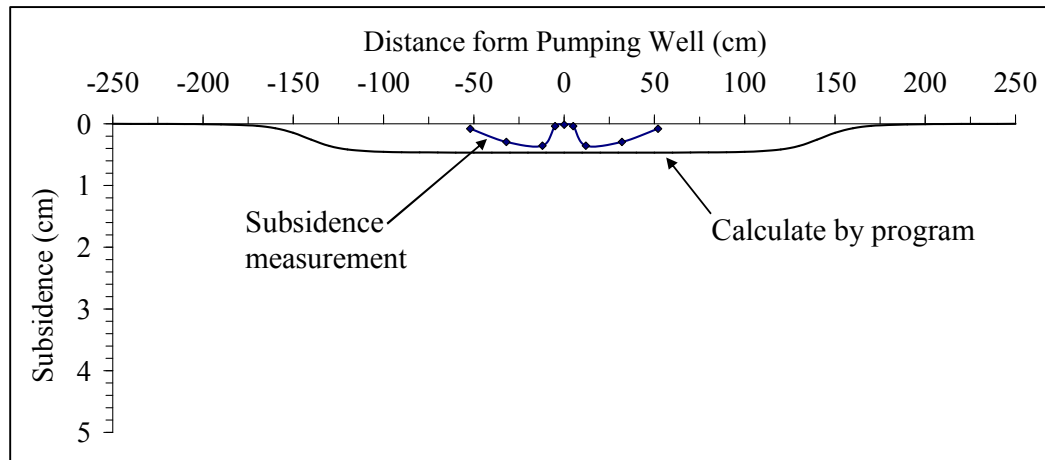
Figure 6.21 Results of Salt_ SUBSID calculation (case 4) for vertical infiltration,

$d_s = 11$ cm, $h_p = 2$ cm, $h_w = 10$ cm and the continuous

pumping $Q = 20$ cc/min and $Q = 100$ cc/min.

CHAPTER VII

COMPUTER SIMULATION

7.1   Introduction

This research simulated the flowing of underground water by using the computer simulation to study the characteristics of the water flow through the overburden feature.   It describes the parameters and the flowing form in the simulation including results from computing. Results from the computer simulation (Finite Element Subsurface & Transport Simulation System) will be used to create the ratio of the flowing in overburden to the pumping rate and the permeability by using the FEFlow program (Wasy, 2006) In the simulation, there is various rate of the water flow underneath the surface which depends on the area either in two or three dimensions. The parameters in calculating are the area the water has flow through, the rate of permeability, the rate of flowing and the transportations of sediment. The parameters are the overburden thickness, the water pressure, the water level and the position of the pumping, the water flowing in from the top and flow out on the side. The results of this simulation will be compared with the physical model results and the solubility, focusing on the water flow direction from formation surface leaching the salt layer to pumping well.

7.2   Results of The Computer Simulation

The result of the simulation is shown in the groundwater flowing in overburden thickness and pumping rate which is used in this simulation was the same rate as in the

physical model. It observed the water flowing through formation surface or the water has dissolved the salt. The results of each testing show in Figures C-1 though C-11. It shows that the depth of pumping or the distance of the tube to the salt surface has influenced to the solubility salt. This mean the salt will be dissolved more if the pumping tube is near the salt surface. (Figure C-1 in Appendix C) If the tube was moved further, then the pumping would make salt soluble into a large area which conforms to the results from the physical model. When the pumping well is installed near to the salt layer (h_p = 0.5 cm), the permeability of fresh water is near to the salt surface is small (Figure C-1 in Appendix C). When the pumping well position is far from the salt layer (h_p = 2 cm), the permeability of fresh water is far to the salt surface (Figure C-2 in Appendix C). When the pumping well is moved to further distance from salt layer (hp = 3.5 cm), the permeability of fresh water is moved to further the salt surface is large (Figure C-3 in Appendix C). The computer simulation can be made for continuous pumping only. The results of the groundwater flowing has been affected from the overburden thickness. The extent of water flowing was followed the overburden thickness. The thicker the overburden is, the less the water permeability to dissolve the salt is affected from the pumping. These were in the line with the physical model results. When the thickness is small (d_s = 11 cm), the permeability of fresh water occurs around the pumping area (Figure C-4 in Appendix C). When the overburden thickness has increased (d_s = 25 cm), the permeability of fresh water becomes large ((Figure C-5 in Appendix C). When the overburden thickness has increased a lot more (d_s = 50 cm), the permeability of fresh water becomes larger (Figure C-6 in Appendix C). The flow direction of the brine in the vertical infiltration in the computer simulation has been in the line with the results of the physical model. The result shows the flow

direction of groundwater into pumping well, the most of water flows from the horizontal infiltration. The results of physical model, the small amount of salt dissolved were surrounding under the tube because the water in that area has moved in a small amount. So it creates up cone in the centre under the tube in vertical infiltration. For results of horizontal flow, the groundwater flow from the sources. Which conforms to the physical model result, that means the salinity is in only the area that the water flows through from the vertical flow in the tube. As the physical model results show that the most salinity is in the area that water has flown in (Figures C-7 though C-11 in Appendix C). And the computer results shows that salts will be dissolved from the water flowing in. These can be seen as the results in the chapter IV.

CHAPTER VIII

DISCUSSIONS, CONCLUSIONS AND

RECOMMENDATIONS FOR FUTURE STUDIES

8.1 Discussions

Four series of tests were performed by using a physical model. These four test series are to assess the effects of depth of pumping, overburden thickness, groundwater level and withdrawal rate. The results obtained from the periodic and continuous pumping under vertical and horizontal water flow directions are given in chapter IV. The results of each series described the effect of various test parameters on the test. The formation and surface subsidence have been caused from those parameters. For the flow direction, it seems that the horizontal flow direction has more influenced on the subsidence than the vertical infiltration under the same groundwater level. The pumping rate results indicate that the formation subsidence increases with increasing of pumping rate, but it seems to be opposite with the extent of formation subsidence. When the pumping rate is high, the subsidence area becomes smaller.

Overall results seem similar among each other as the subsidence occurs around the pumping area. The subsidence happens outside the pumping area in reality under the horizontal flow of fresh water. More tests should be conducted on this research topic. Cone underneath the pump well was observed in vertical infiltration condition. The cone was occurred from the effects of flowing rate of water movement into pumping pipe. The middle pipe flows were slower than those around the pipe.

Moreover, the water that comes into pumping pipe has dissolved the salt from the salt layer around the pumping area. The pumping pipe position that made the solubility decreased in area near to the pipe causing the cavern under the pipe.

8.2 Conclusions

Physical scaled-down 2-dimensional models have been used to simulate the surface and formation subsidence induced in the salt basin by brine pumping practice. Sorted sand (0.6-0.8 mm) is used to simulate the overburden. Pure crushed salt (0.6 mm) simulates the underlying salt bed. The effects of well depth (distance between pumping tube and top salt), overburden thickness, groundwater level, pumping rate and flow direction are assessed. The results suggest that deeper pumping tube (closer to the salt surface) induces greater magnitudes of surface and formation subsidence than does the shallower tube. The subsidence magnitude induced over shallow salt bed is greater than that over the deeper salt bed. The extent of the surface subsidence over the shallow salt bed is smaller than that over the deeper salt bed. The deeper groundwater level tends to show greater magnitude of surface and formation subsidence. The groundwater level however has no impact on the extent of the subsidence area. The higher rate of brine pumping, the greater magnitude and the lesser extent of the subsidence is obtained. The location of subsidence is mainly controlled by the positions of the fresh water sources and of the pumping well. The results provide an understanding of the magnitude and severity of the surface and formation subsidence in the brine pumping areas, and hence practical guideline can be drawn, and mitigation plan can be implemented. Comparison between the profile function results of the computing and physical model is made. Results from the Salt_SUBSID can be concluded that this

program should not calculate the subsidence of the physical model testing. The subsidence in the program is in 3-dimensional which can not be related to the subsidence in the physical model. Results from computer simulation show how the groundwater flows into the overburden to dissolve the salt layer.

8.3 Recommendations for Future Studies

The scope of this research is relatively narrow, emphasizing on the correlations between the surface profile and the cavern configurations. This leads to the following research needs.

- The test should be performed on the simulated overburden with various permeability values to access the impacts of the overburden characteristics.

- The effect of the pumping rate should be studied under a broader range. In addition the knowledge of the effect of multiple brine wells on the subsidence characteristics is desirable.

- The test should be conducted under a much slower pumping rate to study the change of the pumped water salinity.

- The overburden rock with different stiffness values should be tested to study their relation with the surface subsidence.

REFERENCES

Aracheeploha, S., Horkaew, P., and Fuenkajorn, K. (2009). Prediction of cavern configurations from subsidence data. In **Proceedings of the Second Thailand Symposium on Rock Mechanics** (pp. 116-176). Suranaree University of Technology

Asadi, A., Shahriar, K., Goshtasbi, K., and Najm, K. (2005). Development of new mathematical model for prediction of surface subsidence due to inclined coal-seam mining, **J. S. Afr. Inst. Min. Metall**, 105(11): 15-20.

Crosby, K. (2007). Integration of rock mechanics and geology when designing the Udon South sylvinite mine. In **Proceedings of the First Thailand Symposium on Rock Mechanics** (pp. 3-22). Suranaree University of Technology.

Fuenkajorn, K. (2002). Design guideline for salt solution mining in Thailand. **Research and Development journal of the Engineering Institute of Thailand**. 13(1): 1-8.

Ge, H., and Jackson, M. P. A. (1998). Physical modeling of structures formed by salt withdrawal; implications for deformation caused by salt dissolution, **AAPG Bulletin,** Vol 82 no.2 (pp. 228-250).

Gil Victor M. S., and Paiva, João C. M. J. (2006). Computer Simulations of Sal Solubility, **JCE WebWare**, Vol. 83 (pp. 173).

Japakasetr, T., and Workman, D. R. (1981). Evaporite deposits of northeast Thailand. **Circum-Pacific Conferences** (pp. 179-187). Hawaii.

Japakasetr, T., and Suwanich, P. (1982). Potash and Rock Salt in Thailand Appendix A Nonmetallic Minerals Bulletin No. 2. **Economic Geology Division, Department of Mineral Resources** (pp. A1-A252). Bangkok, Thailand**.**

Japakasetr, T. (1985). Review on rock salt and potash exploration in Northeast Thailand. **Conference on Geology and Mineral Resources Development of the Northeast**, Thailand, 26-29 November 1985 (pp. 135-147). Khon Kaen University.

Japakasetr, T. (1992). Thailand's mineral potential and investment opportunity. **National Conference on Geologic Resources of Thailand: Potential for Future Development**, November 1992, DMR, Bangkok, Thailand (pp. 641-652).

Jenkunawat, P. (2005). Results of drilling to study occurrence of salt cavities and surface subsidence Ban Non Sabaeng and Ban Nong Kwang. Amphoe Ban Muang, Sakon Nakhon. **International Conference on Geology, Geotechnical and Mineral Resources of Indochina (GEOINDO 2005)** (pp. 259-267). Khon Kaen University.

Jenkunawat, P. (2007). Results of drilling to study occurrence of salt cavities and surface subsidence Ban Non Sabaeng and Ban Nong Kwang, Sakon Nakhon. In **Proceedings of the First Thailand Symposium on Rock Mechanics** (pp. 257-274). Suranaree University of Technology.

Lourenco, S. D. N. Sassa, K.,and Fukuoka, H. (2006)**.** Failure process and hydrologic response of a two layer physical model: Implications for rainfall-induced landslides, **Geomorphology,** Vol 73 (pp. 115-13).

Nieland, J. D. (1991).   Salt_SUBSID: A PC-Based Subsidence Model**. Solution Mining Research Institute**(p. 67), Report No.1991-2-SMRI, California, USA.

Potter, R. W. (1981). Chemical Proper ties Among Components in Salt Deposits. **Physical Properties Data for Rock Salt** (p. 66), L.H. Gevantman, NBS. 167.

Rattanajarurak, P. (1990). Formation of The Potash Deposits, Khorat Plateau, Thailand. **M.S. Thesis, School of Mine, Kensington, Australia.**

Sattayarak, N., and Polachan, S. (1990). Rock salt beneath the Khorat plateau (in Thai), In **Proceedings of the Conference on Geology and Mineral Resources of Thailand** (pp. 1-14). Bangkok, Thailand: Department of Mineral Resources.

Sattayarak, N. (1983).   Review of continental Mesozoic stratigraphy of Thailand. In **Proceeding Stratigraphic correlation of Thailand and Malaysia** (pp. 127-148). Geol. Soc. Thailand.

Sattayarak, N. (1985). Review on Geology of Khorat plateau**. Conference on Geology and Mineral Resources Development of the Northeast** (pp. 23-30). Thailand 26-29 November 1985, Thailand: Khon Kaen University.

Singh, M. M. (1992).   Mine Subsidence. **SME Mining Engineering Handbook. Hartman**, H. L. (ed).   (pp.938-971). Society for mining metallurgy and exploration, Inc Colorado.

Supajanya, T., Vichapan, K., and Sri-israporn, S. (1992).   Surface expression of shallow salt dome in Northeast Thailand, **National Conference on Geologic Resources of Thailand** (pp. 89-95). Potential for Future Development, 17-24 November 1992, DMR, Bangkok, Thailad.

Suwanich, P. (1986).   Potash and Rock Salt in Thailand : Nonmetallic Minerals Bulletin No.2, **Economic Geology Division, Department of Mineral Resources**, Bangkok, Thailand.

Utha-aroon, C. (1993). Continental origin of the Maha Sarakham evaporites. Northeastern Thailand, **Journal of Southeast Asian Earth Sciences**, Great Britain, 8(1-4): 193-203.

Wannakao, L., and Walsri, C. (2007). Subsidence models in salt production area. In **Proceedings of the First Thailand Symposium on Rock Mechanics** (pp. 311-321). Suranaree University of Technology.

Wannakao, L., Janyakorn, S., Munjai, D., and Vorarat, A. (2004). **Geological and geotechnical properties analysis of overburden and salt formations in the northeast for surface subsidence model**. final research report, Department of Geotechnology, Khon Kaen University (in Thai).

Wannakao, L., Munjai, D., and Janyakorn, S. (2005). Geotechnical investigation of surface subsidence at Ban Non Sabaeng salt production area. Sakon Nakhon, Thailand. **International Conference on Geology, Geotechnical and Mineral Resources of Indochina (GEOINDO 2005)** (pp. 282). Khon Kaen University.

Warren, J., 1999. Evaporites: Their Evolution and Economics, **Oxford: Blackwell Science.**

Wasy, GmbH. (2006). FEFlow Finite Element Subsurface & Transport Simulation System, Version 5.3, **User Manual. German engineering company, Walterdorfer Strate 105, D-12526 Berlin, Germany.**

Yumuang, S., Khantapab, C., and Taiyagupt, M. (1986). The evaporate deposits in Bamnet Narong area, Northeastern Thailand, In **Proceedings of the GEOSEA V** (Bullrtin 20, Vol. 2, pp. 249-267). Geological Society of Malasia.

APPENDIX C

RESULT OF COMPUTER SIMULATION (FEFlow)
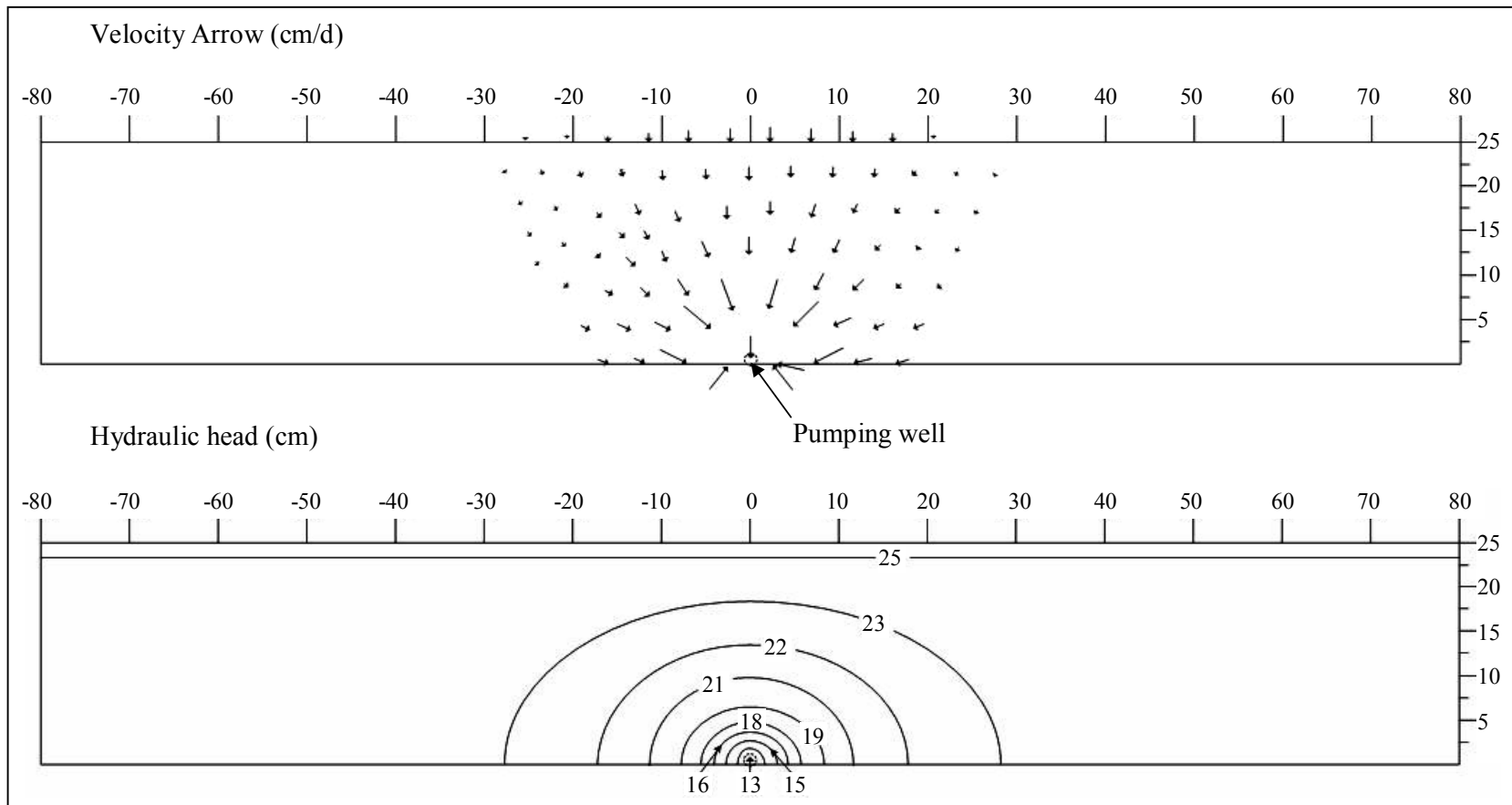
Figure C-1 Computer simulation results of 25 cm overburden thickness, 0.5 cm depth of pumping and 100 cc/min pumping rate
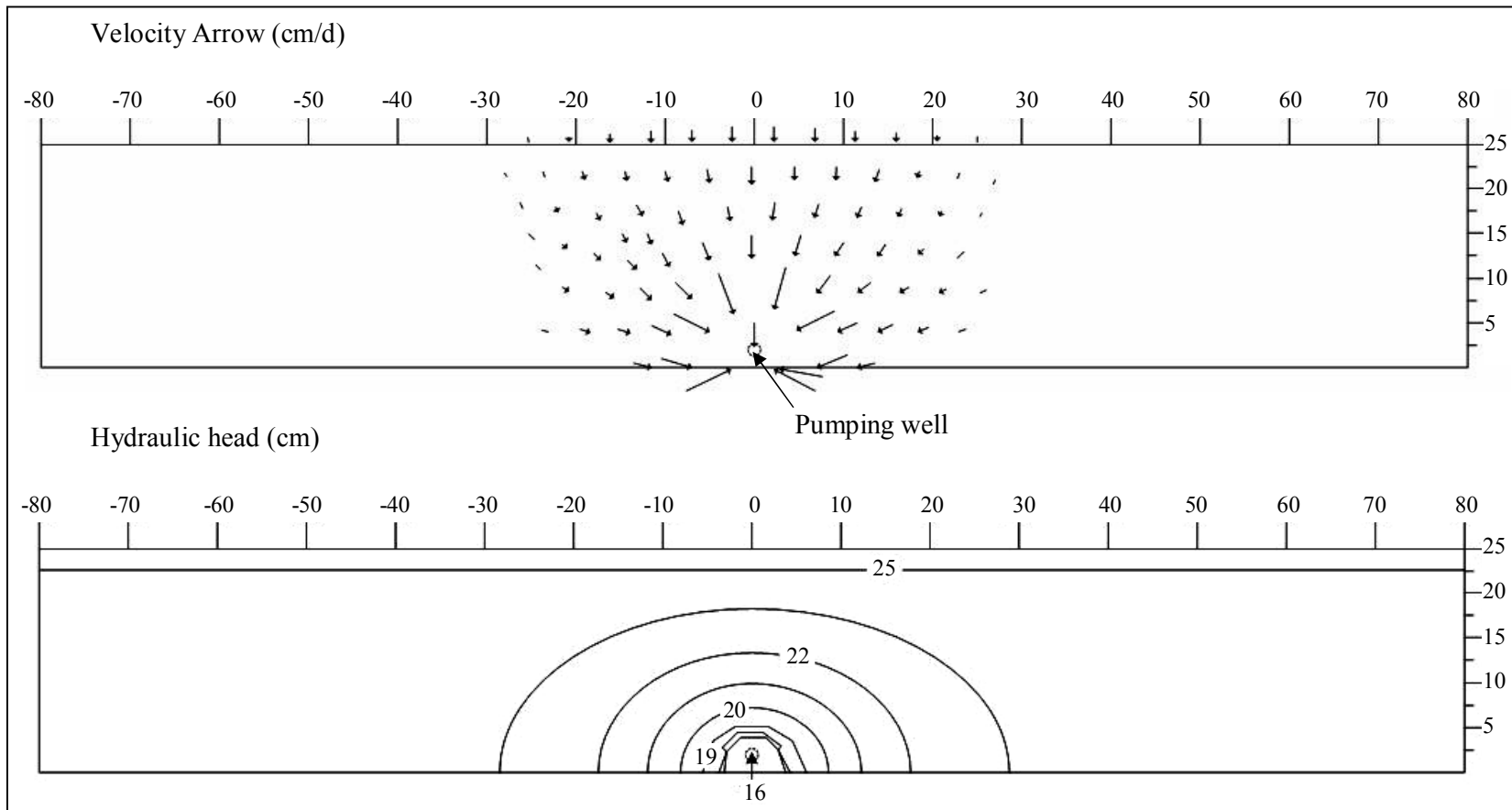
Figure C-2 Computer simulation results of 25 cm overburden thickness, 2 cm depth of pumping and 100 cc/min pumping rate
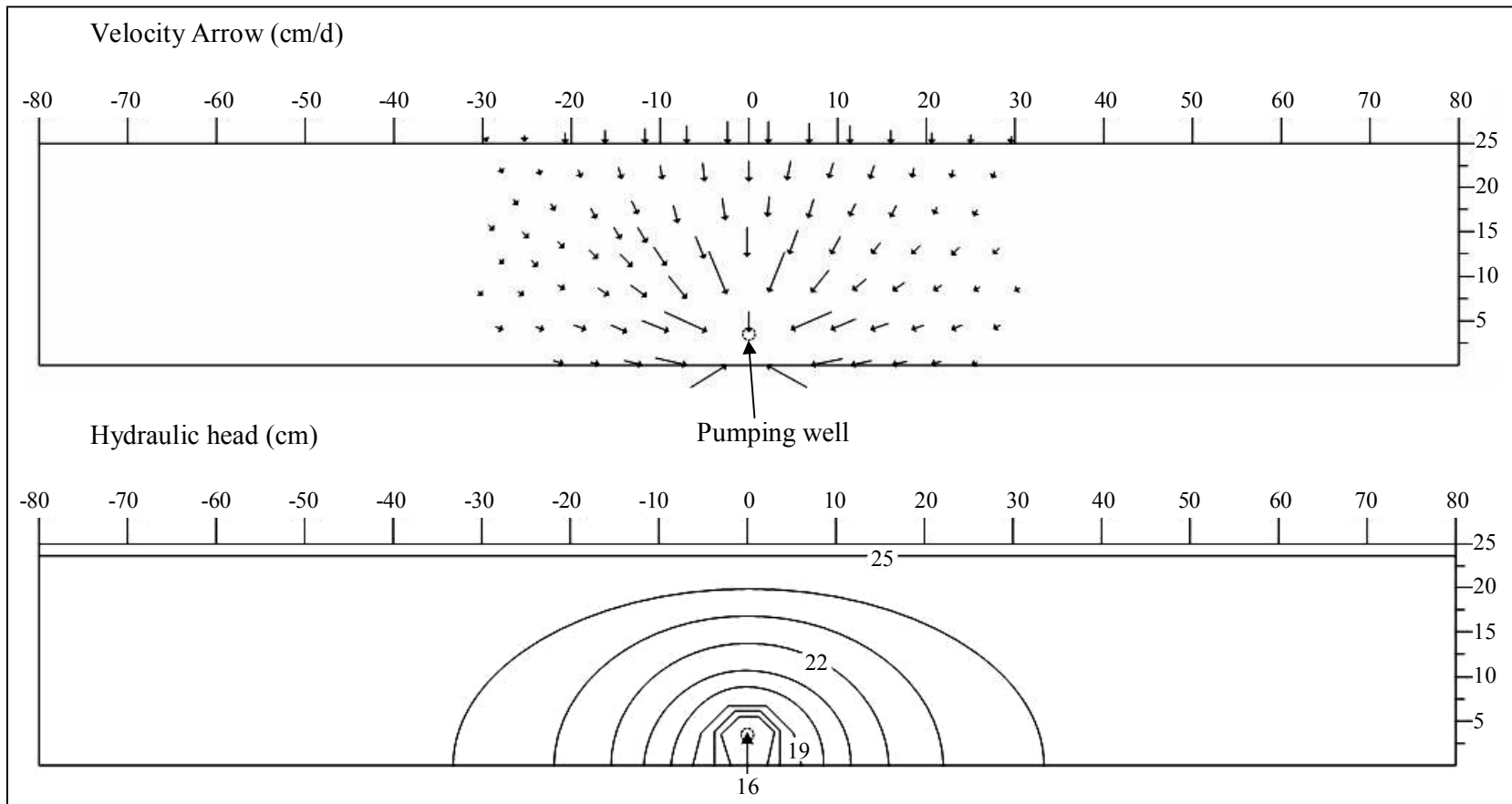
Figure C-3 Computer simulation results of 25 cm overburden thickness, 3.5 cm depth of pumping and 100 cc/min pumping rate
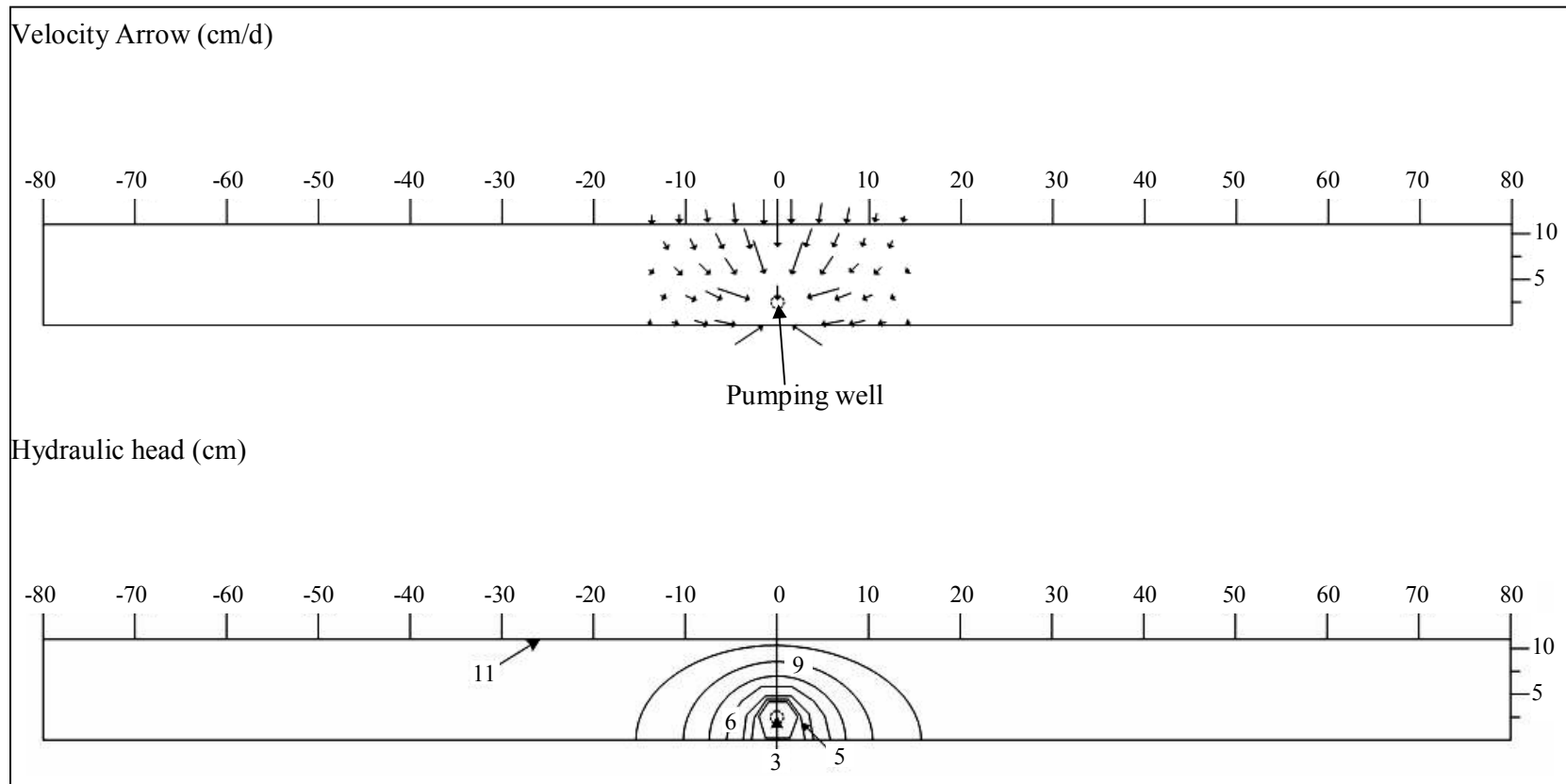
Figure C-4 Computer simulation results of 11 cm overburden thickness, 2 cm depth of pumping and 100 cc/min pumping rate
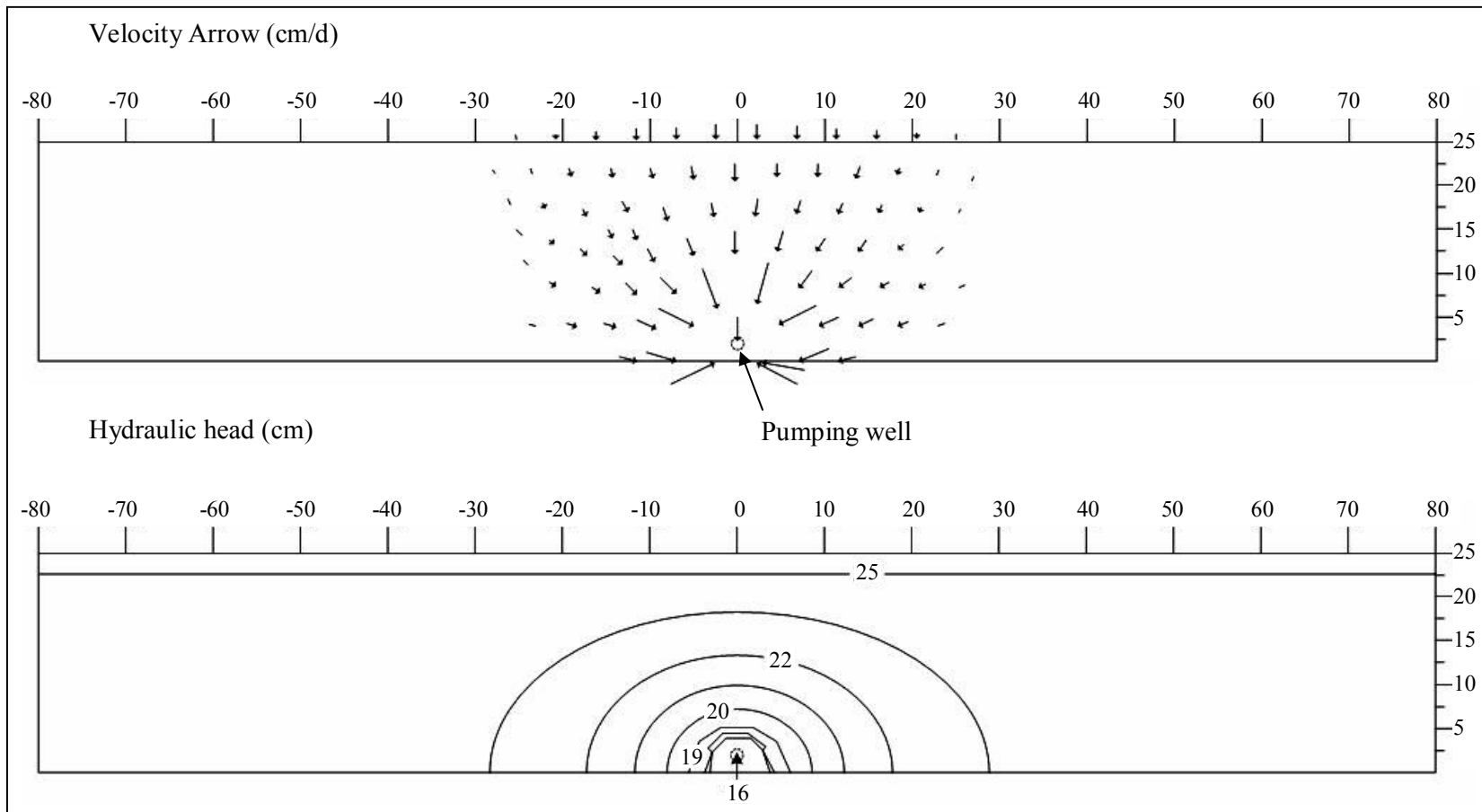
Figure C-5 Computer simulation results of 25 cm overburden thickness, 2 cm depth of pumping and 100 cc/min pumping rate
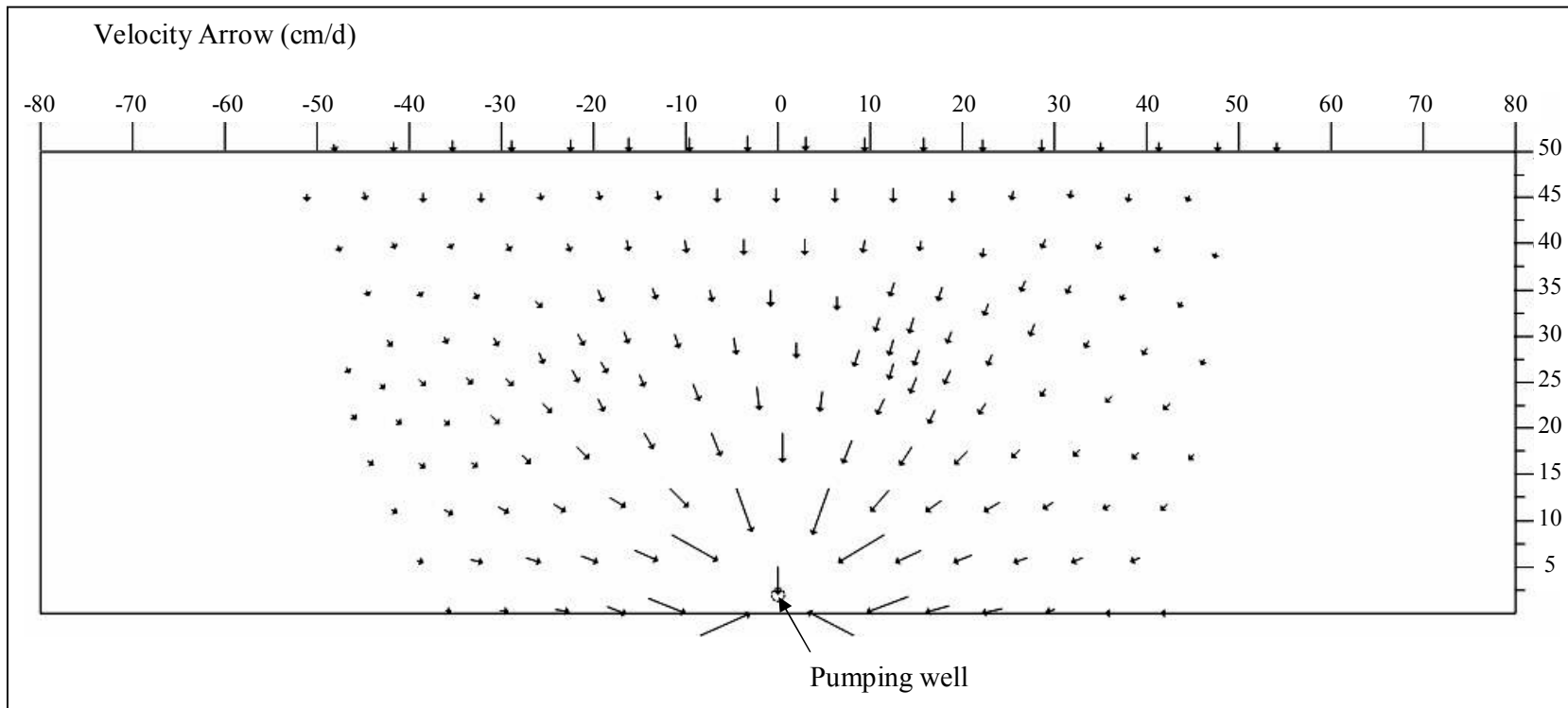
Figure C-6 Computer simulation results of 50 cm overburden thickness, 2 cm depth of pumping (distance from pumping well to

formation surface) and 100 cc/min pumping rate
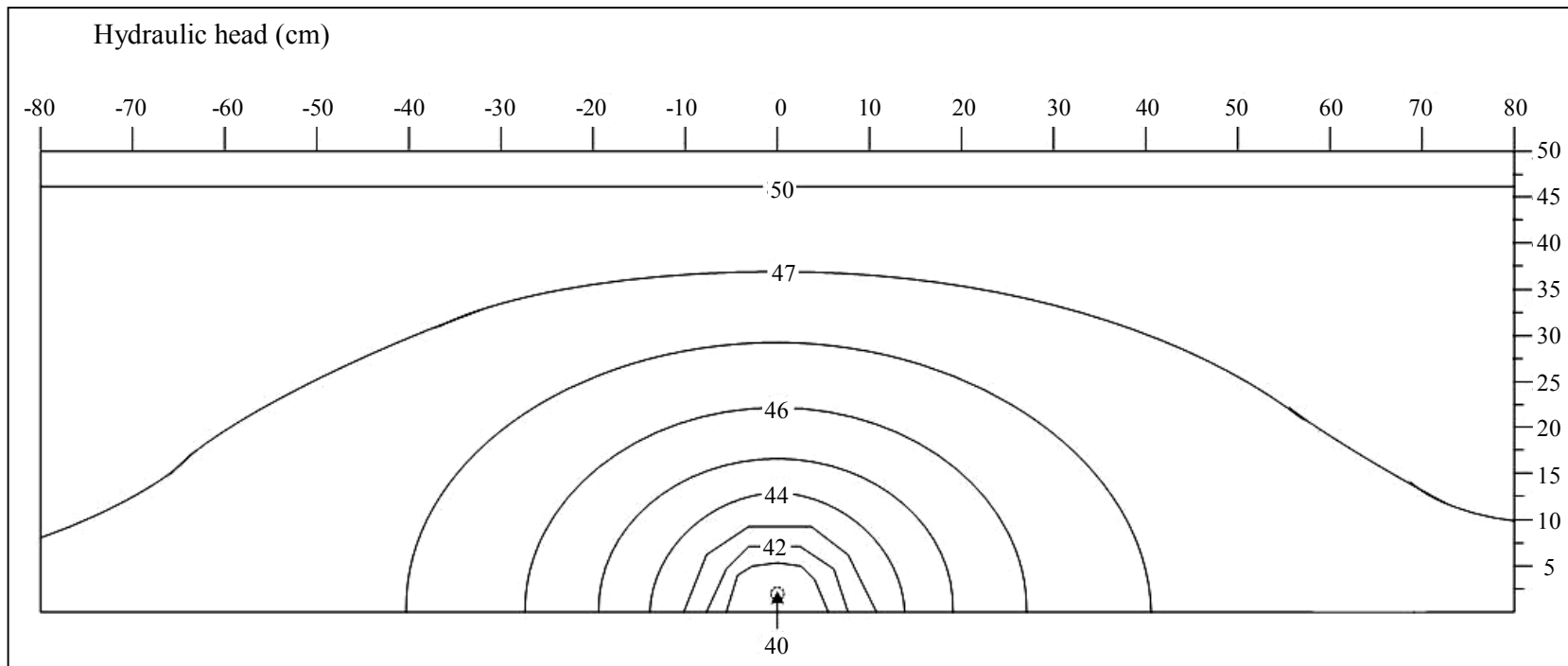
Figure C-6 Computer simulation results of 50 cm overburden thickness, 2 cm depth of pumping (distance from pumping well to

formation surface) and 100 cc/min pumping rate.(continue)
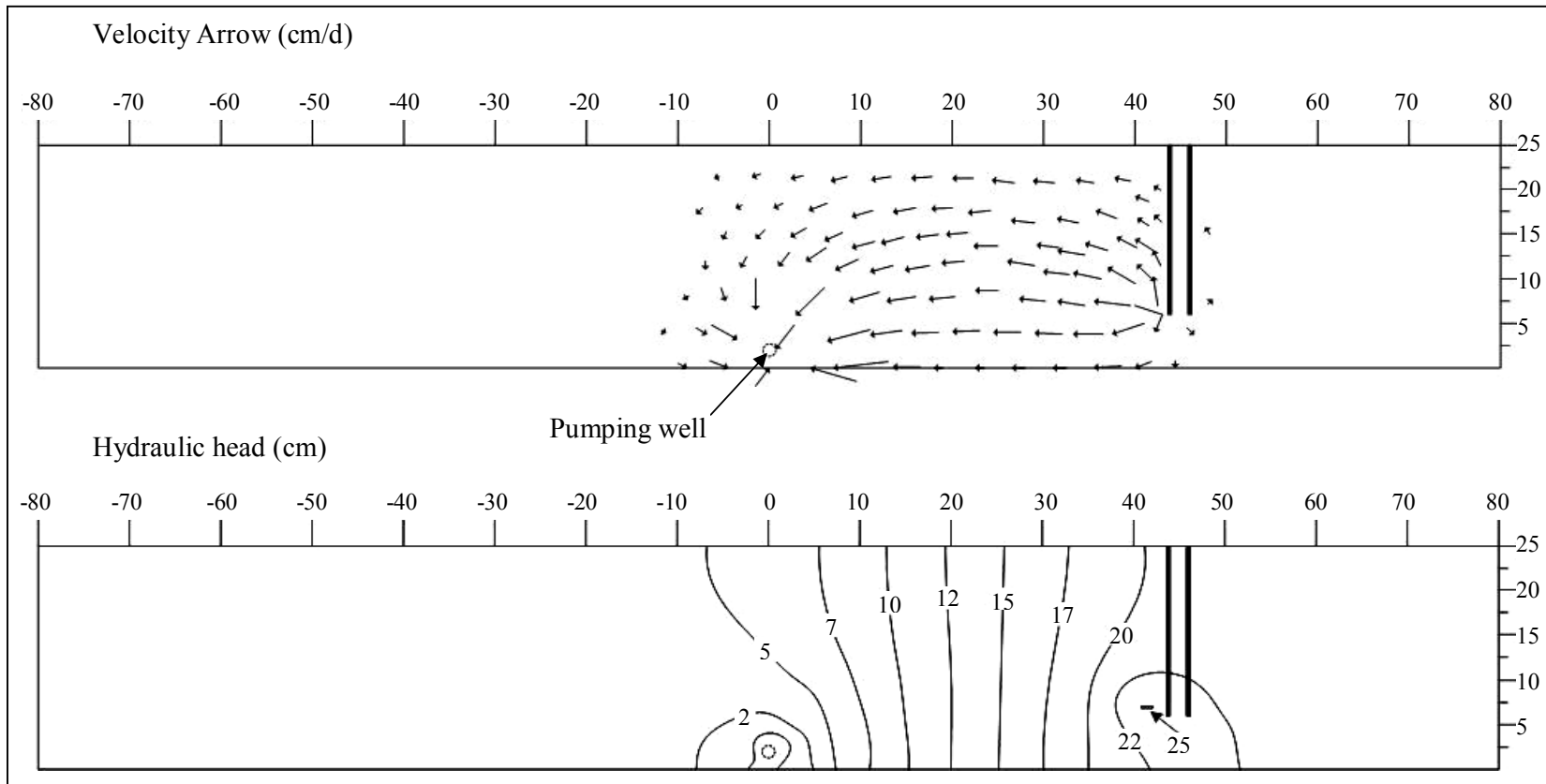
Figure C-7 Computer simulation results of 25 cm overburden thickness, 6cm groundwater level and 100 cc/min pumping rate under horizontal flow direction.
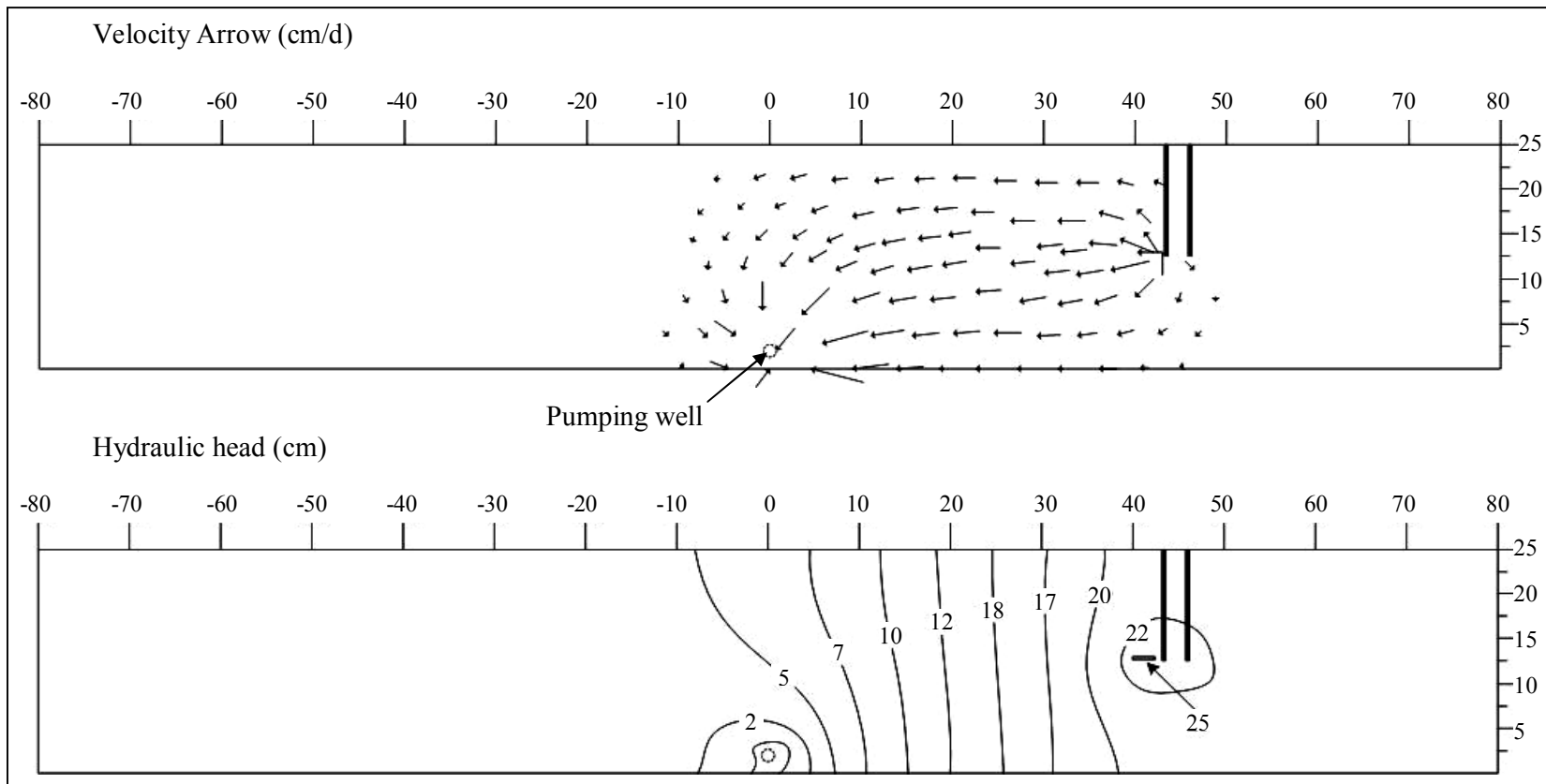
Figure C-8 Computer simulation results of 25 cm overburden thickness, 12.5 cm groundwater level and 100 cc/min pumping rate under the horizontal flow direction.
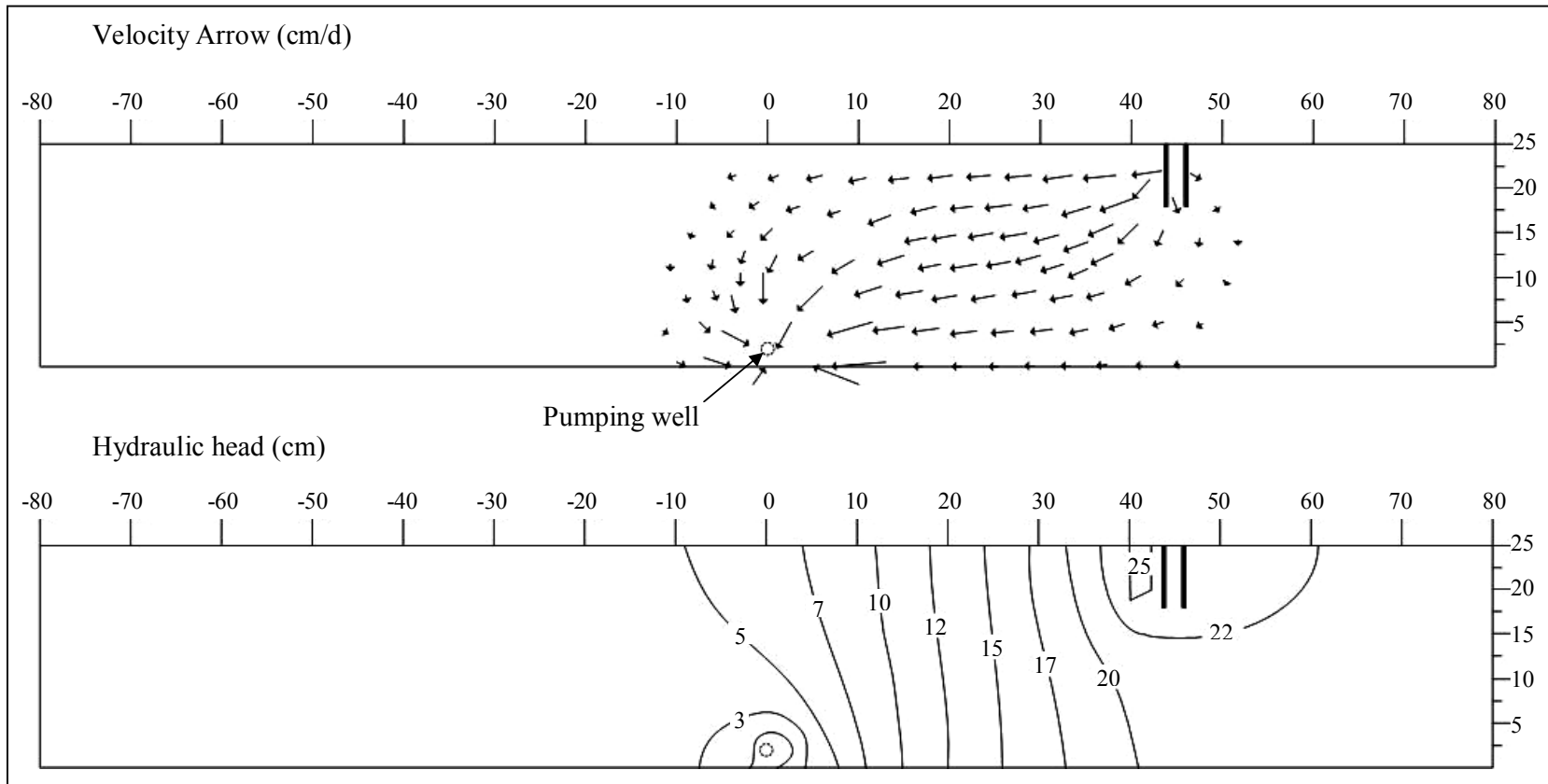
Figure C-9 Computer simulation results of 25 cm overburden thickness, 18 cm groundwater level and 100 cc/min pumping rate under the horizontal flow direction.
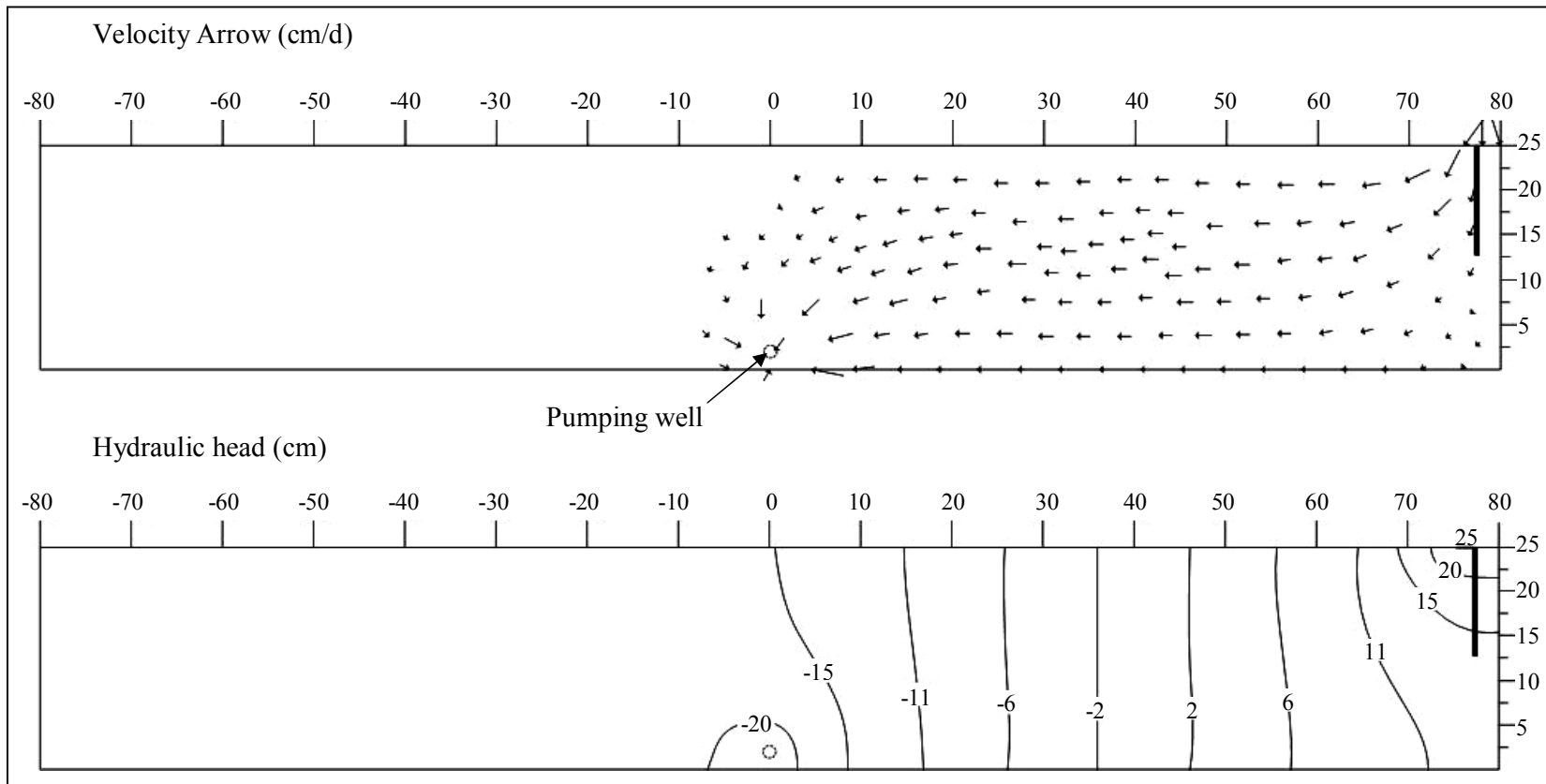
Figure C-10 Computer simulation results of 25 cm overburden thickness, 2 inch in recharge area, 12.5 cm groundwater level and

100 cc/min pumping rate under horizontal infiltration.
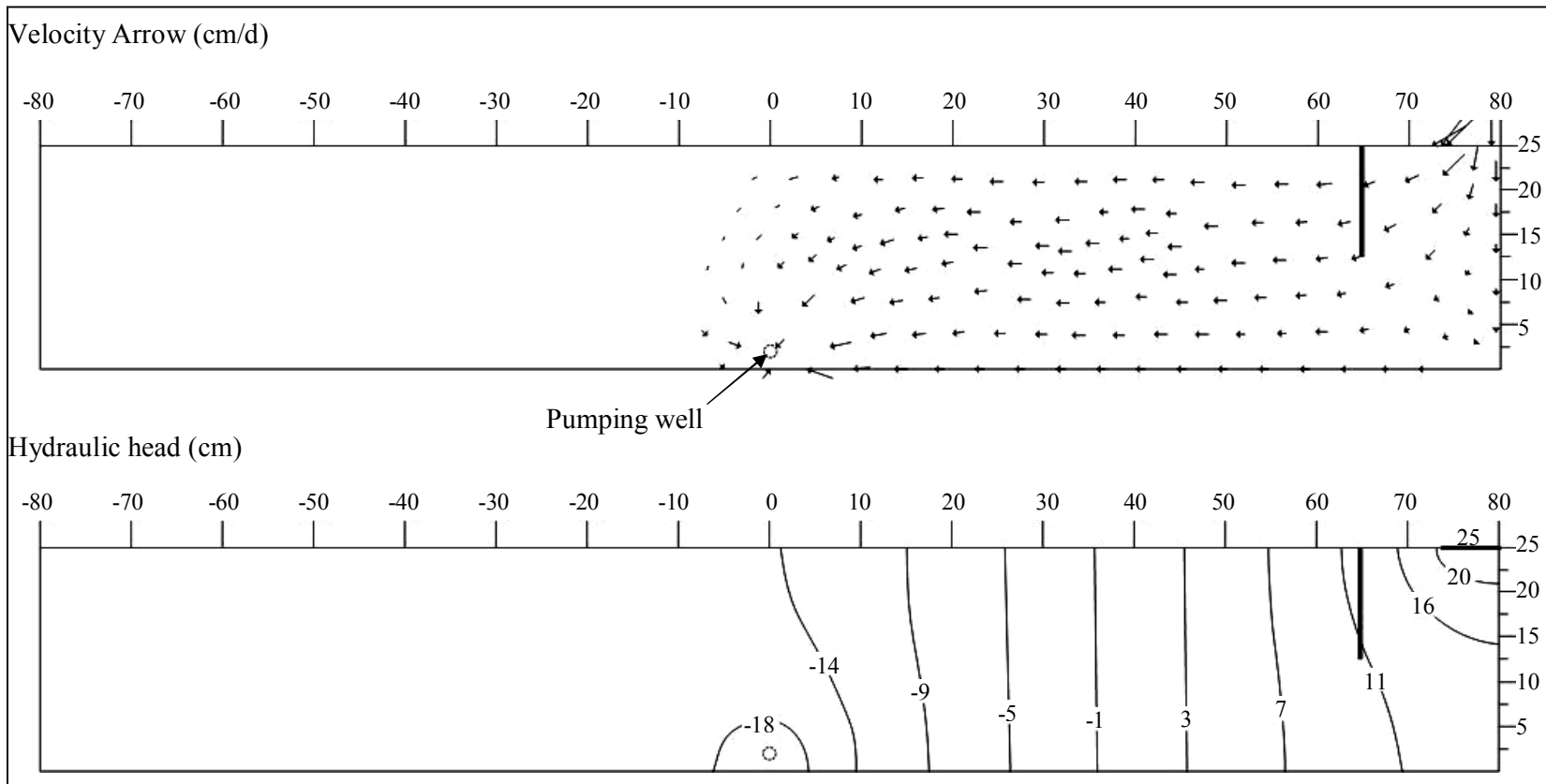
Figure C-11 Computer simulation results of 25 cm overburden thickness, 6 inch in recharge area, 12.5 cm groundwater level and 100 cc/min pumping rate under horizontal flow direction.